EPA-650/4-74-011

July 1973

Environmental Monitoring Series

MATHEMATICAL SIMULATION OF ATMOSPHERIC PHOTOCHEMICAL REACTIONS: MODEL DEVELOPMENT, VALIDATION, AND APPLICATION

Office of Research and Development
U.S. Environmental Protection Agency
Washington DC 20460

EPA-650/4-74-011

MATHEMATICAL SIMULATION OF ATMOSPHERIC PHOTOCHEMICAL REACTIONS: MODEL DEVELOPMENT, VALIDATION, AND APPLICATION

by

Thomas A. Hecht, Philip M. Roth, and John H. Seinfeld

Systems Applications, Inc.
950 Northgate Drive
San Rafael, California 94903

Contract No. 68-02-0580
Task No. 10
Project No. 26AAD
Program Element No. A11008

EPA Project Officer: Marcia C. Dodge

Chemistry and Physics Laboratory
National Environmental Research Center
Research Triangle Park, North Carolina 27711

Prepared for

OFFICE OF RESEARCH AND DEVELOPMENT
U.S. ENVIRONMENTAL PROTECTION AGENCY
WASHINGTON, D.C. 20460

July 1973

This report has been reviewed by the Environmental Protection Agency and approved for publication. Approval does not signify that the contents necessarily reflect the views and policies of the Agency, nor does mention of trade names or commercial products constitute endorsement or recommendation for use.

ACKNOWLEDGEMENTS

We wish to acknowledge the contributions of Dr. Charles Wells, Dr. Robert Shainker, Dr. David Stepner, and Mrs. Ilana Siegall of Systems Control, Inc. of Palo Alto, California. Under a subcontract to their firm, they carried out the digital and analog sensitivity studies reported in Chapters II and III and in Appendix A, and were the authors of Appendix A and a portion of Chapter II.

Abstract

The results of a number of individual tasks involving the development, evaluation, exercise, and analysis of kinetic mechanisms for photochemical smog are described in this document. First, we have carried out a sensitivity analysis of the simplified Hecht-Seinfeld (HS) mechanism. The mechanism was then used in the planning of a number of smog simulation experiments for the University of North Carolina outdoor chamber program. Major aspects of this study were the simulation of the chemical dynamics of proposed experiments under conditions of varying temperature, light intensity, and ratios. While these two tasks were in progress, we were also preparing a detailed planning document focusing on experimental and observational areas of inquiry in which further work is vital to the understanding of smog formation and the development of mathematical models. That report has been submitted to EPA as a separate document EPA-R4-73-031; thus, we only briefly review its contents here.

Results of the sensitivity study of the HS mechanism and our analysis of kinetic mechanisms in the planning report demonstrated deficiencies in the HS mechanism. We therefore undertook the development of an improved kinetic mechanism. The new mechanism, which treats the inorganic reactions in substantial detail and the organic reactions in general terms, has been formulated to strike a balance between accuracy of prediction and compactness of representation. The results of the initial evaluation of the new mechanism using n-butane/NO_x, propylene/NO_x, and n-butane/propylene/NO_x smog chamber data are included.

TABLE OF CONTENTS

LIST OF FIGURES

LIST OF TABLES

I. INTRODUCTION

The goal of the project about which we report here, "The Mathematical Modeling of Photochemical Smog", was the development and validation of a kinetic mechanism capable of describing atmospheric photochemical reactions. The project itself, however, involved a series of tasks, most of which are related to mechanism evaluation, but each being a separate and distinct piece of work. In reporting on the accomplishments of the year, we have elected to discuss each undertaking on an individual basis and in the order carried out. The four main tasks were the following:

1. Exercise and analysis of a simplified kinetic mechanism, as developed by Hecht and Seinfeld (1972), the "best" available mechanism as of the inception of the project.
2. Consultation in the planning of experiments to be carried out in twin 6000 cubic foot outdoor chambers located on the campus of the University of North Carolina.
3. Preparation of a detailed planning document concerned with appraising the current state of knowledge in atmospheric photochemisty and pinpointing specific areas of inquiry in which further experimental work is vital to the advancement of knowledge.

4. Evaluation of an improved, lumped, 39-step kinetic mechanism. Data used for validation were provided by EPA.

It had been clear for some time that there was no kinetic mechanism available, as of mid-1972 that was truly adequate for describing the dynamics of atmospheric reactions. Each mechanism that had been proposed suffered some obvious deficiency (or deficiencies) that required rectification. Furthermore, it was apparent that available smog chamber data were not suitable for use in critically evaluating the capabilities of existing mechanisms. Thus, we were faced at the outset with inadequacies in both models and data. Given these circumstances, we entered into discussions with Dr. M. C. Dodge of EPA, the project officer, in an effort to define an appropriate course of action. As a consequence of these discussions, the following plan was adopted:

- *To carry out sensitivity analyses using the Hecht-Seinfeld (HS) mechanism.* While we were aware of the weaknesses of the mechanism, we felt it important to gain some understanding of the sensitivity of predicted concentration-time profiles to variations in the magnitudes of the parameters of the mechanism, the reaction rate constants and the stoichiometric coefficients. Such analyses were expected to provide further insight into model deficiencies, as well as information helpful in identifying

parameters which should be most accurately determined. In addition, these studies afforded us an opportunity to experiment with both the analog and digital computers in integrating the coupled, first order differential equations. This work is discussed in Chapter II.

To use the HS mechanism to simulate the dynamics of chemical reactions in the outdoor chamber, in response to temporal variations in temperature and radiation intensity. In particular, after consultation with Dr. B. Dimitriades of EPA and Dr. H. Jeffries of the Univeristy of North Carolina, we carried out the following calculations for the toluene system (the "best" surrogate for atmospheric hydrocarbon mixture of the various reactive systems we had studied to date).

1. Determined maximum oxidant levels as a function of initial NO_x for constant initial hydrocarbon at 0.1, 0.5, 1.0, 2.5 and 5.0 ppm. Range of NO_x was 0 to 1 ppm.
2. Determined the effect of variations in light intensity on maximum NO_2 and O_3 and on dosage of both for five light intensity profiles. This calculation was carried out for several pairs of initial conditions of HC and NO_x, where initial conditions within each pair differed only in terms of HC concentration.

3. Determined the effect of temperature on maximum NO_2 and O_3 and on dosage of both. This calculation was carried out over a wide range of ambient temperature levels for four pairs of initial HC and NO_x conditions, as above.

The results of this effort are presented in Chapter III.

- *To prepare a recommendations document* for the Chemistry and Physics Laboratory (CPL) that will serve as an aid in planning for the support of future contracts and grants in experimental and observational aspects of atmospheric chemistry. The core of the report focuses on laboratory studies concerned with the kinetics and mechanisms of individual reactions, on smog chamber studies, and on programs involving atmospheric observations. Also included is a thorough review of the status of modeling of photochemical reaction processes in both the presence and absence of transport-limiting phenomena. This report, "Existing Needs in the Experimental and Observational Study of Atmospheric Chemical Reactions: A Recommendations Report", by J. H. Seinfeld, T. A. Hecht, and P. M. Roth, (EPA-R4-73-031), has been submitted to EPA as a separate document. We will thus only briefly review its contents in this report (Chapter IV).
- *To develop and evaluate an improved photochemical kinetics mechanism.* Development of the improved mechanism, which

was documented originally in the planning report, was taken to completion more rapidly than was originally anticipated, thus allowing time for a relatively extensive validation effort. The model and the validation results are described in detail in Chapter V. We would note here only that the results are quite favorable.

We conclude the report (Chapter VI) with an evaluation of the work carried out to date and a summary of future needs.

II. Sensitivity Analysis of the Hecht and Seinfeld Kinetic Mechanism.

Chemical kinetics mechanisms of varying degrees of complexity are presently being developed for inclusion in urban scale air pollution simulation models. These models, in turn, may be used in the planning and development of air pollution abatement and control strategies. The degree of confidence that one can place in the predictions of such simulation models depends, among other considerations, on the uncertainties associated with the parameters of the model (for example, the reaction rate constants). More important, however, is the sensitivity of the model's predictions to variations in the magnitudes of inaccurately known parameters. Thus, an important step in the development of an accurate, as well as compact kinetic mechanism for photochemical smog is the determination of the sensitivity of concentration-time profiles predicted by the mechanism to variations in each of the various input parameters, rate constants, parameterized stoichiometric coefficients, and initial reactant concentrations. By carrying out such studies, those parameters can be identified which must be accurately determined to insure reliable prediction of pollutant concentrations.

A promising generalized kinetic mechanism (see Table 1.), formulated by Seinfeld et al, (1971) and further developed by Hecht (1972), was chosen as the subject of a detailed sensitivity analysis carried out by us as a part of this contract effort. This mechanism was selected for the study because, in comparing it with other mechanisms that have been developed, we judged it "best" in terms of accuracy and reliability. The

TABLE 1. The HS Kinetic Mechanism

$$NO_2 + h\nu \xrightarrow{1} NO + O$$

$$O + O_2 + M \xrightarrow{2} O_3 + M$$

$$O_3 + NO \xrightarrow{3} NO_2 + O_2$$

$$O_3 + NO_2 \xrightarrow{4} NO_3 + O_2$$

$$NO_3 + NO \xrightarrow{5} 2NO_2$$

$$NO_3 + NO_2 \xrightarrow[6]{H_2O} 2HNO_3$$

$$NO + NO_2 \xrightarrow[7]{H_2O} 2HNO_2$$

$$2HNO_2 \xrightarrow{8} NO + NO_2 + H_2O$$

$$HNO_2 + h\nu \xrightarrow{9} OH + NO$$

$$CO + OH \xrightarrow[10]{O_2} CO_2 + HO_2$$

$$HO_2 + NO \xrightarrow{11} OH + NO_2$$

$$HO_2 + NO_2 \xrightarrow{12} HNO_2 + O_2$$

$$O + HC \xrightarrow{13} \alpha RO_2$$

$$OH + HC \xrightarrow{14} \beta RO_2$$

$$O_3 + HC \xrightarrow{15} \gamma RO_2$$

$$RO_2 + NO \xrightarrow{16} NO_2 + \varepsilon OH$$

$$RO_2 + NO_2 \xrightarrow{17} PAN$$

$$O + HC_2 \xrightarrow{18} \alpha_2 RO_2$$

$$OH + HC_2 \xrightarrow{19} \beta_2 RO_2$$

$$O_3 + HC_2 \xrightarrow{20} \gamma RO_2$$

$$NO_2 \xrightarrow{21} \text{WALL OR PARTICLE}$$

mechanism, termed by us the HS mechanism, has been evaluated for several hydrocarbons and for a wide range of values of the HC/NO_x ratio (see references cited). In this section we report on the sensitivity analysis, the design of the study, and the results of the work.

Simultaneously with our carrying out the sensitivity analysis, we undertook development of a more detailed mechanism, with the intent of eliminating a number of deficiencies in the HS mechanism. During the course of this development work, it soon became apparent that the new mechanism, which we present in Chapter V, represented a substantial improvement over the HS mechanism. Thus, the sensitivity results to be reported here are of limited interest in the sense that the HS mechanism has been substantially improved upon since the task was carried out. Nevertheless, we have elected to fully disclose the results of the work here because

- it is the first such sensitivity study performed
- the methods employed are generally applicable
- the HS mechanism contains the same general chemical dependencies as the improved kinetics, so that the results are of interest and value for making qualitative sensitivity judgements concerning the new mechanism

  the task itself was a clearly defined portion of the overall effort.

We would note, however, that the sensitivity study itself was limited to a detailed analysis of an $HC-NO_x$ system of low reactivity and a partial analysis of a more reactive hydrocarbon-NO_x system, particular attention being given to those parameters which were different for the two systems. This scope

of work, in our judgment, provided a reasonable approach, limiting the expenditure of effort in light of the limited value of the results.

There are several points to be noted about the HS mechanism as we used it. First, reactions 5 and 8, although a part of the mechanism as originally formulated, were found to be unimportant in subsequent validation work (Hecht, 1972) and are now deleted from the mechanism. Reactions 10 to 12 apply only when CO is present initially. To facilitate the interpretation of the results we chose to study only single hydrocarbon reactions systems. As a consequence of this simplification, we were able to delete four additional reactions--reactions 18 to 21. Reactions 18 to 20 are needed when simulating the behavior of binary hydrocarbon mixtures. Reaction 21 is included to account for the observed behavior of auto exhaust when irradiated in smog chambers. To summarize, because we did not consider binary hydrocarbon mixutres, auto exhaust, or systems containing CO in this sensitivity study, the mechanism which we ultimately examined consisted of only of twelve reactions: 1-4, 6, 7, 9, 13-17.

The sensitivity analysis was carried out in the following manner. For the two hydrocarbon-NO_x systems evaluated in the current project, nominal (or base) values for all parameters were taken to be those reported in Hecht (1972). Base concentration-time profiles for hydrocarbon, NO, NO_2, O_3 were obtained by integrating the governing rate equations with each parameter at its nominal value. One of the parameters was then increased and decreased by a fixed percentage, with all other parameters held at

their nominal values. The equations were then integrated twice, once for each of the two new settings (+x% and -x%) of the selected input parameter. This process was repeated for each parameter of interest. Thus, for n parameters, integrations were carried out for a base case and 2n parameter variations. Finally, for each of the 2n+1 integrations, values of "decision variables" were determined. The magnitudes of the decision variables for each variation in a parameter were compared with those computed for the base case, and rankings of sensitivities of the parameters were obtained by tabulating the magnitudes of the differences.

It is appropriate to comment at this point about what constitutes a decision variable. By a decision variable, we have in mind any measure that can be constructed or derived from the predicted responses (in this case, concentration) that is of use in characterizing the sensitivity of the model or mechanism to changes in the magnitudes of the parameters. Measures that are simply calculated include, as noted before, the maximum ozone concentration measured, the time to the NO_2 peak, and the time of "cross-over" of the NO and NO_2 concentration profiles. In none of these simple cases, however, is the decision variable suggested a measure of sensitivity over the <u>entire</u> time period of the integration for <u>each</u> species determined experimentally. Instead of adopting a simple measure, then, we have had to construct one that meets our needs.

Consider the following. Assume that the solid line in Figure 1 is the time history of species y_i (i being one of m species present) for a set of nominal reaction rate constants, $k_1, \ldots, k_n$. Assume

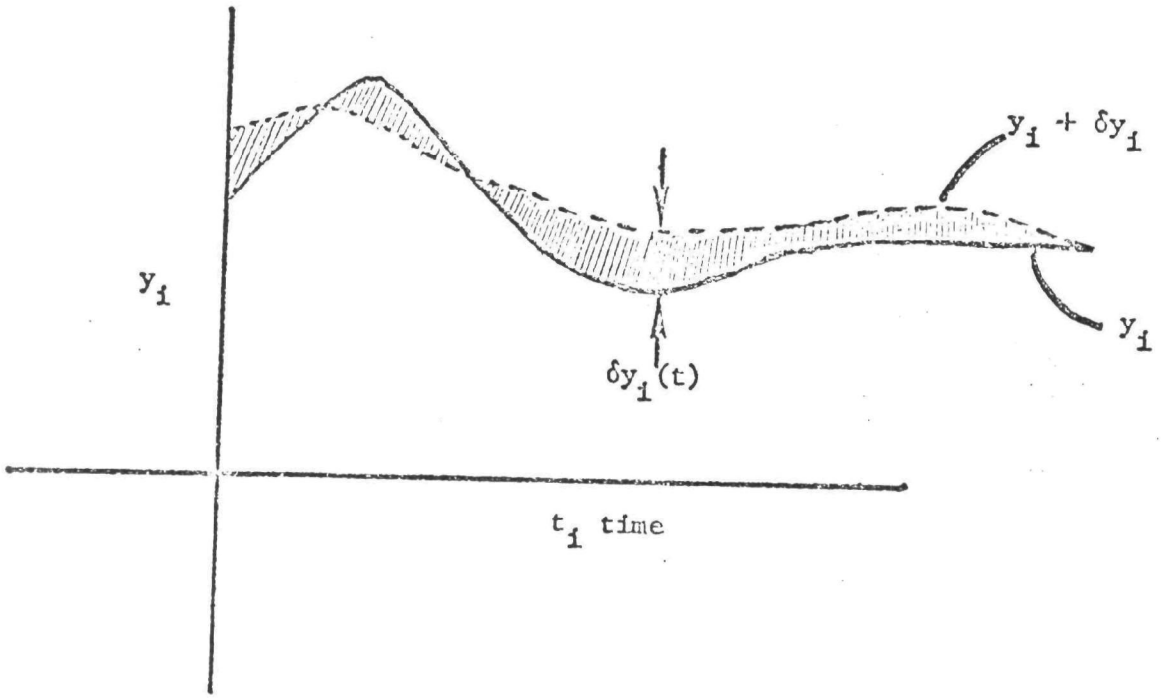

FIGURE 1. SENSITIVITY ANALYSIS

further that one of the reaction rate constants k_j (j representing one of n rate constants, stoichiometric coeffecients, or initial conditions) is altered by a small, fixed percentage. The time history of all the reaction constituents will be altered in some manner in response to this change. For example, the change in y_i, $y_i + \delta y_i$, may be shown by the dotted line. The vertical distance between the lines is the value of $\delta y_i(t)$ at each time point t, and the shaded area is a measure of the effect that a small change in k_j has on the time history of y_i. The total change in y_i, using squared values to allow for both positive and negative differences, is given by

$$\int_0^t (\delta y_i(t))^2 \, dt \qquad (1)$$

If this same operation were performed for the m constituents, the total effect (squared) of a small change in k_j is given by

$$\sum_{i=1}^{m} \int_0^t (\delta y_i(t))^2 \, dt \qquad (2)$$

This is clearly a measure of the sensitivity of the constituent values to variations in the rate constant k_j. If the time histories are greatly altered, indicating a large sensitivity to that particular rate constant, then the expression in equation (2) will have a large value. If the sensitivity is small, there will be very little change in the time histories of constituent values, and the expression in equation (2) will also be small. A measure of sensitivity such as that described can be easily calculated

using a digital computer. However, if an analog computer is used to carry out the analysis, then only more limited (or simpler) measures of sensitivity can be used, as they must be observed visually.

For the purposes of the present study, we elected to employ an analog computer to carry out the necessary calculations. This decision was based on several factors. First, the experimental data from which the nominal values of the rate constants and stoichiometric coefficients were derived [see Hecht (1972)] were corrupted by error to a large enough degree that the base concentration-time profiles were subject to greater than desirable levels of uncertainty. Second, experimental concentration-time profiles were determined only for four of the eleven chemical constituents in the mechanism; thus, the value of a complete sensitivity analysis for each species over the course of the entire irradiation is limited. Third, a digital sensitivity analysis based on equation (2) is extremely expensive to carry out. Given these various considerations, we did not feel that the use of the digital computer was justified. The digital computer was therefore used primarily as a means for checking the results of the analog computations (although we did perform a few sensitivity runs on the digital computer to demonstrate the potential power of this approach).

The availability of a previously wired circuit board also influenced our decision to a degree. As part of the contract effort, we had, at an earlier stage, programmed the HS mechanism for analog usage. As the reader may be aware, analog programming requires a substantial expenditure of effort; once the circuits have been wired, however, the analog provides

virtually instantaneous "turn around" time at a very low cost. Aside from rapid and direct response, other advantages of analog computation include flexibility in use and the opportunity the device provides for "getting a feel" for the effect that varying the parameters has on predicted concentrations. However, only four place accuracy is available on the analog, scaling of variables can, under certain conditions, be a serious problem, and personnel are required for operation at all times. Despite these latter shortcomings, the analog seemed to be the wisest choice for the work at hand.

As we noted earlier, the selection of the analog for use limited our choice of decision variables to those scalars which can be observed visually, i.e., the variables, time to the NO_2 peak, T, and the magnitude of the O_3 maximum, M. These are logical choices inasmuch as the onset of smog symptoms, as characterized by the time to the NO_2 peak, and the intensity of smog, as generally evidenced by the O_3 concentration, are often taken as two major indicators of smog formation and severity. Further, both of these variables are quite sensitive to variations in the values of the input parameters. If consideration is limited to a six hour simulation, as was done in this study, T occurs most often between the first and third hours of irradiation and M between the third and sixth hours. During the first hour the principal occurrence is the oxidation of NO to NO_2, which in turn is reflected in T. Thus, except for the first hour (the "induction" period), T and M serve as sensitive and explicit indicators of the course of the experiment.

In this chapter we present the results of the sensitivity study of the HS mechanism. We examine the parameters displaying the greatest sensitivity, exploring the reasons for the uncertainties associated with each. We then conclude by discussing the basis for our decision to develop the new kinetic mechanism presented in Chapter V. Should the reader be interested, a detailed description of the mathematical representation of the HS mechanism and the techniques used for carrying out both the analog and digital sensitivity analyses can be found in Appendix A.

A. Analog Studies

Use of a large, powerful EAI 8800 analog computer was provided at no cost by the NASA Ames Research Center. The 8800 at Ames is one of the largest analog computers in existence. As such, it has far greater capacity than is required to integrate the governing equations. The computer also has many features which ease programming and debugging. For example, potentiometers can be set directly from the control panel, and the components are versatile enough to allow the programming of coupled differential equations whose individual scales differ by many orders of magnitude. (For this particular application voltage ranges had to be scaled over eleven orders of magnitude.) It also has two attached CRTs, an X-Y plotter, 16 strip chart recorders, and a digital printer for permanently recording integrator initial conditions and pot settings. In short, we found it to be very suited for our use.

In using the analog, special consideration had to be given to the form of the governing equations. In particular, in order to avoid the

need for solving nonlinear algebraic equations, the steady-state assumption was not invoked for any of the species. Thus, instead of employing five differential equations and six steady-state algebraic equations to describe the kinetics (the complete set of equations for this representation can be found in Seinfeld et al, 1971), we solved the full set of eleven differential equations. Equipment requirements for integration of the equations embodying the mechanism were the following: 11 integrators, 15 multipliers, approximately 50 pots, and 65 summing amplifiers. Following initial preparations, the 11 differential equations were time and amplitude sealed, based on the peak amplitudes of the 11 state variables obtained from a digital simulation of the kinetic mechanism using the rate parameters.

A low and a high reactivity hydrocarbon-NO_x system were evaluated in this sensitivity study, with toluene and propylene, respectively, serving as representative hydrocarbons. These hydrocarbons were chosen because extensive validation studies have been carried out for each over a range of initial hydrocarbon to NO_x ratios (Hecht, 1972) and because they demonstrate behavior typical of the low and high "reactivity" organic species that participate in atmospheric reactions.

1. Toluene

   We carried out a comprehensive sensitivity study on the analog computer for the rate constants and stoichiometric coefficients associated with the toluene-NO_x system. Parameters were varied ± 50% from their base values and predicted values of T, the time to the NO_2 peak, and M, the asymptomatic O_3 level, were noted. Base values of

the parameters are tabulated in Table 2; effects of parameter variations on T and M are shown in Table 3. In Tables 4 and 5, respectively, we have "rank-ordered" the parameters in terms of the magnitude of change in T and M observed as a result of the ±50% variations in rate constants and stoichiometric coefficients. T is most sensitive to variations in β , ϵ , α , k_1 , k_2 , and k_{13}., M to variations in β , ϵ , α , and k_1. In addition, decreases in k_2 and k_3 significantly increase M, while a decrease in k_{13} causes a large decrease in M.

2. Propylene

The kinetic mechanism and rate parameters were the same for the propylene-NO_x system as for the toluene-NO_x system; except for changes in the stoichiometric coefficients, in the rates of the hydrocarbon oxidation reactions, and in the rate of PAN formation. We began the analysis of the propylene-NO_x system by examining the sensitivities of k_1 , k_2 , k_3 , and k_{16} , parameters whose nominal values are identical in both systems, and found that their sensitivities followed the same "rank ordering" observed for the toluene-NO_x system. For this reason and the reasons already outlined in the introduction to this chapter, we limited the sensitivity runs for the propylene system to eight of the input rate constants and one of the initial conditions.

Base values of the parameters used in the propylene sensitivity runs are presented in Table 6. Effects of parameter variations on T and M are shown in Table 7. In Tables 8 and 9, respectively, we have "rank-ordered" the parameters examined in terms of the magnitude of change in T and M that have resulted from the indicated variations in rate constants. Both T and M are most sensitive to variations in k_1 and k_2. In addition, a 50% decrease in k_{13} results in a large decrease in T and M, and a 50% increase in k_{15} results in a substantial decrease in M. Formal evaluation of the sensitivity of the stoichiometric coefficients was not performed. From our experience with this system, however, we can conclude that α, β, and ϵ are extremely sensitive parameters, as was the case for the toluene system.

B. Digital Studies

Our principal interests in digital computation techniques are in performing routine validation experiments, such as those presented in Chapter V, and in estimating the magnitude and uncertainty (i.e. variance) of "sensitive" parameters through the analysis of experimental data. However, we have also used the digital computer in what amounted to a pilot study, to carry out a limited sensitivity analysis of the toluene-NO_x system. Specifically, we examined the effect on predicted concentration-time profiles of varying the magnitude of four parameters--k_1, k_3, k_4, and k_{16}.

TABLE 2. Base Values of Parameters for the Toluene-NO_x System

Rate Constants *

k_1	0.266	min^{-1}
k_2	2.76×10^6	min^{-1}
k_3	21.8	$ppm^{-1}min^{-1}$
k_4	0.006	$ppm^{-1}min^{-1}$
k_6	0.1	$ppm^{-1}min^{-1}$
k_7	5.0×10^{-4}	$ppm^{-1}min^{-1}$
k_9	5.0×10^{-3}	min^{-1}
k_{11}	1.8×10^3	$ppm^{-1}min^{-1}$
k_{12}	10.0	$ppm^{-1}min^{-1}$
k_{13}	6.0×10^3	$ppm^{-1}min^{-1}$
k_{14}	1.5×10^4	$ppm^{-1}min^{-1}$
k_{15}	7.5×10^{-5}	$ppm^{-1}min^{-1}$
k_{16}	1.8×10^3	$ppm^{-1}min^{-1}$
k_{17}	30.0	$ppm^{-1}min^{-1}$

Stoichiometric Coefficients

α	6.0
β	1.2
γ	4.0
ϵ	0.61

Dilution

$Q = 5.4$ liters/min.

* $k_5 = k_8 = k_{10} = k_{18 \text{ through } 21} = 0.0$

TABLE 3. Effects of Parameters Variations On Time to NO_2 Peak and On Magnitude of Asymptotic O_3 Concentration (or Concentration at 400 Minutes) for the Toluene-NO_x System

Parameter Varied, and Magnitude of Varied Parameter	Time to NO_2 Peak	c_{O_3} max (in ppm) or c_{O_3} @400 min
Base Values	162	.24
$k_1 = .133$	278	.11
$k_1 = .399$	119	>.3
$k_2 = 1.38 \times 10^6$	94	>.3
$k_2 = 2.07 \times 10^6$	128	.27
$k_2 = 4.14 \times 10^6$	224	.19
$k_3 = 10.9$	164	>.3
$k_3 = 32.7$	160	.205
$k_4 = .003$	162	.28
$k_4 = .009$	160	.21
$k_4 = .06$	148	.09
$k_6 = .05$	162	.24
$k_6 = .15$	160	.24
$k_7 = .00025$	162	.24
$k_7 = .00075$	162	.24
$k_9 = .0025$	162	.24
$k_9 = .0075$	158	.24
$k_{13} = 3000$	286	.14
$k_{13} = 9000$	118	.28
$k_{14} = 7500$	163	.24
$k_{14} = 22500$	160	.24
$k_{15} = 3.75 \times 10^{-15}$	161	.24
$k_{15} = 1.125 \times 10^{-4}$	160	.24
$k_{16} = 900$	186	.17
$k_{16} = 2700$	151	.29

TABLE 3. (Continued)

Parameter Varied, and Magnitude of Varied Parameter	Time to NO_2 Peak	c_{O_3} max (in ppm) or c_{O_3} @ 400 min
Base Values	162	.24
$k_{17} = 15$	163	.29
$k_{17} = 45$	161	.21
$\alpha = 3$	300	.12
$\alpha = 9$	114	.30
$\beta = .6$	360	.09
$\beta = 1.8$	48	>.3
$\gamma = 2$	160	.24
$\gamma = 6$	160	.24
$\varepsilon = .305$	336	.12
$\varepsilon = .915$	56	>.3
$(NO_2)_o = .02$	186	.24
$(NO_2)_o = .04$	142	.24
$(NO)_o = .45$	158	.23
$(NO)_o = .65$	165	.25
$(O_3)_o = .05$	124	.25
$(HC)_o = 1.34$	194	.20
$(HC)_o = 2.00$	136	.27

TABLE 4. Rank Order of Parameters: Sensitivity of "Time to NO_2 Peak" to Parameter Variations of ± 50% for the Toluene-NO_x system.

THOSE CHANGES CAUSING GREATEST DELAY IN TIME TO NO_2 PEAK

Parameter Change	T
β - 50%	360
ε - 50%	336
α - 50%	300
k_{13} - 50%	286
k_1 - 50%	278
k_2 + 50%	224
k_{16} - 50%	186
k_3 - 50%	164
k_{14} - 50%	163
k_{17} - 50%	163

No Effect: k_4 - 50%
k_6 - 50%
k_7 ± 50%
k_9 - 50%

THOSE CHANGES CAUSING GREATEST REDUCTION IN TIME TO NO_2 PEAK

Parameter Change	T
β + 50%	48
ε + 50%	56
k_2 - 50%	94
α + 50%	114
k_{13} + 50%	118
k_1 + 50%	119
k_{16} + 50%	151
k_9 + 50%	158
k_3 + 50%	160
k_4 + 50%	160
k_6 + 50%	160
k_{14} + 50%	160
k_{15} + 50%	160
γ - 50%	160
γ + 50%	160
k_{15} - 50%	161
k_{17} + 50%	161

TABLE 5. Rank Order of Parameters: Sensitivity of "Asymptotic Ozone Concentration, or Ozone Concentration at 400 Minutes" to Parameter Variations of ± 50% for the Toluene-NO_x system.

THOSE CHANGES CAUSING GREATEST INCREASE IN O_3 LEVELS (at 400 Minutes)

k_1 + 50%	>.3
k_2 - 50%	>.3
k_3 - 50%	>.3
β + 50%	>.3
ϵ + 50%	>.3
α + 50%	.3
k_{16} + 50%	.29
k_{17} - 50%	.29
k_4 - 50%	.28
k_{13} + 50%	.28

THOSE CHANGES CAUSING GREATEST DECREASE IN O_3 LEVELS (400 Minutes)

β - 50%	.09
k_1 - 50%	.11
α - 50%	.12
ϵ - 50%	.12
k_{13} - 50%	.14
k_{16} - 50%	.17
k_2 + 50%	.19
k_3 + 50%	.205
k_4 + 50%	.21
k_{17} + 50%	.21

TABLE 6. BASE VALUES OF PARAMETERS FOR THE PROPYLENE-NO_x SYSTEM

Rate Constants*

k_1	0.266	min^{-1}
k_2	2.76×10^6	min^{-1}
k_3	21.8	$ppm^{-1}min^{-1}$
k_4	0.006	$ppm^{-1}min^{-1}$
k_6	0.1	$ppm^{-1}min^{-1}$
k_7	5.0×10^{-4}	$ppm^{-1}min^{-1}$
k_9	5.0×10^{-3}	min^{-1}
k_{11}	1.8×10^3	$ppm^{-1}min^{-1}$
k_{12}	10.0	$ppm^{-1}min^{-1}$
k_{13}	4.0×10^4	$ppm^{-1}min^{-1}$
k_{14}	2.5×10^4	$ppm^{-1}min^{-1}$
k_{15}	0.016	$ppm^{-1}min^{-1}$
k_{16}	1.8×10^3	$ppm^{-1}min^{-1}$
k_{17}	3.0	$ppm^{-1}min^{-1}$

Stoichiometric Coefficients

α	16.0
β	0.2
γ	4.0
ε	0.22

Dilution:

Q = 6.95 liters/min.

*$k_5 = k_8 = k_{10} = k_{18}$ through $k_{21} = 0.0$

TABLE 7. EFFECTS OF PARAMETER VARIATIONS ON TIME TO NO_2 PEAK AND ON MAGNITUDE OF ASYMPTOTIC O_3 CONCENTRATION (OR CONCENTRATION AT 400 MINUTES) FOR THE PROPYLENE-NO_x SYSTEM.

Parameter Varied; Value of Parameter	Time to NO_2 Peak	c_{O_3} max (in ppm) or c_{O_3} @ 400 min
Base Values	130	.47
$k_1 = .133$	250	.25
$k_1 = .312$	114	.51
$k_2 = 1.38 \times 10^6$	66	>.58
$k_2 = 4.14 \times 10^6$	194	.36
$k_3 = 10.9$	142	.48
$k_3 = 32.7$	124	.47
$k_{13} = 20,000$	260	.24
$k_{13} = 60,000$	88	.58
$k_{14} = 12,500$	130	.48
$k_{14} = 37,500$	130	.47
$k_{15} = .024$	134	.30
$k_{16} = 900$	128	.46
$k_{16} = 2700$	130	.48
$k_{17} = 1.5$	130	.48
$k_{17} = 4.5$	130	.46
$(NO_2)_0 = .02$	164	.46
$(N)_2)_0 = .06$	112	.49

TABLE 8. RANK ORDER OF PARAMETERS: SENSITIVITY OF "TIME TO NO_2 PEAK" TO PARAMETER VARIATIONS FOR THE PROPYLENE-NO_x SYSTEM

Those Changes Causing Greatest Delay in Time to NO_2 Peak

Parameter Change	T
k_{13} - 50%	260
k_1 - 50%	250
k_2 + 50%	194
$(NO_2)_0$ - 50%	164
k_3 - 50%	142
k_{15} + 50%	134

Those Changes Causing Greatest Reduction in Time to NO_2 Peak

Parameter Change	T
k_2 - 50%	66
k_{13} + 50%	88
$(NO_2)_0$ + 50%	112
k_1 + 25%	114
k_3 + 50%	124
k_{16} - 50%	128

No Effect $k_{14} \pm 50$

k_{16} + 50

k_{17} - 50

* Changes and ordering about the same as for toluene, with exception of k_{16}, which is less sensitive for propylene

TABLE 9. RANK ORDER OF PARAMETERS: SENSITIVITY OF "ASYMPTOTIC OZONE CONCENTRATION, OR OZONE CONCENTRATION AT 400 MINUTES", TO PARAMETER VARIATIONS FOR THE PROPYLENE-NO_x SYSTEM

Those Changes Causing Greatest Increase in O_3 Levels (Maximum or at 400 Min., Whichever is Greatest)

Parameter Change	T
k_2 - 50%	>.58
k_1 + 25%	.51
$(NO_2)_o$ + 50%	.49
k_3 - 50%	.48
k_{14} - 50%	.48
k_{16} + 50%	.48
k_{17} - 50%	.48

Those Changes Causing Greatest Decrease in O_3 Levels*

k_{13} - 50%	.24
k_1 - 50%	.25
k_{15} + 50%	.30
k_2 + 50%	.36
k_{16} - 50%	.46
k_{17} + 50%	.46
$(NO_2)_0$ - 50%	.46

No Effect k_3 + 50%

k_{14} + 50%

* Effects about the same as for toluene, except that, for propylene system, k_{15} - 50% causes greater reduction in O_3 than k_1 - 50%. The effect occurs, however, because NO_2 peak has been delayed.

Details of the methods employed can be found in Appendix A.

The measure of sensitivity employed for the digital studies was the "root sum square" criterion, equation (2), which can be expressed in the expanded form,

$$K_j = \left[\sum_{i=1}^{11} \int_0^t (y_i^B(t) - y_{ij}^V(t))^2 \, dt \right]^{1/2}$$

where y_i^B = predicted concentration of the i^{th} species using base values of parameters

y_i^V = predicted concentration of i^{th} species using base values of all parameters, except one. This parameter was varied 1% in magnitude.

t = time at which simulation was terminated

j = index of parameter that was varied

The summation is carried out over the integrated, squared, predicted differences for 11 species--NO, NO_2, O_3, HC, HC_2, RO_2, OH, O, HNO_2, NO_3, and HO_2. The results of the analysis are shown in Table 10. As we noted in the introduction this measure of sensitivity would have been of greater significance if all the chemical constituents had been determined experimentally. During the experiments only NO, NO_2, O_3, and HC were monitored. Comparison of these results (Table 10) with those in Tables 4 and 5, however, shows that the resultant "rank-ordering" of the digital and analog sensitivity methods agree.

TABLE 10. Results of Limited Sensitivity Study Carried Out On the Digital Computer for the Toluene-NO_x System

Reaction Rate Constant*	$k_j K_j$**
k_1	1.46
k_{16}	0.271
k_3	0.256
k_4	0.144

* In *decreasing* order of sensitivity

** K_j is defined in text. The criterion $K_j k_j$ is derived from $K_j \times (k_j^B - k_j^V)$, where $k_j^B - k_j^V = .01 k_j^B \simeq .01 k_j$. Thus, the tabulated values are $.01 k_j K_j \times 10^2$, or $k_j K_j$.

C. Conclusions

In the analysis of the HS mechanism that we have described, we found the concentration predictions to be most sensitive to changes in the same rate constants and stoichiometric coefficients, where T and M have been employed as decision variables. These input parameters are k_1, k_2, k_{13}, α, β, and ε. The only major difference in behavior observed between the two systems is that variations in the rate of the ozone-hydrocarbon reaction (reaction 15) affect the ozone concentrations predicted for the propylene system, but not for the toluene system. This, of course, reflects the fact that ozone does not react with aromatics at a significant rate; hence, changes in k_{15} for this system have virtually no effect. Nevertheless, individual variations in each of the input parameters results in some observable change in the concentration-time profiles for at least one of the hydrocarbon-NO_x systems. As a result, one may conclude that the HS mechanism cannot be made more compact without having a deleterious effect on the quality of description.

The fact that several parameters are "sensitive" does not imply that predictions of the mechanism are necessarily uncertain. Nor is the uncertainty in prediction related in a simple manner to the completeness of the kinetic representation or to the accuracy with which input parameters are known. Rather, it is uncertainty in sensitive parameters or, for that matter, in the mechanism itself which results in uncertain predictions. Thus, the uncertainty in prediction associated with one of the sensitive rate constants, k_2, is very low because good agreement

exists among the many experimental determinations of the rate constant, and the stoichiometry of the elementary reaction is well known. As for the other parameters, the following recommendations can be made. Careful measurement of the light intensity in future studies will substantially reduce the uncertainty associated with k_1. The magnitudes of the stoichiometric coefficients and k_{13}, however, have been established by means of model fitting procedures, as there is no *a priori* technique presently available for determining these parameters. Rather, their magnitudes must, in the future, be based on values established in successfully completed validation studies. Thus, the uncertainty in k_{13}, α, β, and ε will decrease as the number of different systems for which successful validation studies are carried out increases. While parameter estimation, as opposed to parameter determination, is not particularly desirable, it is a necessary consequence of adopting a compact, generalized mechanism.

Finally, we might note that, despite the high probability that the new kinetic mechanism (Chapter V) alluded to in the introduction will prove to be more reliable a predictor, the sensitivity study performed here using the HS mechanism is still of value for the following reasons:

- Both mechanisms contain the same skeleton of important elementary reactions, so that "patterns of sensitivity" in the HS mechanism may well be similar to patterns of sensitivity observed using the larger mechanism.
- In addition to characterizing patterns of sensitivity, we have been able to identify several parameters for which it is important to reduce uncertainties in the future both in and through experimental studies.

For example, in reviewing the plans for the U.C. Riverside chamber studies that were initiated this summer, we have been guided by the results of the sensitivity studies in suggesting that emphasis be placed on accurate determination of both k_i, and the initial NO_2 concentration, parameters that in the past have not been controlled with precision. Moreover, we have recommended to the staff of CPL that work be supported that would lead to more accurate determination of the sensitive rate constants including that for the RO_2-NO reaction.

In summary, then, while the sensitivity studies that we carried out are surely not of long range or lasting value, they have provided both information and insights that have been of use. Furthermore, the techniques explored in this work will prove to be of considerably greater use when they are applied in a future study of the new, expanded mechanism.

III. PLANNING OF OUTDOOR CHAMBER EXPERIMENTS

A novel type of smog chamber has recently been constructed out-of-doors in a rural community near Research Triangle Park, North Carolina. This structure, an A-frame covered with transparent Teflon film, is divided by a membrane into two 6,000 cubic foot reactors. In carrying out an experiment, these reactors are filled with ambient air (the pollutant content of which is typically quite low) and charged with varying amounts of hydrocarbons and NO_x. Chemical reactions are then allowed to proceed under conditions of natural sunlight, temperature, and humidity. The initial concentrations of reactants for these experiments are chosen so as to demonstrate the changes in "air quality" which may result from various pollution control strategies presently under consideration.

We have participated in the planning of these experiments through the simulation of the proposed chamber runs using the simplified HS mechanism (Table 1). At the request of Dr. B. Dimitriades of EPA and Dr. H. Jeffries of UNC, we undertook the following calculations.

(i) computed maximum oxidant as a function of initial NO_x for constant initial hydrocarbon at 0.1, 0.5, 1.0, 2.5, and 5.0 ppm. The range of NO_x concentrations is 0 to 1 ppm.

(ii) determined the effect of variations in light intensity on maximum NO_2 and O_3 and on dosage* of both for five light intensity profiles. This calculation was carried

---

* All dosage calculations were based on an irradiation time of 1000 minutes.

out over a wide range of ambient temperature levels for four pairs of initial conditions for HC and NO_x.

(iii) determined the effect of temperature on maximum NO_2 and O_3 and on dosage* of both. This calculation was carried out over a wide range of ambient temperature levels for four pairs of initial conditions for HC and NO_x.

We selected toluene as a surrogate for the atmospheric mixture for the purposes of this calculation because, of the various hydrocarbons for which we have carried out validation studies, it has a reactivity most similar to that of the observed hydrocarbon mix in the atmosphere. While we are aware that the HS mechanism may provide uncertain predictions for reactant systems for which evaluative studies have not been undertaken, our success in validating the toluene-NO_x system for a large variety of initial conditions lends a reasonable degree of credence to the predictions of the mechanism for this particular system. In this chapter we report the results of each of these three tasks using the toluene-NO_x system as a model of the atmospheric hydrocarbon mixture.

A. Effect of Initial NO_x Concentration on Maximum Oxidant

The purpose of this calculation was to generate plots of maximum oxidant as a function of initial NO_x for fixed hydrocarbon levels. The rate constants determined for toluene in previous validations were used in generating the required predictions. The input parameters for these simulations are shown in Table 2. In addition, a dilution rate of 5.4 liters/second, necessitated by the sampling procedure, was assumed. In order to minimize computer time and decrease the probability of numerical instabilities, the free radical equi-

*All dosage calculations were based on an irradiation time of 1000 minutes.

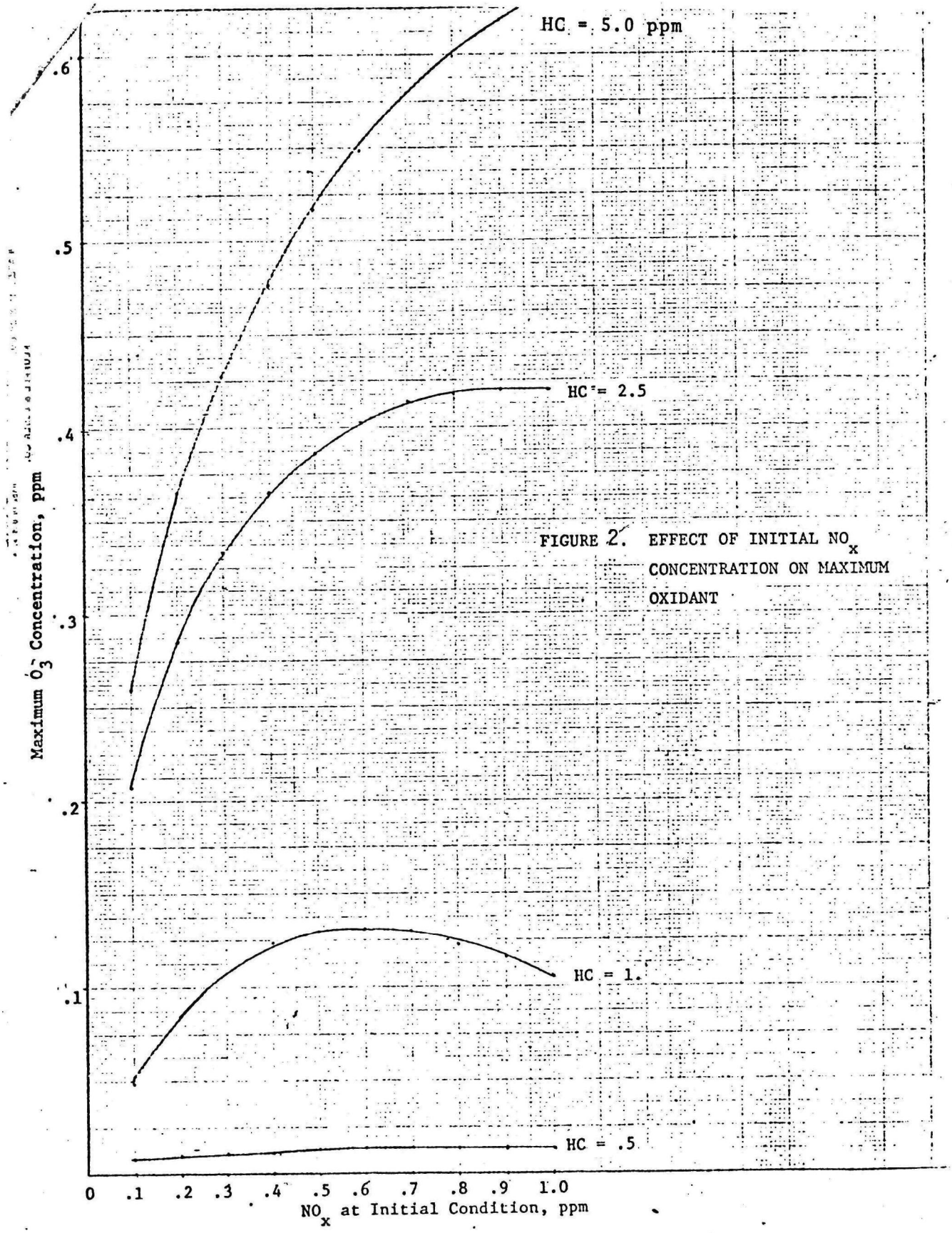

FIGURE 2. EFFECT OF INITIAL NO_x CONCENTRATION ON MAXIMUM OXIDANT

Figure 2 Continued....

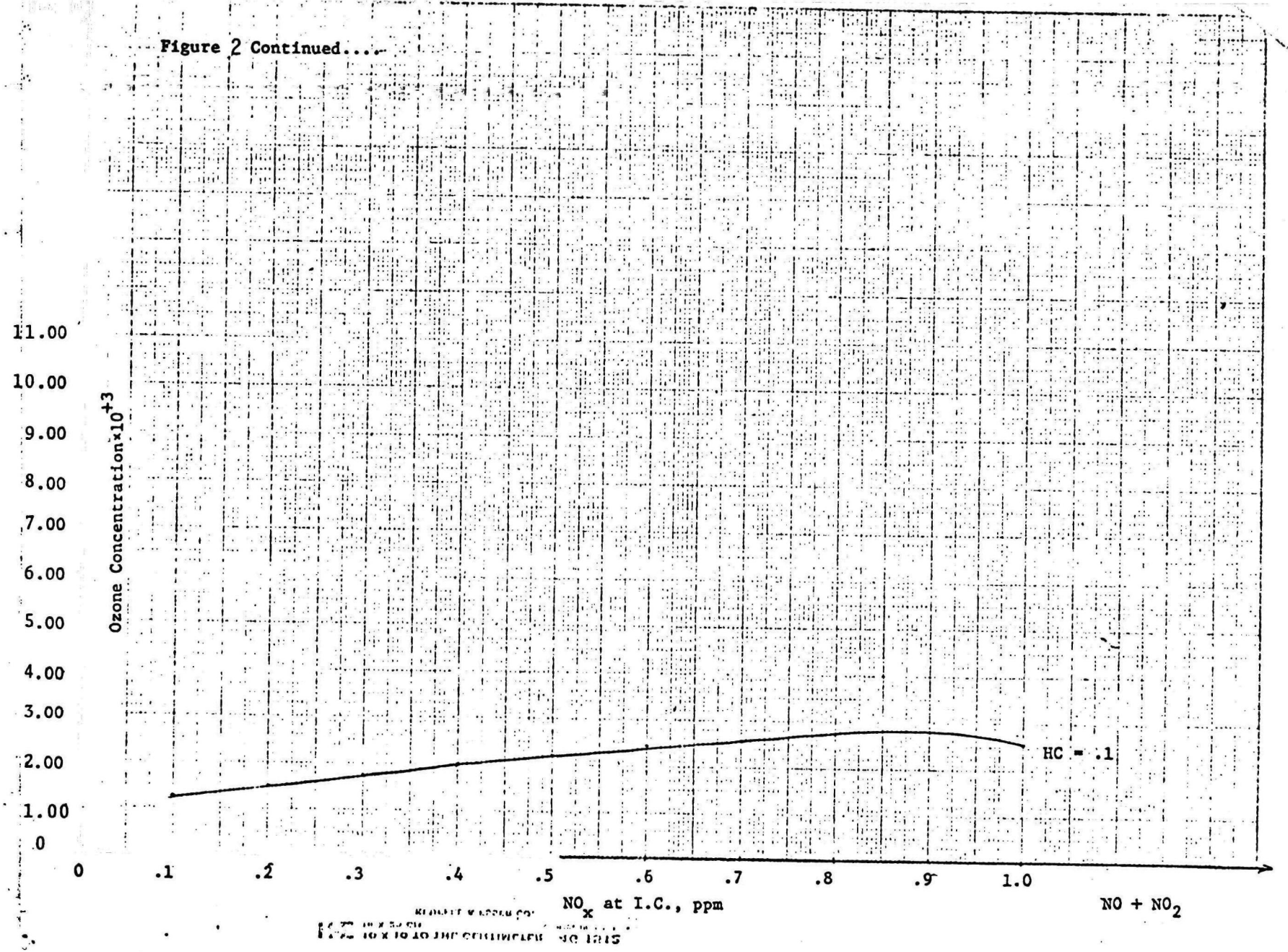

librium assumption was made. Invocation of this assumption reduces the number of differential equations to be integrated from eleven to four.

The results of 50 executions of the model are plotted on Figure 2. In this figure, the maximum ozone concentrations over a six hour integration period is plotted versus initial NO_x concentration. The initial NO_x concentration is fixed at a NO/NO_2 ratio 13.7/1.0 and varies from 0 to 1.0 ppm. A family of five curves representing constant initial hydrocarbon concentrations are plotted. It is evident that negligible O_3 is generated when the initial HC is less than 0.1 ppm. However, as the initial HC level increases to approximately 0.5 ppm, the oxidant level becomes measurable, although it still does not show a great dependency on initial NO_x concentration. At and above an initial HC concentration of 1.0 ppm, however, the maximum ozone level displays marked dependency on initial NO_x concentration, first increasing with increasing NO_x, then going through a maximum, and finally decreasing as the NO_x is increased still further.

B. Effect of Diurnal Light Intensity Variations on NO_2 and O_3 Maximums and Dosages.

The objective of this task was to investigate the effect of varying light intersities on the maximum values of NO_2 and O_3, and on their respective dosages, for both summer and winter conditions. To simulate the effect of the diurnal variation of light intensity on the reaction

$$NO_2 + h\nu \xrightarrow{k_1} NO + O ,$$

it was assumed the k_1 is related to time, t, in the following manner (see Leighton (1961), p. 163):

$$k_1 = a_i \cdot f_s \qquad \text{Summer}$$

$$k_1 = a_i \cdot f_w \qquad \text{Winter}$$

where $f_s = 1.0 - 0.694\tau^2$ and is ≥ 0.0 for all τ

$f_w = 0.774 - 1.07\tau^2$ and is ≥ 0.0 for all τ

and

$$\tau = \frac{t - 12}{6}; \quad 0 \leq t \leq 24$$

Note that t is in units of hours past midnight. The peak light intensity occurs at 12:00 hours and the ratio of the peak winter intensity to peak summer intensity of 0.774/1.000, as given in Leighton. We carried out diurnal light intensity simulations for three values of the coefficient a_i for both summer and winter conditions as given in the first column to Table 11. These values correspond roughly to high average, and low sunlight intensity conditions which might occur at noon on clear days at about the time of the summer solstice, the vernal and autumnal equinoxes, and the winter solstice, respectively, at the latitude of North Carolina.

The simplified mechanism was modified to include variations of k_1

TABLE 11. EFFECT OF DIURNAL LIGHT INTENSITY VARIATIONS ON THE HS REACTION MODEL

	a_1	HC	NO_x	O_3 max	NO_2 max	O_3 dosage	NO_2 dosage
	.37	2.0	.5	.34914	.31393	100.833	165.597
	.37	.8	.35	.2435	.2467	36.819	132.27
	.37	.5	.35	.0358	.1416	8.3486	
	.37	.24	.35	.007027	.07358	3.4108	54.102
	.266	.5	.35	.00378	.05687	2.585	56.744
	.266	3.	.5	.34171	.31485	233.915	136.702
SUMMER							
	.166	.24	.35	.001912	.05373	.8112	38.542
	.166	.5	.35	.00895	.12571	2.3651	81.216
	.166	.8	.35	.00567	.10993	1.936	69.601
	.286	.24	.35	.00318	.05454	1.189	39.494
	.286	.5	.35	.00561	.10518	1.900	51.193
	.286	.8	.35	.0551	.1620	6.981	74.336
	.286	1.	.5	.08795	.2453	17.986	126.229
WINTER							
	.206	.5	.35	.00351	.0778	1.69	57.928
	.206	3.	.5	.2189	.2722	44.816	136.633
	.128	.24	.35	.00112	.0412	.722	48.827
	.128	.5	.35	.001974	.0837	.916	56.372
	.128	.8	.35	.00295	.1109	1.034	57.057

with time, as described by the expressions for k_1 for summer and winter given earlier. The observed O_3 and NO_2 maxima and dosages for six values of a_i (three each for summer and winter) and for several sets of initial conditions for toluene and NO_x are reported in Table 11. In general, the magnitudes of each of the four responses decreased as light intensity (a_1) decreased. An exception to this behavior, however, was an increase in the NO_2 dosage with decreasing light intensity for hydrocarbon to NO_x ratios below 1.5. This behavior results from a reduced rate of oxidation of NO as a result of low ambient hydrocarbon concentrations and from a reduced rate of conversion of NO_2 to products.

C. Effect of Temperature Variations on NO_2 and O_3 Maxima and Dosages

Most of the reactions contributing to smog formation are thermal rather than photolytic. Because the rates of thermal reactions depend on the temperature of the reaction system, it is reasonable to expect that variations in temperature will result in a change in the rate at which smog forms. In the HS mechanism, for example, all the reactions except the first and ninth (photolysis of NO_2 and HNO_2, respectively) are thermal.

In this task it was our goal to evaluate the effects of temperature variations on selected responses, notably NO_2 and ozone maxima and dosages. To evaluate the effect of changes in temperature on the predictions of the HS mechanism, one must first determine the activation energy (E_A) or thermal dependency of each reaction. The activation energies for several of the reactions in the HS mechanism have been determined experimentally (Johnston et al., 1970), and we have used these values wherever possible. For those

cases in which no experimentally determined value of E_A is available, we either estimated or approximated the activation energy by analogy with similar reactions for which activation energies have been measured. The activation energies which we used for the temperature varying calculations are presented in Table 12. In view of uncertainties in the mechanism and our estimates of unmeasured activation energies, the results which follow probably have an uncertainty of about ±50%.

The temperature range considered in our study was 264°K to 315°K. This range spans the majority of temperature conditions which might be encountered during the year-round operation of the outdoor chamber in North Carolina. The temperature effects were studied for four sets of initial reactant concentrations:

Toluene (ppm)	NO_x (ppm)
1) 0.6	0.35
2) 0.8	0.35
3) 1.0	0.50
4) 1.7	0.50

In Table 13 we present the NO_2 and O_3 maxima and dosages for each of these cases.

In surveying the results of the simulations, we observed the following general trends:

(i) As the temperature increases, the peak NO_2 concentration increases. The effect of changes

TABLE 12: ACTIVATION ENERGIES OF THE REACTIONS IN THE HS MECHANISM

REACTION	E(kcal/mole)
1	0
2	-2.1
3	2.5
4	7.0
5	-
6	0
7	0 (est.)
8	-
9	0
10	1.08
11	1.0 (est.)
12	8.0 (approx.)
13	3.0 (approx.)
14	8.0 (approx.)
15	1.0 (approx.)
16	0
17	0

Source of activation energies: Project Clean Air

TABLE 13: EFFECT OF CHANGES IN TEMPERATURE ON NO_2 AND O_3 CONCENTRATIONS

SYSTEM	TEMP.	O_3 PEAK (ppm)	NO_2 PEAK (ppm)	O_3 DOSAGE* (ppm min)	NO_2 DOSAGE* (ppm min)
$(NO_x)_o$ = 0.35 ppm	264°K	0.018	0.092	10.5	87.7
	279°K	0.047	0.144	29.0	175.7
	288°K	0.075	0.171	40.9	172.3
$(Toluene)_o$ = 0.6 ppm	301°K	0.095	0.201	90.0	234.6
	311°K	0.100	0.219	113.73	217.5
$(NO_x)_o$ = 0.35 ppm	273°K	0.076	0.156	25.6	121.6
	290°K	0.131	0.203	113.9	246.5
$(Toluene)_o$ = 0.80 ppm	305°K	0.143	0.231	121.1	160.6
	315°K	0.145	0.244	125.5	126.3
$(NO_x)_o$ = 0.5 ppm	273°K	0.140	0.266	54.6	211.9
	290°K	0.174	0.321	143.7	276.4
$(Toluene)_o$ = 1.0 ppm	305°K	0.180	0.353	153.3	187.9
	315°K	0.177	0.368	141.5	141.5
$(NO_x)_o$ = 0.5 ppm	264°K	0.251	0.295	170.5	310.7
	279°K	0.296	0.343	230.2	234.7
$(Toluene)_o$ = 1.7 ppm	288°K	0.303	0.362	248.5	185.6
	301°K	0.298	0.382	286.4	125.1
	311°K	0.288	0.394	350.6	94.96

*Dosage calculated over a 1000 minute simulation.

in temperature on the peak NO_2 concentration is proportionately greater at lower temperatures than at higher temperatures.

(ii) The NO_2 dosage goes through a maximum; the temperature at which the maximum occurs depends on the HC/NO_x ratio.

(iii) The peak O_3 concentration increases sharply when the temperature is raised form 264^oK to 290^oK. Further increases in the temperature however, have little effect on the peak concentration.

(iv) The O_3 dosage also increases substantially when the temperature is raised from 264^oK to 290^oK. But, as is the case of the peak ozone concentration, further increases in temperature affect the ozone dosage only slightly.

These results suggest that extreme caution must be exercised in interpreting and comparing the results of smog chamber experiments performed under different temperature conditions, especially for the range, 264^oK to 290^oK.

D. Conclusions

Using the simplified mechanism we have demonstrated that, for toluene (a surrogate for the atmospheric hydrocarbon mixutre), variations in light intensity and temperature substantially influence the predicted NO_2 and O_3 maxima

and dosages. We have also shown that the predicted maximum ozone level is quite sensitive to the initial hydrocarbon concentration--much more so than to the initial NO_x concentration. Finally, while influences on the NO_2 and O_3 maxima and dosages due to variations in light intensity and temperature are not at all unexpected, the calculations presented here suggest the magnitudes of the changes that might be expected.

The study of smog formation in an outdoor chamber results in some obvious disadvantages, namely lack of control over light intensity, temperature, and humidity. With these three parameters uncontrolled, it is not possible to truly replicate experiments. If, however, the non-linear changes in the concentration-time behaviors of the pollutants resulting from variations in these three parameters can be properly accounted for, it may still be possible to compare runs which are otherwise identical (i.e. same initial concentrations, etc.). One means of analyzing the data is to program the observed diurnal temperature and light intensity profiles into a kinetic mechanism, comparing the predicted profiles for the "replicate" runs with those profiles which were observed in the experiments. Such an approach may still be inadequate in the sense that variations in other experimentally undetermined parameters may subsequently be shown to be important. But, without some type of mathematical analyses, no quantitative evaluation of the reproducibility of the outdoor chamber experiments will be possible.

IV. PREPARATION OF A RECOMMENDATIONS REPORT, "EXISTING NEEDS IN THE OBSERVATIONAL STUDY OF ATMOSPHERIC CHEMICAL REACTIONS"

A great many experimental and observational programs have been carried out over the years in an effort to increase our knowledge of atmospheric chemical reactions. Carefully conceived laboratory experiments have provided the basis for estimation of individual rate constants. Smog chambers studies have served as an important aid in establishing a qualitative understanding of the overall smog formation process. Atmospheric observations have also proven valuable in this respect and, in addition, in the identification of pollutant species. Within the last four years, however, advances in the development of mathematical descriptions of the photochemical reaction process have created a need for refined experimental and observational programs, programs geared to yielding information either of much greater accuracy than seemed necessary five or ten years ago or of a type or kind that has rarely been collected in the past.

Two major "breakthroughs" have spurred the interest in increasingly complex and sophisticated experimentation in the field of atmospheric chemistry--

- the development of photochemical kinetics mechanisms capable of describing the concentration-time behavior of major reactants and products, as monitored in a smog chamber. While the comparisons between prediction and

observation have often been good for experiments having a variety of initial conditions, the hydrocarbon reactant has generally been a single species or binary mixture.

- the development of mathematical models capable of predicting the concentrations of photochemical pollutants as a functions of location and time over a region of the order of two to five thousand square miles (i.e., a major metropolitan airshed). The spatial resolution of such models is typically of the order of one to two miles.

While development of both types of models has proceeded rather smoothly and swiftly over the past three years, it became apparent at an early stage that *there presently exists no data base of sufficient accuracy and detail to properly support model validation studies*. As a part of this contract effort we have prepared a separate report, "Existing Needs in the Experimental and Observational Study of Atmospheric Chemical Reactions", in which we made detailed recommendations for data collection programs that might be carried out in order to meet a broad spectrum of needs.

But the collection of data for model validation purposes alone suggests a rather narrow horizon. We see as a primary value of model development the codification of knowledge in the field of study, the "pulling together" of the many bits and pieces in an attempt to gain

an expanded understanding of the whole. When viewed in this way, the mounting of an experimental program with a model, models, or modeling as the structural foundation for the pursuit is a major step forward--from gaining knowledge in a piecemeal fashion (and understanding often with long delays) to gaining knowledge efficiently, in quantity, and in a coordinated manner.* It is the purpose of the recommendations report to discuss future needs in the measurement and observation of atmospheric reaction processes with the broader perspective--with the unifying element of the mathematical model, our best descriptor of the dynamic processes that we are attempting to understand.

If we are to deal with the subject of atmospheric reactions in a unified manner, it is necessary to discuss mathematical modeling at an early stage. In Chapter II of the report, we examine the nature of the photochemical mechanism (i.e., its mathematical structure, the degree of detail it incorporates, etc.) and present a short history of model development. We then discuss the need for lumping of hydrocarbon and radical species and suggest a mechanism (presently being subjected to verification--see Chapter 5 of this report) that has strong potential

---

* The notion of *coordinating* all elements of an experimental and observational program is of great importance. For example, if the concentration-time predictions of a validated kinetic mechanism are relatively insensitive to the magnitude of a particular rate constant, there is little point in expending effort to improve the accuracy of its estimated value. Science is better served by concentrating efforts in areas in which an increase in knowledge pays a greater reward. The model serves admirably as a tool for identifying such efforts.

for accurately describing the concentration-time behavior of all measurable species (except, of course, those that are lumped). Model assumptions are carefully stated and the validation procedure is described. Finally, we outline the alterations that must be made in any kinetic mechanism if it is to be incorporated into an urban airshed model.

In Chapter III, we present a full discussion of the two major classes of urban airshed models--the Eulerian and the Langrangian. Fundamental equations are presented and applied forms of the equations are derived so that the assumptions on which the latter are based can be clearly discerned. The two commonly applied types of models--the grid and the trajectory--are detailed, and their advantages and shortcomings are discussed. Levels of uncertainty associated with input variables to these models--emissions and meteorological--are presented. The chapter concludes with a section summarizing possible avenues of pursuit for improving the present generation of models.

The remaining three chapters, IV, V, and VI, are, in many ways, the core of the report. They deal, respectively, with laboratory studies concerned with the kinetics and mechanisms of individual reactions, smog chamber studies, and atmospheric observations. In each, we discuss existing deficiencies in knowledge, examine in detail

the types of studies needed, and recommend specific studies and/or general programs. Thus, these three chapters, taken as a whole, constitute a comprehensive review, analysis, and diagnosis of needs in experimentation and observation of the atmospheric chemistry of contaminants.

V. DEVELOPMENT OF AN IMPROVED GENERAL KINETIC MECHANISM

In the two years since simplified mechanisms such as that of Hecht and Seinfeld (1972) (Table 1) were developed, signficant advances have been made in our knowledge of the mechanisms and rate constants of the individual reactions contributing to smog formation. These advances have set the stage for the development of a new kinetic mechanism, one which does not suffer many of the deficiencies of the three existing mechanisms. In particular, a new mechanism should be rigorous in its treatment of inorganic reactions (because of their importance), sufficiently detailed to distinguish between the reactions of various classes of hydrocarbons and free radicals, free of poorly defined adjustable parameters, and as compact as possible. In Chapter II of the recommendations report, "Existing Needs in the Experimental and Observational Study of Atmospheric Chemical Reactions", we have presented a new formulation which meets the requirements; it is restated in Table 14.

TABLE 14

A Lumped Kinetic Mechanism for Photochemical Smog

$NO_2 + h\nu \xrightarrow{1} NO + O$	The NO_2-NO-O_3 Cycle
$O + O_2 + M \xrightarrow{2} O_3 + M$	
$O_3 + NO \xrightarrow{3} NO_2 + O_2$	
$O + NO + M \xrightarrow{4} NO_2 + M$	Important Reactions of O with Inorganic Species
$O + NO_2 \xrightarrow{5} NO + O_2$	
$O + NO_2 + M \xrightarrow{6} NO_3 + M$	
$O_3 + NO_2 \xrightarrow{7} NO_3 + O_2$	The Chemistry of NO_3, N_2O_5, and HNO_3
$NO_3 + NO \xrightarrow{8} 2NO_2$	
$NO_3 + NO_2 \xrightarrow{9} N_2O_5$	
$N_2O_5 \xrightarrow{10} NO_2 + NO_3$	
$N_2O_5 + H_2O \xrightarrow{11} 2HNO_3$	
$NO + HNO_3 \xrightarrow{12} HNO_2 + NO_2$	Reactions of HNO_3 with Inorganic Species
$HNO_2 + HNO_3 \xrightarrow{13} H_2O + 2NO_2$	
$NO + NO_2 + H_2O \xrightarrow{14} 2HNO_2$	Chemistry of HNO_2
$2HNO_2 \xrightarrow{15} NO + NO_2 + H_2O$	
$HNO_2 + h\nu \xrightarrow{16} OH + NO$	

TABLE 14 (Continued)

$OH + NO_2 \xrightarrow{17} HNO_3$	}	Important Reactions of OH with Inorganic Species
$OH + NO + M \xrightarrow{18} HNO_2 + M$		
$OH + CO + (O_2) \xrightarrow{19} CO_2 + HO_2$		
$HO_2 + NO \xrightarrow{20} OH + NO_2$	}	Oxidation of NO by HO_2
$H_2O_2 + h\nu \xrightarrow{21} 2OH$	}	Photolysis of H_2O_2
$HC_1 + O \xrightarrow{22} ROO + \alpha RCOO + (1-\alpha)HO_2$ (RCOO: O)	}	Hydrocarbon Oxidation Reactions Where HC_1 = olefins, HC_2 = aromatics, HC_3 = paraffins, HC_4 = aldehydes
$HC_1 + O_3 \xrightarrow{23} RCOO + RO + HC_4$ (RCOO: O)		
$HC_1 + OH \xrightarrow{24} ROO + HC_4$		
$HC_2 + O \xrightarrow{25} ROO + OH$		
$HC_2 + OH \xrightarrow{26} ROO + H_2O$		
$HC_3 + O \xrightarrow{27} ROO + OH$		
$HC_3 + OH \xrightarrow{28} ROO + H_2O$		
$HC_4 + h\nu \xrightarrow{29} \beta ROO + (2-\beta)HO_2$		
$HC_4 + OH \xrightarrow{30} \beta RCOO + (1-\beta)HO_2 + H_2O$ (RCOO: O)		
$ROO + NO \xrightarrow{31} RO + NO_2$	}	Reactions of Organic Free Radicals with NO, NO_2, and O_2
$RCOO + NO + (O_2) \xrightarrow{32} ROO + NO_2 + CO_2$ (RCOO: O)		
$RCOO + NO_2 \xrightarrow{33} RCOONO_2$ (RCOO: O)		
$RO + O_2 \xrightarrow{34} HO_2 + HC_4$		

TABLE 14 (Continued)

$RO + NO_2 \xrightarrow{35} RONO_2$	
$RO + NO \xrightarrow{36} RONO$	
$HO_2 + HO_2 \xrightarrow{37} H_2O_2 + O_2$	Peroxy Radical Recombination Reactions
$HO_2 + ROO \xrightarrow{38} ROOH + O_2$	
$2ROO \xrightarrow{39} ROOR + O_2$	

There are two points to be noted regarding this mechanism. First, the unspecified stoichiometric parameters, α and β, can now be estimated a priori with a high degree of confidence. α is the fraction of carbons attached to the double bond in a mono-olefin which are not terminal carbons on the chain. Consider, for example, the O-HC_1 reaction for propylene and 2-butene which contain, respectively, external and internal double bonds.

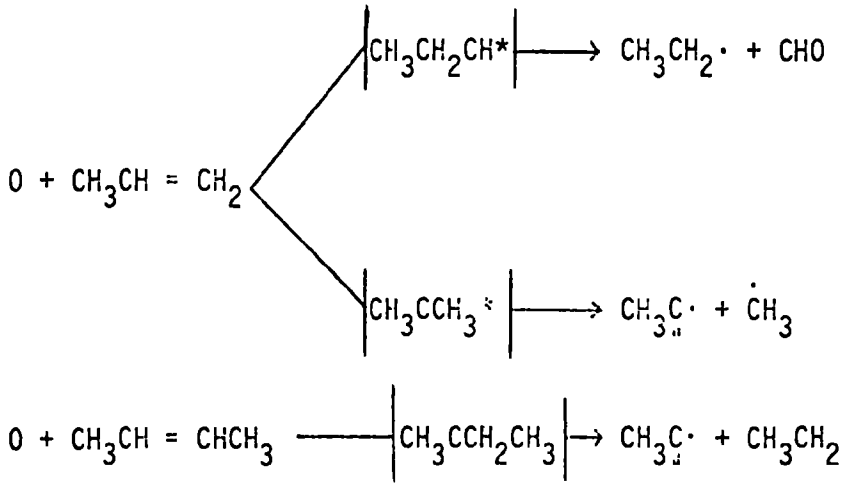

If we assume that allyl and acyl radicals react rapidly with O_2 and that the CHO decomposes into $CO + HO_2$ in the presence of O_2, these reactions can be rewritten in our generalized notation as

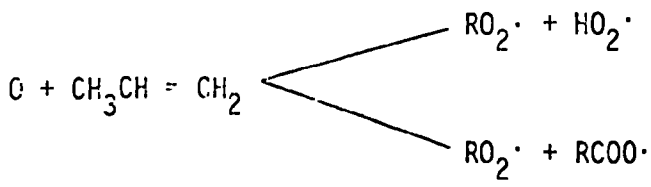

and

If we now further assume that O will react with equal probability at either carbon attached to the double bond, $\alpha = 1/2$ for propylene and $\alpha = 1$ for 2-butene. By the same reasoning α can be shown to be zero for ethylene.

β is the fraction of total aldehydes which are not formaldehyde. During smog chamber studies of the propylene-NO_x system, equal quantities of formaldehyde and higher aldehydes are observed to form; thus, $\beta = 1/2$. In the case of toluene, Altshuller et al. (1970) have observed that only 15% of the aldehydes are formaldehyde; therefore, $\beta = .85$ in this case.

Second, as in earlier studies, we have exercised care in selecting those species whose concentration-time (c-t) behavior is to be described by a differential equation and those whose c-t behavior is to be described by algebraic equations. The most complete mathematical representation of the kinetics of this mechanism would be a description of the time-varying behavior of each reactant and product (exclusive of O_2, CO_2, and H_2O, which are not followed) with a differential equation. But because the computing time required to integrate the governing equations numerically increases at a rate proportional to the square of the number of differential equations*, we are interested

---

* We have used the technique of Gear (1971) to solve the system of coupled differential equations.

in minimizing that number. One way of accomplishing this is to apply the steady-state approximation for those species which reach their equilibrium concentrations on a time scale short relative to that of the majority of reactants and products. Mathematically, this means that the concentration-time behavior of those species assumed to be in steady-state is described by an algebraic rather than a differential equation.

In our validation experiments we have assumed four species to be in pseudo steady-state: O, OH, RO and NO_3. The validity of this approximation for the first three species has been established by comparing the concentrations predicted when the approximation is invoked to those predicted when the species are represented by differential equations. We have found in these comparisons that agreement is excellent, maximum discrepancies in concentration being on the order of 0.01% over a 400 minute simulation. This test shows conclusively that the steady-state approximation is accurate for O, OH, and RO. When we tried to perform an identical test for NO_3, we found that the concentration predicted by a differential equation was negative at startup**. Thus, a meaningful test as to the validity of the steady-state approximation could not be made. We

---

** This reflects the fact that NO_3 forms chiefly after the NO_2 peak by reaction 7. As there is no O_3 present initially, numerical roundoff error at the first time step results in negative NO_3 concentrations.

are, however, reasonably confident that the approximation is "good" in this case as well.

In this chapter we devote our attention to a discussion of the first phase of an evaluation study of the 39-step mechanism. For this portion of the validation program we have used smog chamber data obtained by the Division of Chemistry and Physics of EPA; we begin, then, with a description of the data base and sources of experimental uncertainty. Next, we present validation results for the mechanism using data from three different hydrocarbon-NO_x systems: n-butane-NO_x, propylene-NO_x, and n-butane-propylene-NO_x. We conclude with a discussion of the results, including predictions of the effect of initial hydrocarbon and NO_x reactant concentrations on peak ozone formation.

A. The Data Base and Sources of Experimental Uncertainty

The significance of the validation results for a kinetic mechanism is to a large degree dependent upon the diversity and reliability of the experimental data base. We were fortunate in being able to obtain chamber runs for this study involving both low and high reactivity hydrocarbons, as well as a simple mixture. Moreover, the ratio of HC/NO_x was varied over a wide range for each reactant system. In this section we describe the data base provided by the Division of Chemistry and Physics of the Environmental Protection Agency (EPA) for validation purposes. We examine in some detail the importance of accurately specifying certain experimental variables, notably light intensity and water vapor concentration. We discuss the degree to which wall effects may influence observed chamber results. Finally, we comment on the accuracy and specificity of the analytical instrumentation used to monitor pollutant concentrations and on the reproducibility of the experiments.

1. Data Base

The data base used in this validation study is that supplied by the Division of Chemistry and Physics of EPA. It is comprised of three hydrocarbon-NO_x systems:

(i) n-Butane-NO_x at three different HC/NO_x ratios

(ii) Propylene-NO_x at four different HC/NO_x ratios

(iii) n-Butane-Propylene-NO_x at six different HC/NO_x ratios

All but two of the chamber runs were made between February and May of 1967 by the staff of the Chemical and Physical Research and Development Program at the National Center for Air Pollution Control in Cincinnati, Ohio (Altshuller et al., 1967,1969; Bufalini et al., 1971). The remaining two runs (457 and 459) were carried out in March 1968. The initial conditions for the experiments are given in Table 15.

2. Light Intensity

Radiation intensity is one of the most important parameters in a smog chamber experiment, for it governs the photolysis rate of NO_2 (reaction 1), the reaction which initiates and sustains the smog formation process. Irradiation of the smog chamber was carried out through the use of two banks of externally mounted fluorescent lamps, 148 lamps of three different types. Under normal operation, these lamps have an expected lifetime of 1000 hours, but throughout the program they were operated at a 25% overvoltage to increase radiation intensity. Overload operation results in a more rapid deterioration of the lamps; consequently, approximately 1/7 of the lamps were replaced after every 100 hours of operation.

The average first order "rate constant" for NO_2 disappearance in nitrogen, k_d^* , was determined by the experimenters to be 0.40 min^{-1}, but was not redetermined during the ten-month period over which the

---

*It can be shown that

$$k_d \sim \frac{2k_3}{k_2(M) + k_3} k_a\phi$$

where

$k_1 = k_a\phi$

k_a = photolytic absorption rate constant (continued)

data provided to us were taken. We have assumed, in accordance with the results of Schuck et al. (1966), that k_1, the overall photolysis rate of NO_2, is equal to 2/3 k_d, or 0.266 min^{-1}. Finally, we have estimated that, due to inaccuracies in the determination of k_d, in the factor of 2/3 relating k_d to k_1, and in the estimation of irradiation intensity, k_1 has an uncertainty bound of $\pm$ 0.10 min^{-1}.

3. Water Vapor in the Chamber

Another parameter which is thought to be important in smog chamber runs is the water concentration. Water enters into the smog kinetics via reactions 11 and 14, nitric and nitrous acid production. The latter is important since photolysis of nitrous acid produces OH radicals which, in turn, initiate further reactions. The humidifier control of the inlet air stream to the chambers was set to generate 50% relative humidity at 75°F, but, during very cold, dry weather, relative humidities of only 30% were achieved. The humidity of the inlet air stream was checked only once or twice during the eleven-month study.

(Continued)

ϕ = dissociation efficiency

$$O + NO_2 + M \xrightarrow{k_2} NO_3 + M$$

$$O + NO_2 \xrightarrow{k_3} NO + O_2$$

Thus, k_d is, in essence, a lumped parameter representing the combined rates of all NO_2 reactions in an oxygen-free atmosphere. Unfortunately, the use of k_d leads to difficulties in presenting the kinetics, as the combined reaction which it represents is not first order. However, since the only available data for light intensity in these chamber experiments are based on the validity of k_d as a rate constant, we use it here to estimate k_1.

TABLE 15

Initial Conditions Associated with the Experimental Chamber Data

EPA Run	$(NO_2)_o^*$	$(NO)_o^*$	$(n\text{-Butane})_o^*$	$(Propylene)_o^*$
306**	0.03	0.30	1.60	
314	0.02	0.29	3.17	
345	0.12	1.28	3.40	
318	0.06	1.12		0.51
325	0.04	0.32		0.45
329	0.06	0.26		0.24
459	0.06	1.14		0.78
307	0.05	1.23	3.06	0.36
333	0.08	1.25	3.41	0.23
348	0.08	1.23	3.39	0.50
349	0.03	0.31	3.25	0.44
352	0.07	0.27	3.29	0.26
457	0.05	1.11	3.29	0.81

* Initial concentrations in units of parts per million (ppm)

** 0.12 ppm of aldehyde also present initially

4. Wall Effects

An effect of particular concern in smog chamber studies is the influence of surfaces on chemical dynmaics, and thus on observed reaction kinetics. Of major importance in this regard is the possibility of chemical interactions occurring between adsorbed pollutants and material in the gas phase. Although it is possible that some low reactivity organics such as carboxylic acids and ketones can be found on the walls as a result of hydrogen bonding with adsorbed water, we focus our attention in this discussion on species which have been clearly identified on the surfaces of a small smog chamber (Gay and Bufalini, 1971)--nitric acid, nitrates, and nitrites. We begin, then, by discussing the heterogeneous reactions of the most important oxides of nitrogen, NO and NO_2. In the process we also give attention to various mechanisms that might account for the appearance of HNO_3 as a product of these reactions.

a. NO and NO_2

Even in so-called dry systems it is reasonable to assume that an adsorbed layer of water will be found on the walls of the smog chamber. This is certainly the case for the experiments under consideration in this study, as the chamber was intentionally humidified during all runs. Thus one possible explanation for the appearance of nitrate and nitrite on the walls would be dissolution of NO and NO_2 in the adsorbed water layer. Nitric oxide can be eliminated in this regard because of its extremely low solubility in water; NO_2, however,

dissociates in water by the following reactions (Hill, 1971):

$$6NO_2 + 3H_2O \rightleftarrows 3HNO_3 + 3HNO_2$$

$$3HNO_2 \rightleftarrows HNO_3 + 2NO + H_2O$$

The rate of loss of NO_2 in this manner is dependent upon the amount of water adsorbed, the rate of dissolution of NO_2, and the magnitude of rate constants for the dissociation reactions. In the experiments under consideration, however, NO_2 losses via this mechanism can be neglected because, within experimental error, all of the NO_x initially present can be accounted for at the time of the NO_2 peak as NO_2, NO, and NO and NO_2 lost by sampling and dilution up to the time of the peak. We might thus conclude that no significant amounts of NO or NO_2 were lost directly to the walls during the smog chamber experiments.

b. N_2O_5

After the NO_2 peak occurs, and as O_3 begins to accumulate, N_2O_5 forms by the reactions

$$NO_2 + O_3 \rightarrow NO_3 + O_2$$

$$NO_3 + NO_2 \rightleftarrows N_2O_5$$

N_2O_5 will undergo hydrolysis to form nitric acid by the reaction

$$N_2O_5 + H_2O \rightarrow 2HNO_3$$

If the hydrolysis takes place in the adsorbed layer of water on the wall, HNO_3 will form directly on the walls. However, both the water concentrations in smog chambers (63% relative humidity (RH) at 25°C is

equivalent to 20,000 ppm H_2O) and the rate constants for the primary reactions in nitric acid formation in the gas phase (Table 6) are large enough that the loss of NO_x after the NO_2 peak may be fully ascribed to the formation of nitric acid in the gas phase.

It remains unclear, however, as to whether N_2O_5 hydrolyzes in the gas phase or on the walls. As we have noted, the water concentration during these chamber runs was quite high. As the stationary state concentration of nitric acid* would also have been high, actual HNO_3 concentrations in these experiments were always far from saturation. Thus there would have been a strong tendency for N_2O_5, whether it were found in the gas phase or on the wall, to hydrolyze rather than to decompose, forming NO_2 by the reactions

$$N_2O_5 \rightleftarrows NO_2 + NO_3$$

$$NO_3 + NO \rightarrow 2NO_2$$

However, even if these reactions were favored due to the formation of N_2O_5, the rate of formation of NO_2 would still be low since NO is depleted at this stage of the smog reactions. Thus, in light of the various considerations presented, we conclude that reactions involving N_2O_5 at the walls would have little if any effect on the course of the overall smog reactions.

---

*Leighton (1961), p. 193, calculates that the stationary state concentration of HNO_3 is 3,000 ppm for initial conditions of 0.10 NO_2, 0.10 O_3, 0.01 NO, and 63% RH at 25°C.

c. HNO_3

Nitric acid is very soluble in water because of strong hydrogen bonding. Thus, it is highly likely that a nitric acid molecule in the gas phase that is involved in a collision with the wall would dissolve. The rate of loss of HNO_3 from the gas phase, then, is probably transport-limited and will depend to some degree on the rate of stirring in the chamber. Unfortunately, detection of HNO_3 in the gas phase has until now proven to be a difficult task, perhaps because the acid is lost to the walls of the sampling tubes.

d. Other Chemical and Catalytic Effects of the Walls

It would, of course, be highly desirable to expand our understanding of the degree to which interactions occur between adsorbed pollutants and material in the gas phase. Unfortunately, our knowledge concerning such phenomena is limited, and we can only speculate. We thus offer the following comments:

(i) We expect that the rate of heterogeneous oxidation of NO in chambers is small. For example, in one chamber characterization experiment, 1.6 ppm of NO was irradiated in air for six hours. At the end of that period it was found that 19% of the initial NO had been oxidized to NO_2. We believe that this figure represents an upper limit for the rate of non-photochemical oxidation of NO. The effect would be additionally reduced in reactant systems for which the time to the NO_2 peak is relatively short (i.e., two hours or less).

(ii) As we concluded earlier, we expect that the presence or absence of wall effects would result in no detectable differences in the rate of formation of HNO_3, largely because of the strong tendency of N_2O_5 to hydrolyze at the water concentrations used during these experiments. Similarly, whether HNO_3 is formed in the gas phase, subsequently migrating to the wall, or whether it is formed directly on the wall, it is unlikely that the site of hydrolysis will have much of an effect on the observed chemistry. While nitric acid is commonly used as an oxidant when concentrated (60%) in the liquid phase (Godt and Quinn, 1956), it is ineffective as an oxidant at low concentrations. The highest attainable concentration of HNO_3 during the chamber runs is a value that is numerically equal to the initial NO_x concentration, which never exceeded 1.5 ppm.

We conclude, based on the preceding discussion, that no significant amounts of NO and NO_2 are adsorbed on the walls and that the possible adsorption of N_2O_5 and HNO_3 should not alter the observed photochemistry. However, it is not possible at this time to ascertain the degree to which the presence of surfaces might accelerate the oxidation of NO. Based on these tentative conclusions, we have not taken wall effects into account in our validation efforts.

5. Estimates of Experimental Error

Before comparing model predictions with experimental observations, it is desirable to establish both the accuracy and the precision of the measurements. Accuracy refers to the extent to which a given measurement agrees with the true but unknown value of the parameter being measured. Precision refers to the extent to which a given set of measurements agrees with the mean of the observations. Inaccuracies in determination of concentrations are largely attributable to lack of specificity or accuracy in analytical procedures, particularly in the instrumentation used to monitor concentrations during the course of an experiment. Imprecision is detected through the poor repeatability of an experiment, the results of which may or may not be accurately determined. There may be a wide variety of causes of imprecision, some of which may also be attributable to instrumentation problems.

a. The Accuracy of the Analytical Instruments

The four pollutant species of primary importance in our modeling efforts, NO_2, NO, O_3, and hydrocarbons, were all measured using standard instrumentation and techniques.

(i) Hydrocarbons were determined individually by gas chromatography: the accuracy of these measurements is estimated to be ±10% at a concentration level of 1 ppm.

(ii) Oxidants were measured using two independent techniques: the Mast Ozone Meter and neutral KI analysis. Corrections to KI readings were required to account for interferences

due to PAN and NO_2. Despite the corrections the KI measurements exceeded the Mast readings by an average of 50%. As Dr. S. L. Kopczynski (1972) of the Division of Chemistry and Physics, who was in charge of executing the smog chamber experiments used in this validation study, is of the opinion that the KI technique is the more accurate of the two procedures, we have validated our model using the results of the KI analyses.

(iii) Oxides of nitrogen were sampled manually into fritted bubblers containing Saltzman reagent. Nitric oxide was oxidized to form NO_2 by reaction with sodium dichromate. Dr. Kopczynski has estimated that this conversion is almost 100% efficient. Absorbance was read on a Beckman DU spectrometer reacing 2 ppm at full scale.

In general, the accuracy of these various measurements is a function of the concentration level of the pollutant being measured. Accuracy is poorest over the low concentration range. As most pollutants are present at low concentrations at some time during the course of a reaction, questions of accuracy will inevitably arise with regard to chamber studies. For example, at concentrations of NO_2 below 0.15 ppm, concentrations can be determined no more accurately than ±50%. At the higher concentrations encountered as the reaction proceeds, the accuracy of the reading improves substantially. Unfortunately, no recalibration of the oxidant or the nitrogen oxide

analyzers was performed during the eleven-month study.

b. The Repeatability of Experimental Runs

Because replicate runs were made for only four of the experiments used for our validation studies, we have been unable to calculate a meaningful statistical measure of the reproducibility of the experiments. But, in those few instances for which a replicate run was available, the agreement between the two sets of data was quite good. Our impression of the chamber data is that, in spite of the lack of recalibration of the light intensity and chemical analyzers, the data are in general reproducible, were carefully taken, and are as suitable as any currently available for validation purposes. Although the data were taken in 1967 and 1968, at a time prior to the development of photochemical kinetic mechanisms for atmospheric reactions, the investigators did exercise sufficient care in quantifying most of those parameters important in validation of these models. For example, dilution rates and the rate of conversion of NO to NO_2 in the absence of hydrocarbons were measured for all reactant systems. Probably the greatest weakness in the chamber data with regard to their use in validation is the lack of precise knowledge of the light intensity. As will be shown in Section D1, the magnitude of light intesity has a substantial effect upon the time to the NO_2 peak predicted by the model.

B. Evaluation of the 39-Step Lumped Mechanism

Evaluation of the lumped kinetic mechanism in Table 14 consists of

(i) obtaining estimates of the various input parameters to the mechanism--the reaction rate constants, parameterized stoichiometric coefficients α and β, initial concentration of reactants, and average dilution rate constants.

(ii) carrying out sensitivity studies for these parameters; i.e., establishing the effect of controlled variations in the magnitude of the various parameters on the concentration-time profiles for NO, NO_2, O_3, and hydrocarbon, and

(iii) generating concentration-time profiles for the various reactant mixtures using the specified initial conditions. These predictions are then compared with experimental results to assess the "goodness of fit".

In the first part of this section we discuss the basis for selection of the input parameters. In the second part, we present the validation results for each of the three hydrocarbon systems studied. Results are summarized as a series of plots displaying both predicted and measured concentrations.

1. Estimation of Parameters

Prior to obtaining kinetic information from the lumped mechanism all known parameters must be specified and uncertain parameters estimated. The input parameters to this mechanism include the rate constants, parameterized stoichiometic coefficients, initial reactant concentrations, and average loss rates of the reactants and products due to sampling.

a. The Rate Constants

While the kinetic mechanism is written in a general fashion, we have striven to formulate it in such a way that all important features of the detailed chemistry are retained. Thus, our goal has been to include each elementary reaction thought to contribute to the overall smog kinetics. A reaction has been judged unimportant only if its inclusion in the mechanism results in no significant changes in the predictions of the decision variables, namely, the rate of oxidation of NO, the time to the NO_2 peak, and the rate of accumulation and maximum levels of O_3. By virtue of the mechanism's detail we are able to use directly as input experimental determinations of the rate constants for the individual reactions in every case for which measurements have been made. [One problem associated with the adoption of simplified mechanisms (e.g., HS and EM mechanisms) was that their highly compact nature precluded strict adherence to the use of experimental values of pertinent rate constants.]

Several papers have been published in the past three years which review the vast literature dealing with kinetic studies relevant to the reactions now thought to be important in smog formation. These include the detailed modeling study of Demerjian et al. (1973), the atmospheric chemistry and physics assessment in Project Clear Air (Johnson et al., 1970), and the detailed modeling study of propylene conducted by Niki et al. (1972). Their recommended values for the rate constants of the individual reactions incorporated in the lumped

TABLE 16

Validation Values of the Rate Constants and Their Comparison with the Recommended Values of Other Investigations

Reaction	Validation* Value	Demerjian et al. (1973)	Johnston et al. (1970)	Niki et al. (1972)	Others
1	.266 min^{-1}	DEPENDS ON EXPERIMENTAL SYSTEM			
2	2.0×10^{-5} $ppm^{-2}min^{-1}$	2.0×10^{-5}	2.3×10^{-5}	2.2×10^{-5}	
3	2.3×10^{1}	2.3×10^{1}	2.9×10^{1}	2.9×10^{1}	
4	3.5×10^{-3} $ppm^{-2}min^{-1}$	3.4×10^{-3}	2.5×10^{-3}		
5	1.38×10^{4}	8.1×10^{3}	8.1×10^{3}		1.38×10^{4} †
6	2.2×10^{-3} $ppm^{-2}min^{-1}$	2.2×10^{-3}			
7	1.1×10^{-1}	$0.48\text{-}1.1\times10^{-1}$	1.1×10^{-1}	1.1×10^{-1}	
8	1.5×10^{4}	$0.66\text{-}1.47\times10^{4}$	1.5×10^{4}	1.5×10^{4}	
9	4.5×10^{3}	6.8×10^{3}	4.5×10^{3}	4.4×10^{3}	
10	1.5×10^{1} min^{-1}	1.5×10^{1}	1.4×10^{1}	1.4×10^{1}	
11	1.0×10^{-5}	2.5×10^{-3}	3.0×10^{-3}	1.5×10^{-6}	
12	1.0×10^{1}				
13	5.0				
14	4.3×10^{-6} $ppm^{-2}min^{-1}$	$\leq 4.3\times10^{-6}$	6.9×10^{-6}	3.6×10^{-8}	
15	4.5	≤ 4.5		2.8×10^{-2}	
16	1/10 k_1 min^{-1}	$1/4\times k_1$	$1/10\times k_1$	$1/2000\ k_1$	
17	1.5×10^{4}	$\geq 1.5\times10^{4}$	1.5×10^{3}	6.0×10^{3}	
18	1.2×10^{4}**	$0.8\ k_{14}$		2.1×10^{3}	

TABLE 16 (Continued)

Reaction	Validation* Value	Demerjian et al. (1973)	Johnston et al. (1970)	Niki et al.(1972)	Others
19	2.5×10^{2}	2.5×10^{2}	2.2×10^{2}	2.6×10^{2}	
20	7.0×10^{2}	2.0×10^{2}		2.9×10^{2}	7.0×10^{2} ††
21	$1/250\ k_1 min^{-1}$	$1/160\ k_1$			$1/250\ k_1$ †††
22	6.8×10^{3}	$6.8\ 10^{3}$	$3.7\text{-}4.4\times10^{3}$	4.4×10^{3}	
23	1.6×10^{-2}	$1.5\ 10^{-2}$	$0.9\text{-}1.6\ 10^{-2}$	1.7×10^{-2}	
24	$2.5\ 10^{4}$	9.4×10^{3}		2.5×10^{4}	
25	$1.07\ 10^{2}$		1.07×10^{2}		
26	5×10^{3}				
27	6.5×10^{1}	3.2×10^{1}	$0.16\text{-}6.5\times10^{1}$		
28	3.8×10^{3}	3.8×10^{3}	5.7×10^{3}		6.0×10^{3} ††††
29	$2\times10^{-3} min^{-1}$	$0.4\text{-}2.5\times10^{-3}$		$1/1000\ k_1$	
30	2.3×10^{4}	2.2×10^{4}		2.3×10^{4}	
31	9.1×10^{2}	9.1×10^{2}		2.9×10^{2}	
32	9.1×10^{2}	4.7×10^{2}		1.5×10^{3}	
33	1.0×10^{2}	4.9×10^{2}		2.2×10^{1}	
34	2.4×10^{-2}	$2.4\text{-}5.6\times10^{-2}$		4.4×10^{-3}	
35	4.9×10^{2}	$3.0\text{-}4.9\times10^{2}$		2.9×10^{3}	
36	2.5×10^{2}	$2.0\text{-}2.5\times10^{2}$		9.9×10^{2}	

TABLE 16 (Continued)

Reaction	Validation* Value	Demerjian et al. (1973)	Johnston et al. (1970)	Niki et al.(1972)
37	5.3×10^{3}	5.3×10^{3}	5.3×10^{3}	5.3×10^{3}
38	1.0×10^{2}	1.0×10^{2}		5.3×10^{3}
39	1.0×10^{2}	1.0×10^{2}		4.4×10^{3}

---

*Units of $ppm^{-1}min^{-1}$ unless indicated to the contrary

**Pseudo second order value

† Schuck et al., 1966

††Davis, et al., 1972

†††Dodge, 1973

††††Morris and Niki, 1971

mechanism, as well as more recent or different determinations, are presented in Table 16, along with the values which we used in our validation studies. Note that, for each reaction, the validation value of the rate constant is within the range of values recommended by these three groups or other individuals. For some reactions a considerable span exists between the lowest and highest "best" estimates of the rate constants (e.g., the formation of PAN by reaction 33). This generally indicates that the rate constant has not yet been precisely determined experimentally. In such instances parameter values have usually been estimated by analogy to similar reactions with known rate constants. In Chapter IV of the recommendations report, "Existing Needs in the Experimental and Observational Study of Atmospheric Chemical Reactions", we have discussed in detail the reactions for which considerable uncertainty in either the value of the rate constant or the nature of the elementary mechanism still remains and have made recommendations for further important experimental investigations.

b. Parameterized Stoichiometric Coefficients

As we noted in the introduction to this chapter, two parameterized stoichiometric coefficients must be specified. Since the only olefin which we are considering in this validation study is propylene, a terminal olefin, α is always equal to 1/2. The value of β depends upon the fraction of total aldehydes formed during an irradiation which is not formaldehyde. The approximate values of β for

the three systems validated are

System	β
n-Butane-NO_x	.75
Propylene-NO_x	.50
n-Butane-Propylene-NO_x	.63

The accuracy of these values is probably no better than ±20% because

(i) the ratio of formaldehyde to higher aldehydes fluctuates somewhat during an irradiation,

(ii) all the higher aldehydes may not have been detected with the analytical instruments, and

(iii) the accuracy of the analytical techniques used to determine aldehydes in this study is poor.

This uncertainty, however, introduces no substantial impediment to the validation effort since variation in β over the extremes of the uncertainty bounds have little effect on the predictions of the decision variables, T and M, first defined in the sensitivity study of the Hecht Seinfeld mechanism (Chapter II).

c. Initial Concentrations of Reactants

The initial concentrations of the reactants were not always determined at T = 0.0 minutes, that is, the instant at which the lights were turned on. In those cases for which measurements at zero time were unavailable, we have estimated the initial concentrations by interpolating between the last measurement before and the

first measurement after the irradiation was begun.

d. Average Dilution Rate

In carrying out chemical analyses of reactants and products, large volumes of gas were drawn from the chamber during an experiment. Removal of such large samples for analysis was necessary in order to obtain accurate determinations of contaminant concentrations. Because a volume of clean air, equal in volume to the amount of gas removed for sampling, was added to the chamber to maintain the total chamber pressure at 1 atmosphere, dilution generally amounted to 20-25% of the initial concentrations of reactants during a 6-hour irradiation. In order to determine the amount of dilution, ethane, a hydrocarbon which is virtually unreactive in photochemical smog, was added to the reactant mix as a tracer gas. If ethane is assumed to be chemically inert, its loss from the chamber can be attributed entirely to sampling and dilution, carried out at an average rate given by:

$$\frac{-dc}{dt} = kc$$

The "rate constant" for the reaction is then

$$k = \frac{2.3 \log(c_o/c_f)}{t_f - t_o}$$

where o and f are the beginning and ending times of the irradiation. The average dilution rate constants for the experiments used for

validation were:

EPA Run	k x 10^4(min^{-1})	EPA Run	k x 10^4(min^{-1})
306	7.5	307	9.5
314	8.5	333	10.0
345	7.5	348	7.9
318	8.2	349	9.3
325	8.5	352	9.5
329	8.9	457	6.9
459	4.8		

e. Sensitivity of Kinetic Mechanisms to Variations in the Magnitudes of Parameters

We have carried out a large number of validation runs during this study, many of which involved the investigation of the effect of varying the magnitude of a parameter on the predicted concentration-time profiles. These efforts can thus be viewed, in part, as an informal sensitivity study of the lumped kinetic mechanism. We have also completed a detailed formal sensitivity analyses of the simplified Hecht and Seinfeld (HS) mechanism (Chapter II). In comparing the HS mechanism with the new lumped kinetic mechanism we find the most striking difference to be that a large number of stoichiometric coefficients having a poor correspondence to actual stoichiometries must be specified in the simple mechanism. Otherwise, with the exception of the obvious difference in detail of chemical description, the two mechanisms present the same basic features of the smog formation process. A sensitivity analysis of the HS mechanism thus provides a

useful indication of the sensitivity of parameters in the lumped mechanism.

Among those parameters that are imprecisely known, the predictions of the HS mechanism are most sensitive to variations in the rate of photolysis of NO_2, k_1, the initial concentration of NO_2, and the stoichiometries of the OH-HC and RO_2-NO (which involves regenerating OH) reactions. Variations of ±50% in the water concentration, however, have virtually nc effect on the predictions. In one sensitivity study, using a set of data from the toluene-NO_x system in which the NO_2 peak reoccurred at 162 minutes, ±50% changes from the base values of $(NO_2)_0$, k_1, β , and ε caused the following changes in the time to the peak T.

Parameter Change	Change in T (minutes)
β - 50%	+ 198
ε - 50%	+ 174
k_1 - 50%	+ 116
$(NO_2)_0$ - 50%	+ 24
β + 50%	- 114
ε + 50%	- 106
k_1 + 50%	- 43
$(NO_2)_0$ + 50%	- 20

β and ε both govern the rate of NO oxidation due to the OH-hydrocarbon oxidation reaction. As it is this reaction which is primarily responsible for the hydrocarbon loss rate observed in smog,

and as the rate constant of the reaction correlates most closely with the photochemical reactivity of hydrocarbons in smog chambers, one would expect changes in the stoichiometries of reactions involved in the production or loss of OH to have an impact on the predictions of kinetic mechanisms. In terms of the lumped mechanism, we would expect changes in the stoichiometries of the reactions of OH with the four classes of hydrocarbons and changes in the termination rate of OH through reaction with NO_2 and NO (reactions 17 and 18) to have a material effect on the predictions. We would also expect variations in the two experimental parameters, k_1 (light intensity) and initial NO_2 concentration, to perturb the predictions of the lumped mechanism. During validation of the mechanism we have qualitatively confirmed these expectations.

2. The Validation Results

In this section we present validation results for the lumped mechanism (Table 14) for the following reactant systems:

Reactant System	Number of Sets of Experimental Data
n-Butane-NO_x	3
Propylene-NO_x	4
n-Butane-Propylene-NO_x	6

The input parameters to the mechanism are those presented in Section VB1. The results are depicted as a series of figures. Figure numbers,

EPA experiment identification number, and initial concentrations of reactants are given in the List of Figures, Table 17. Predictions of the mechanism are represented by solid lines, and the experimental data points are coded according to

- □ NO
- △ NO_2
- ◇ O_3
- ○ Propylene
- ⌑ n-Butane
- ⧖ Peroxyacyl nitrates

a. n-Butane-NO_x

Plots of the predicted and experimental values of concentrations with time are shown in Figures 2 through 4. The $(\text{n-butane})_0/(NO_x)_0$ ratios span a range from 2.4 to 10.4.

b. Propylene-NO_x

The propylene-NO_x validation results are presented in Figures 5 through 8. For this system the $(\text{propylene})_0/(NO_x)_0$ ratios for the four experiments vary between 0.4 and 1.3.

c. n-Butane-Propylene-NO_x

The validation results for this binary hydrocarbon system are displayed in Figures 9 through 14. The hydrocarbon/NO_x ratios for the experiments considered here span approximately the same range as those used for the validations of the single hydrocarbon system. The

TABLE 17

List of Figures

Figure	EPA Run	$(NO_2)_0^*$	$(NO)_0^*$	(n-Butane)$_0^*$	(Propylene)$_0^*$
3a,b,c	306†	0.03	0.30	1.60	
4a,b,c	314	0.02	0.29	3.17	
5a,b,c	345	0.12	1.28	3.40	
6a,b,c	318	0.06	1.12		0.51
7a,b	325	0.04	0.32		0.45
8a	329	0.06	0.26		0.24
9a,b	459	0.06	1.14		0.78
10a,b,c	307	0.05	1.23	3.06	0.36
11a,b,c	333	0.08	1.25	3.41	0.23
12a,b,c	348	0.08	1.23	3.39	0.50
13a,b,c	349	0.03	0.31	3.25	0.44
14a,b,c	352	0.07	0.27	3.29	0.26
15a,b	457	0.05	1.11	3.29	0.81

*Initial concentrations in units of parts per million (ppm)

†0.12 ppm of aldehyde also present initially

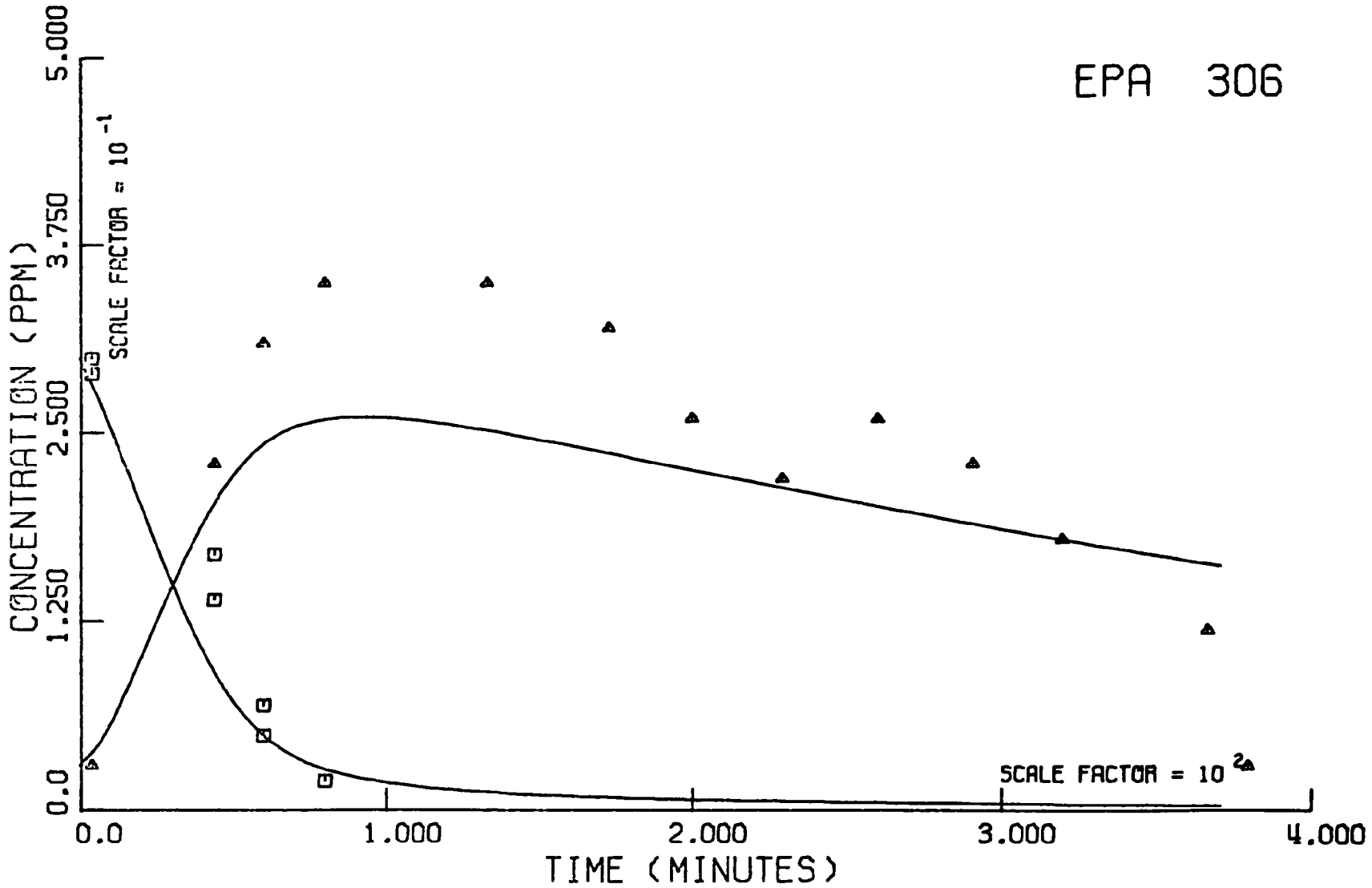

Figure 3a. EPA Run 306

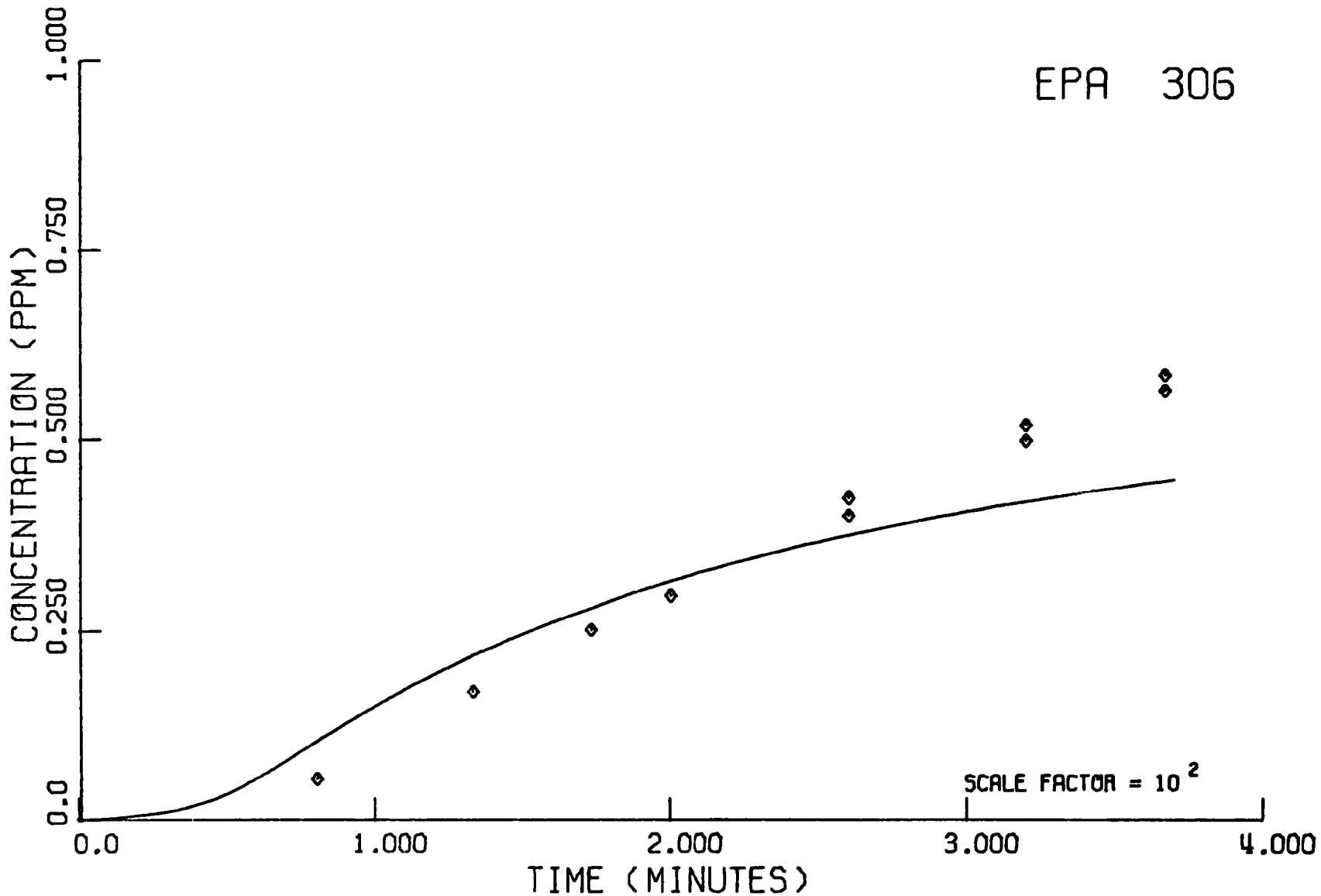

Figure 3b. EPA Run 306

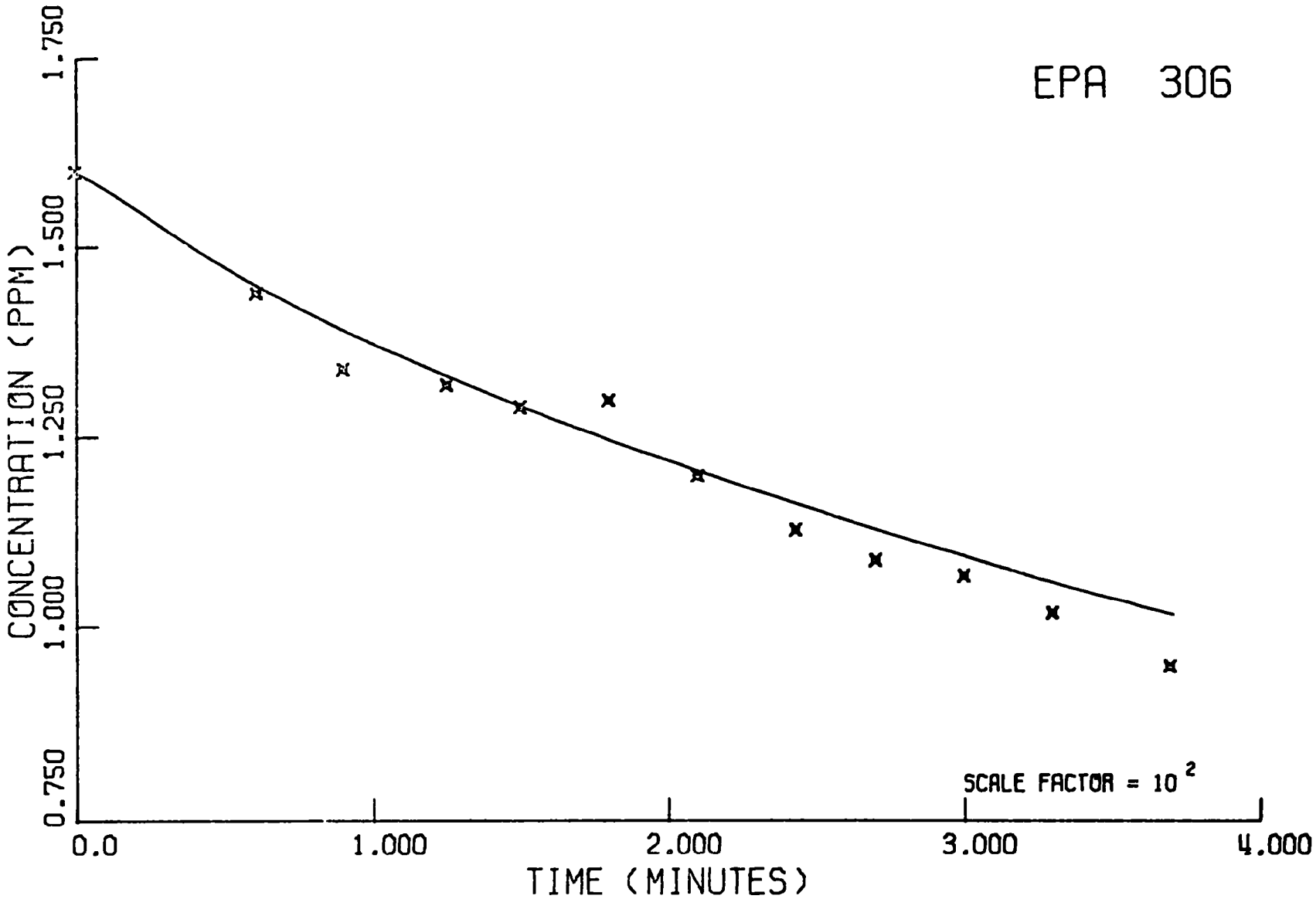

Figure 3C. EPA Run 306

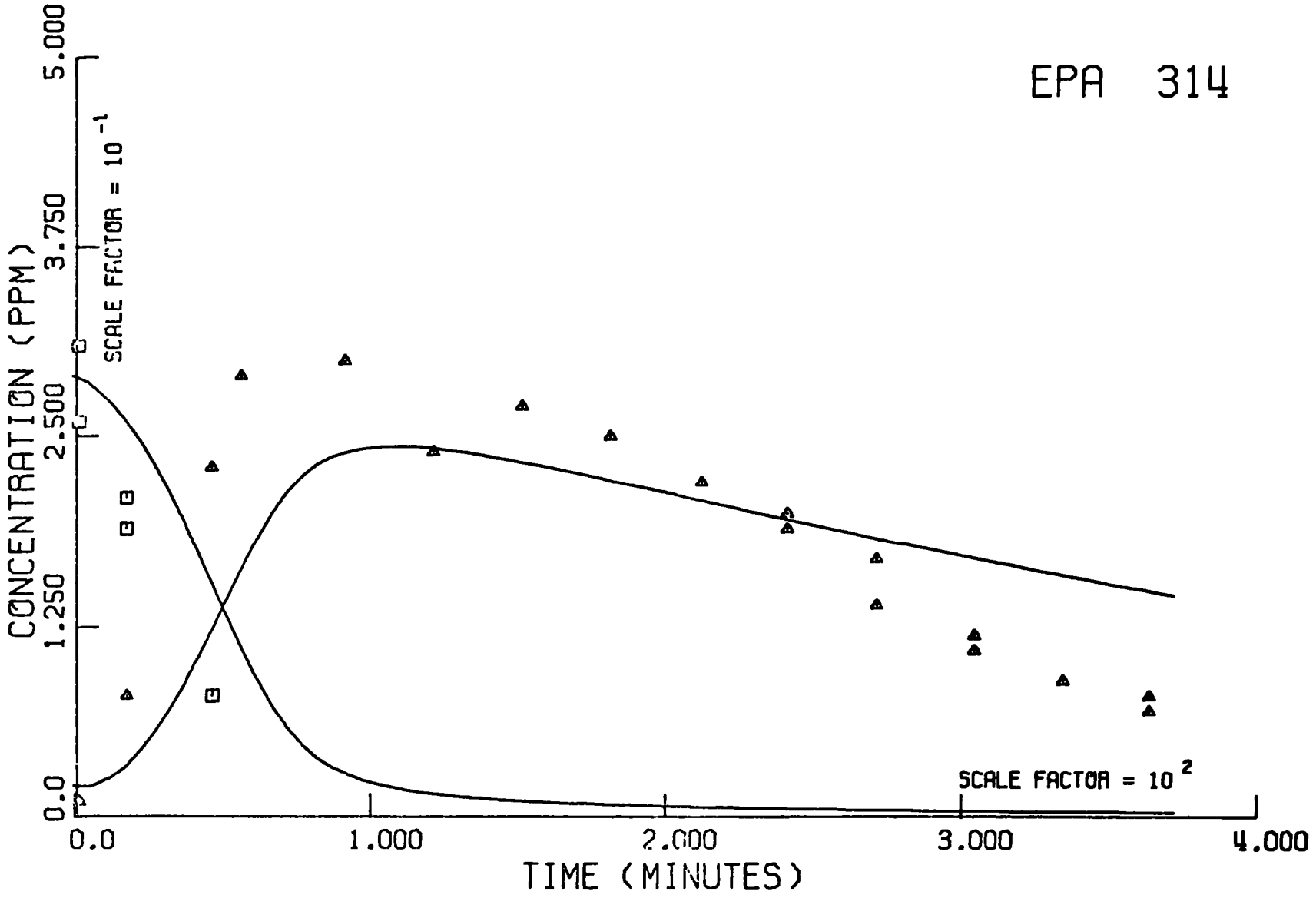

Figure 4a. EPA Run 314

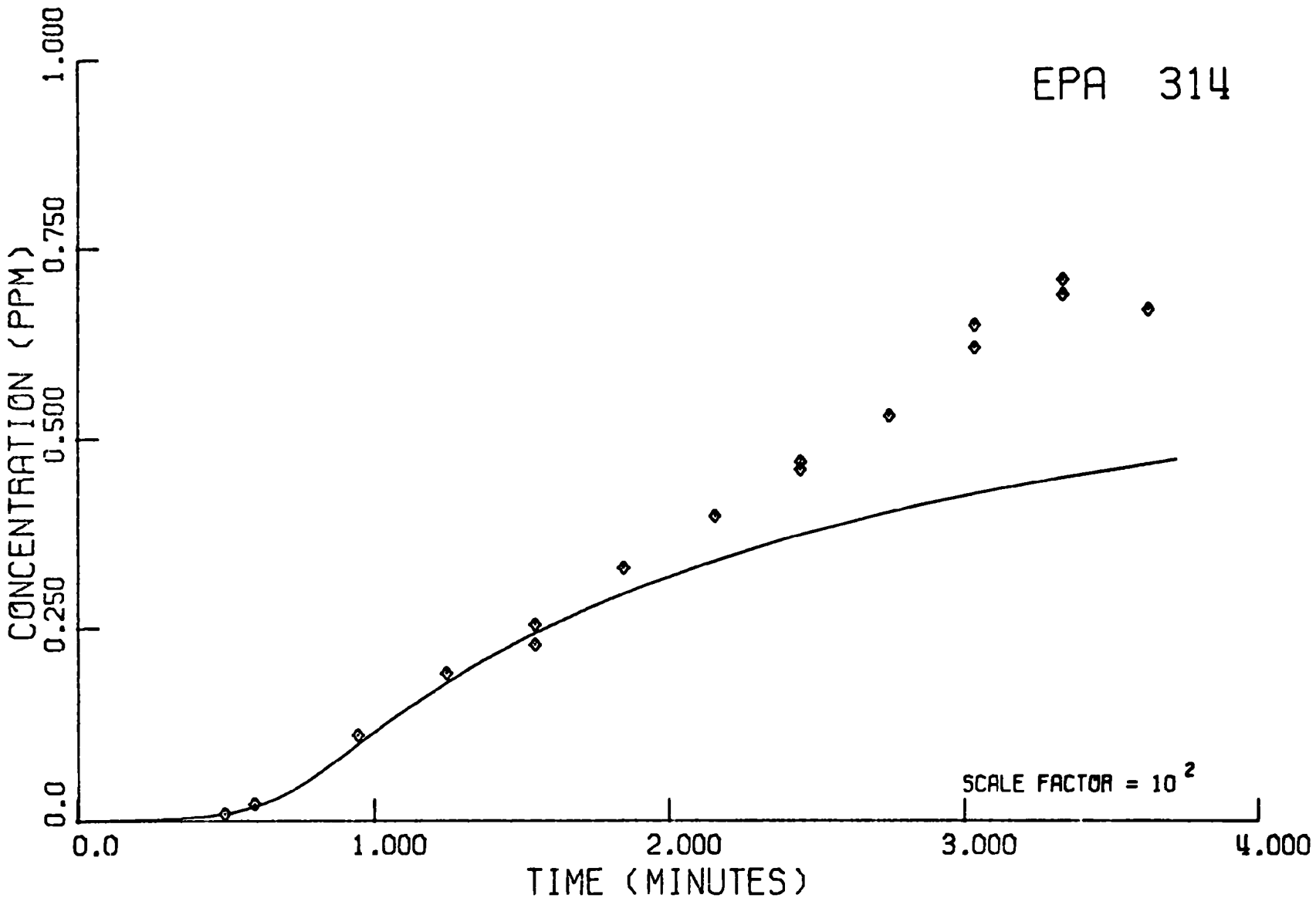

Figure 4b. EPA Run 314

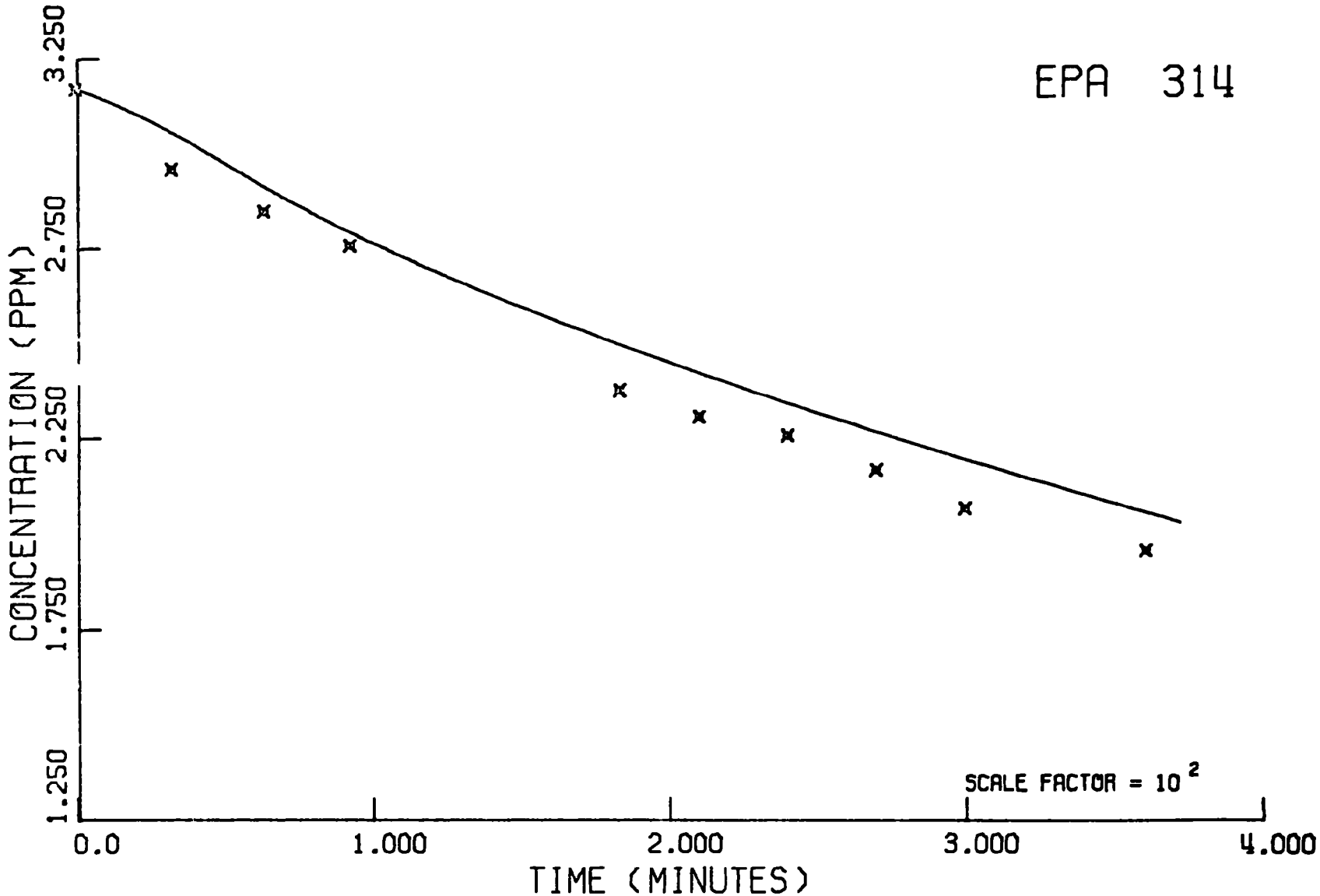

Figure 4c. EPA Run 314

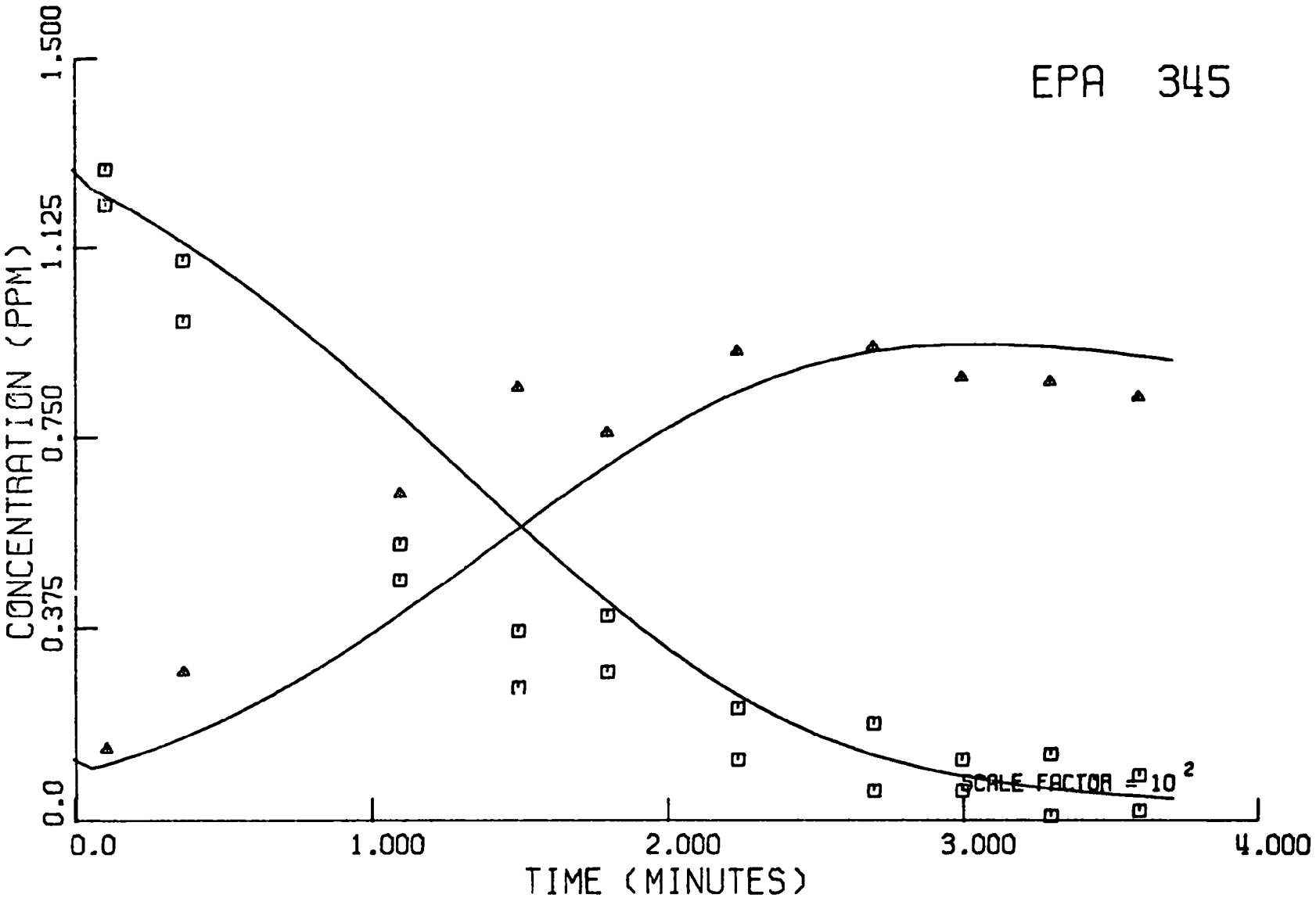

Figure 5a. EPA Run 345

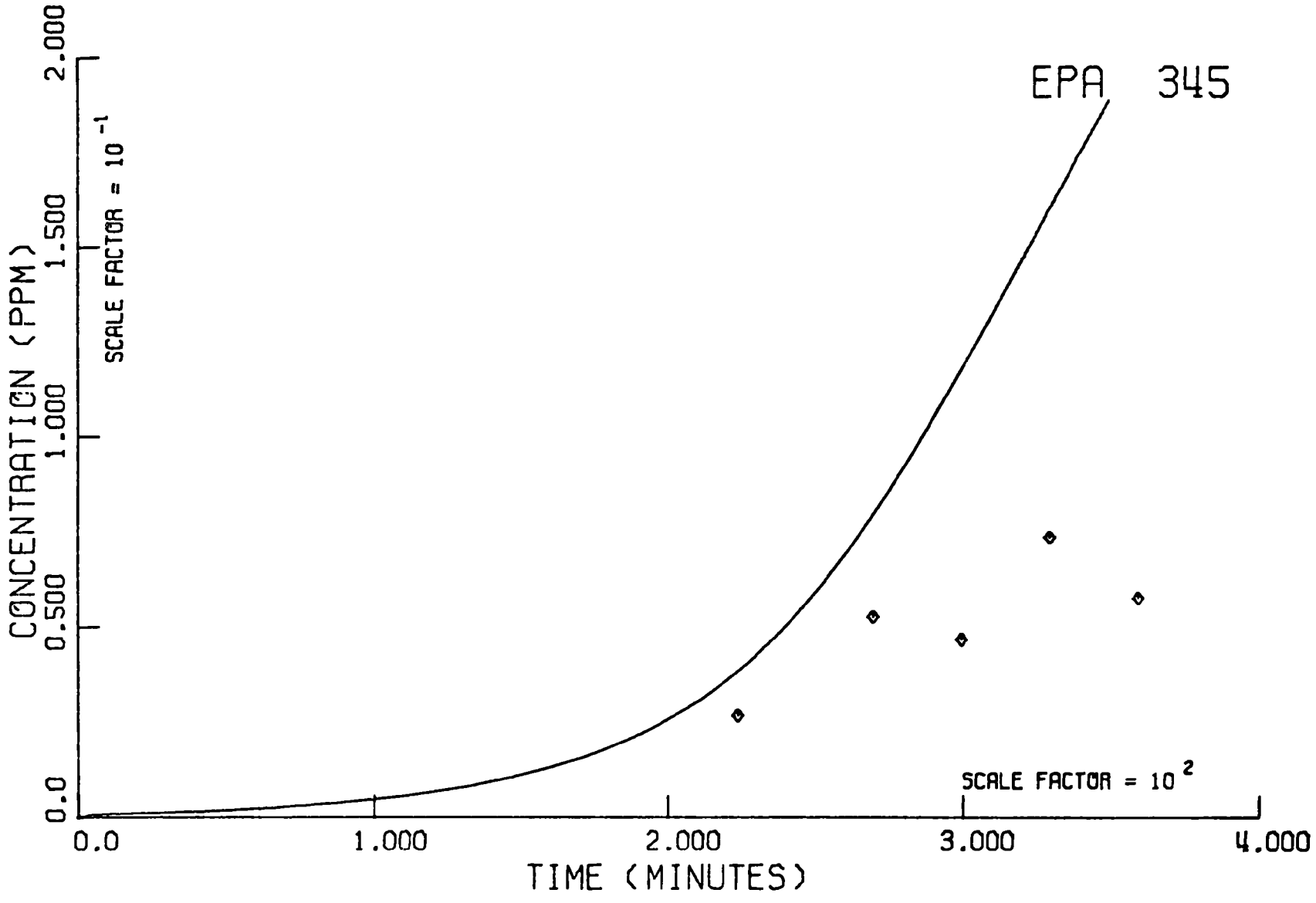

Figure 5b. EPA Run 345

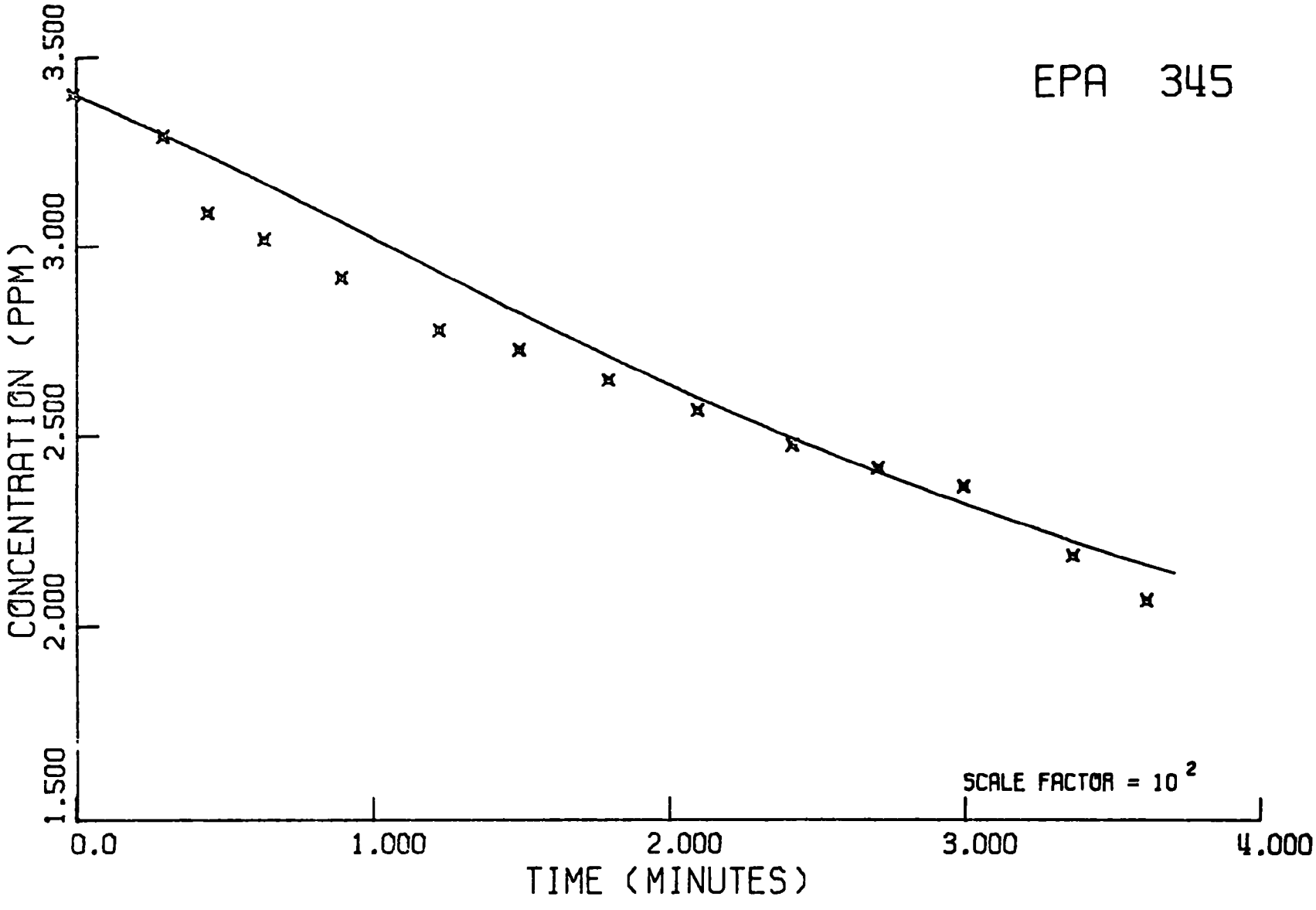

Figure 5c. EPA Run 345

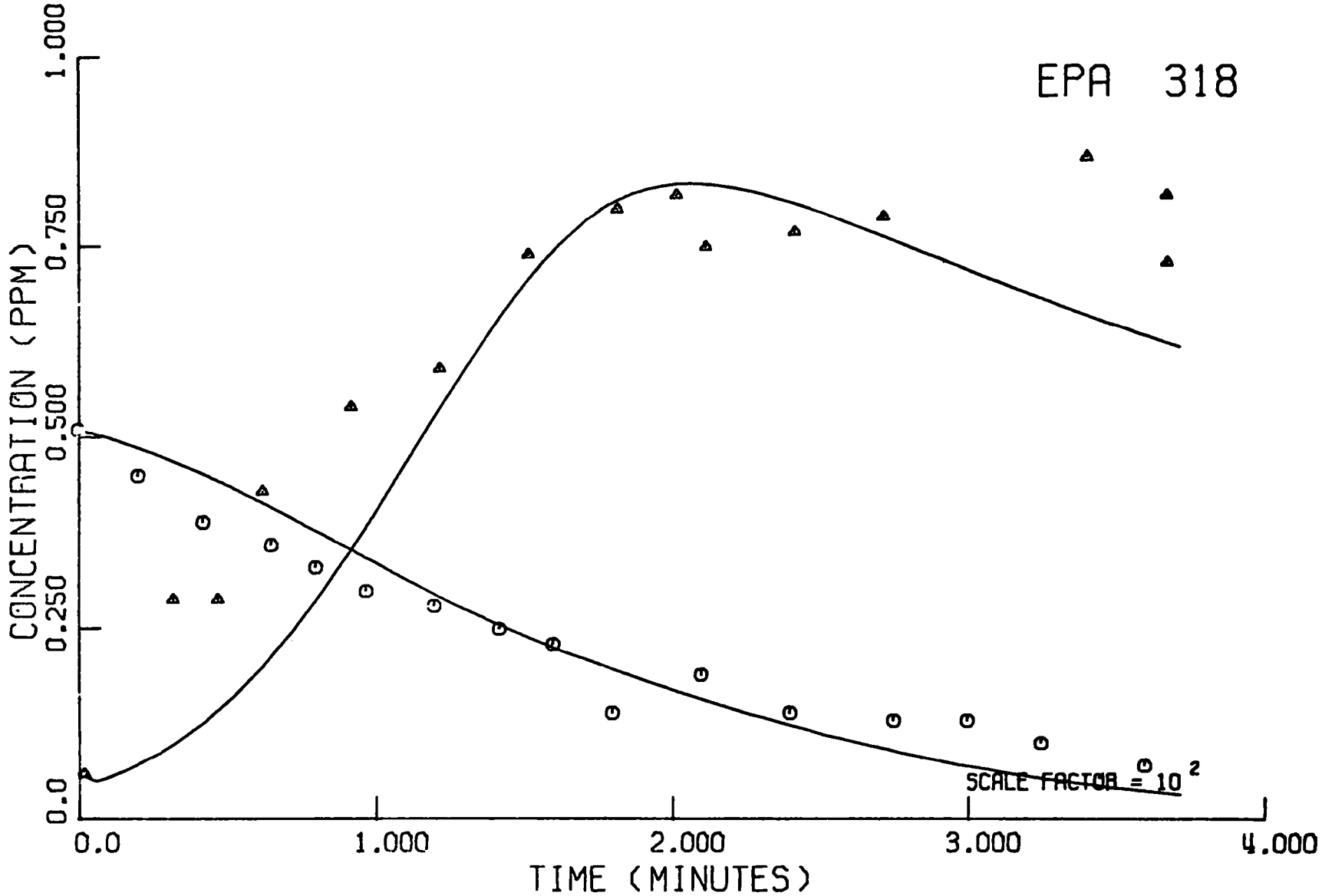

Figure 6a. EPA Run 318

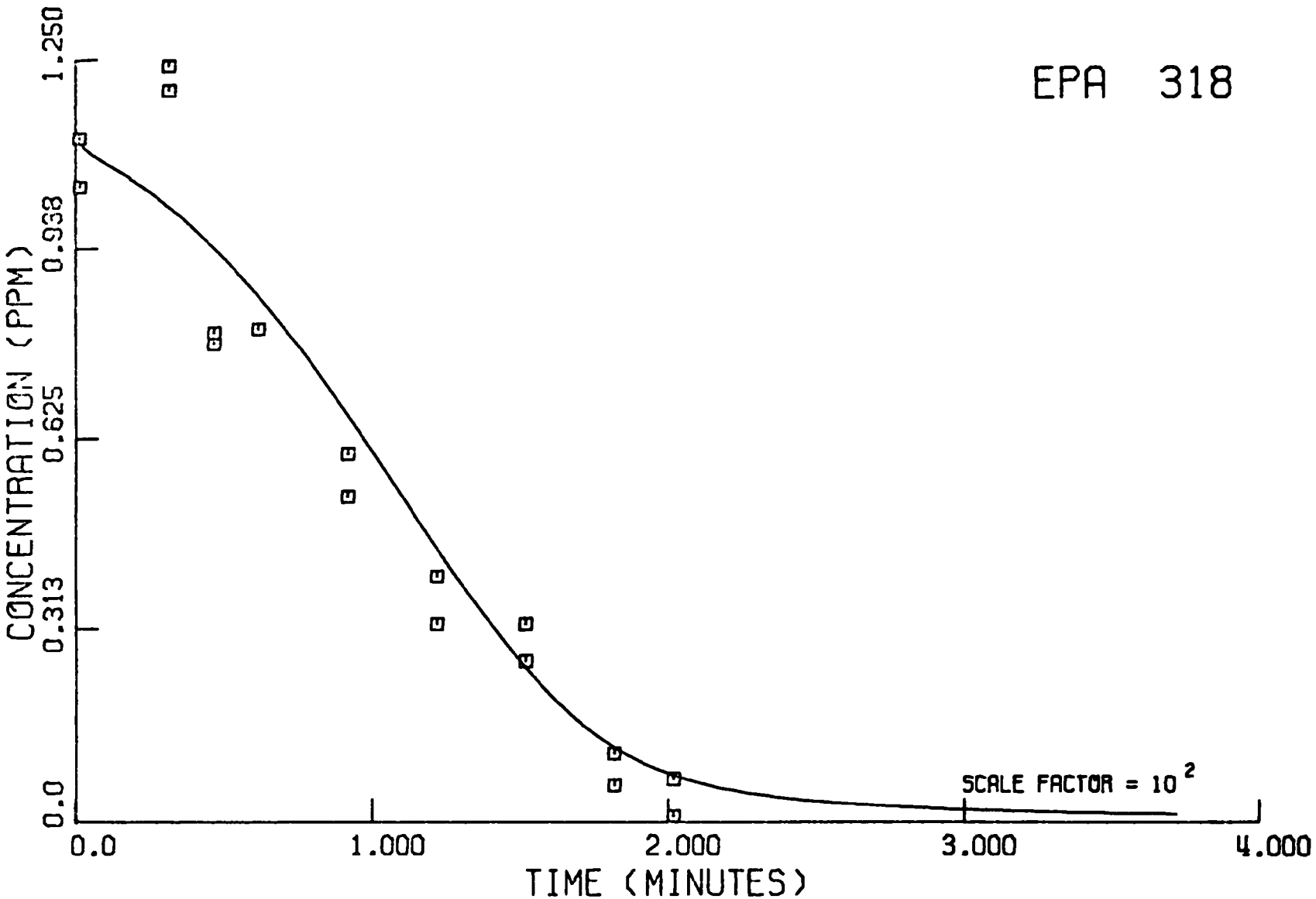

Figure 6b. EPA Run 318

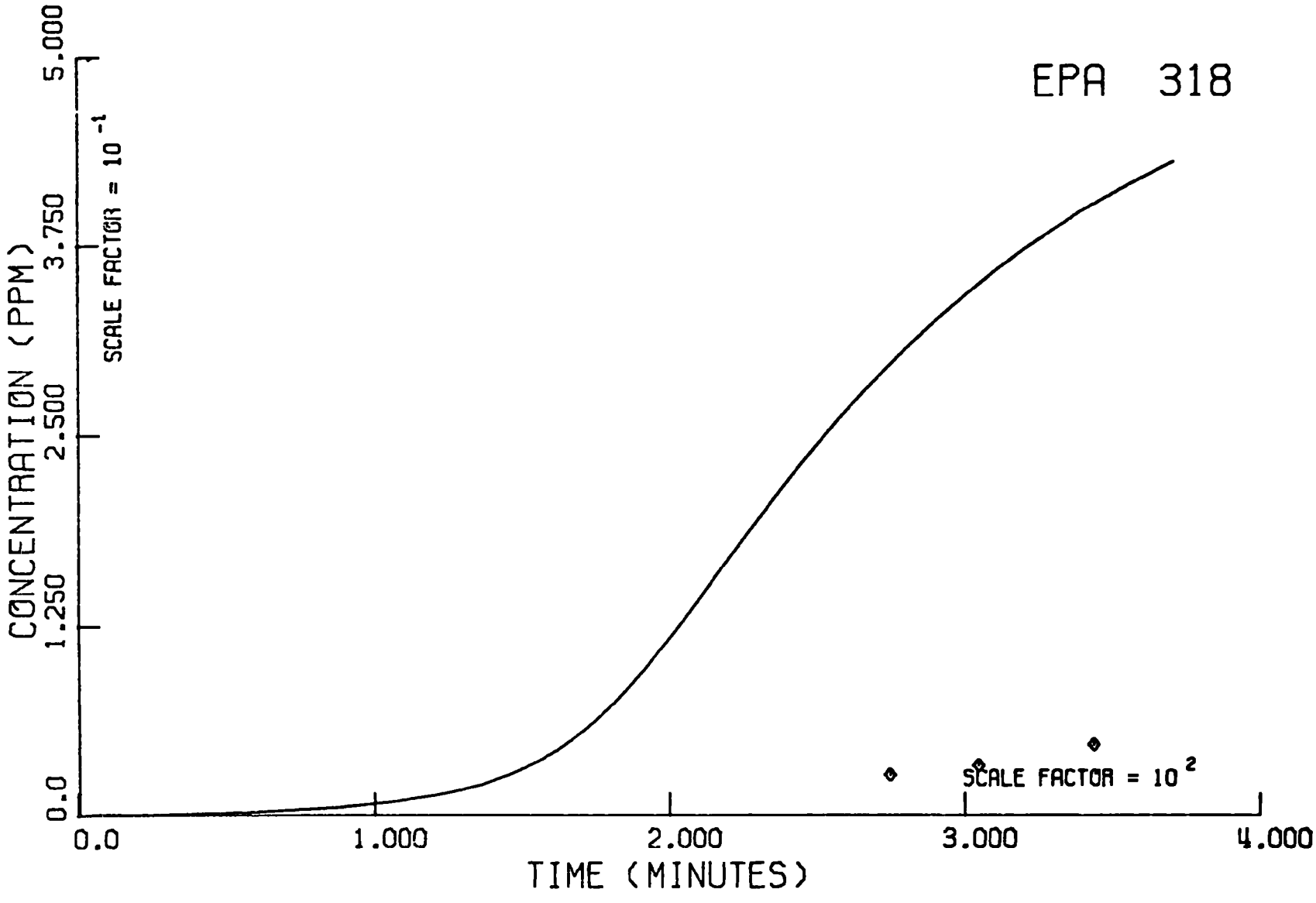

Figure 6c. EPA Run 318

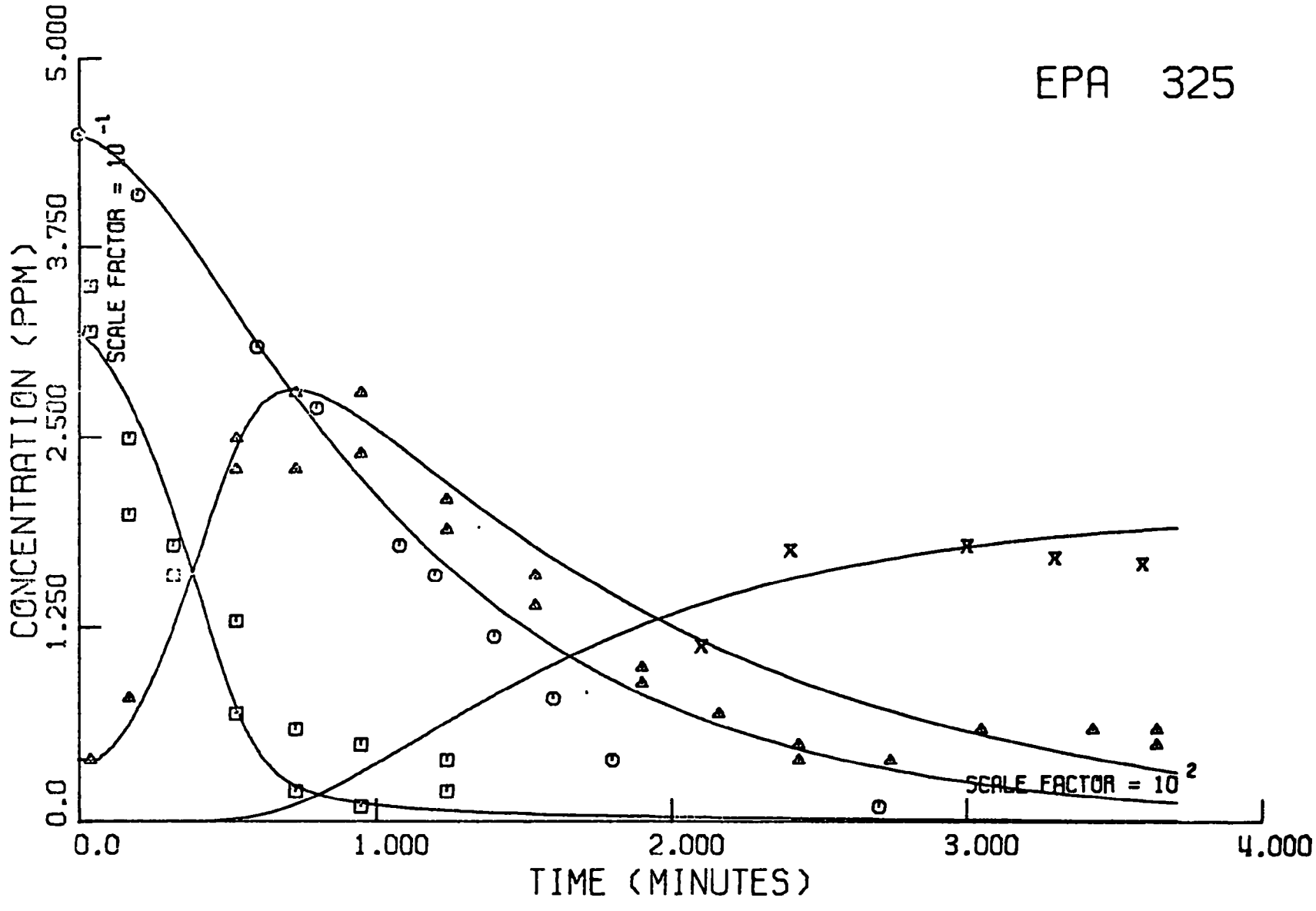

Figure 7a. EPA Run 325

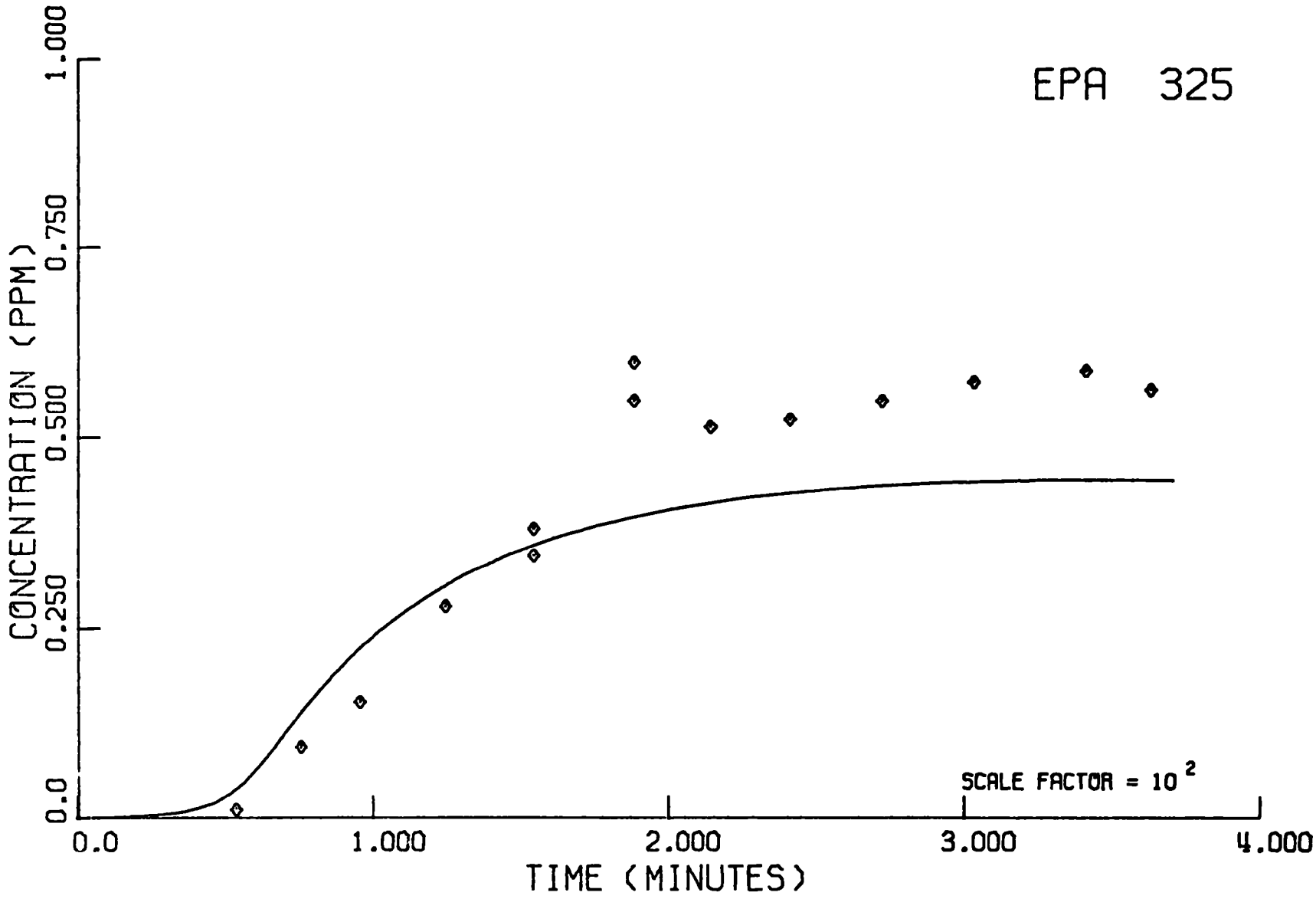

Figure 7b. EPA Run 325

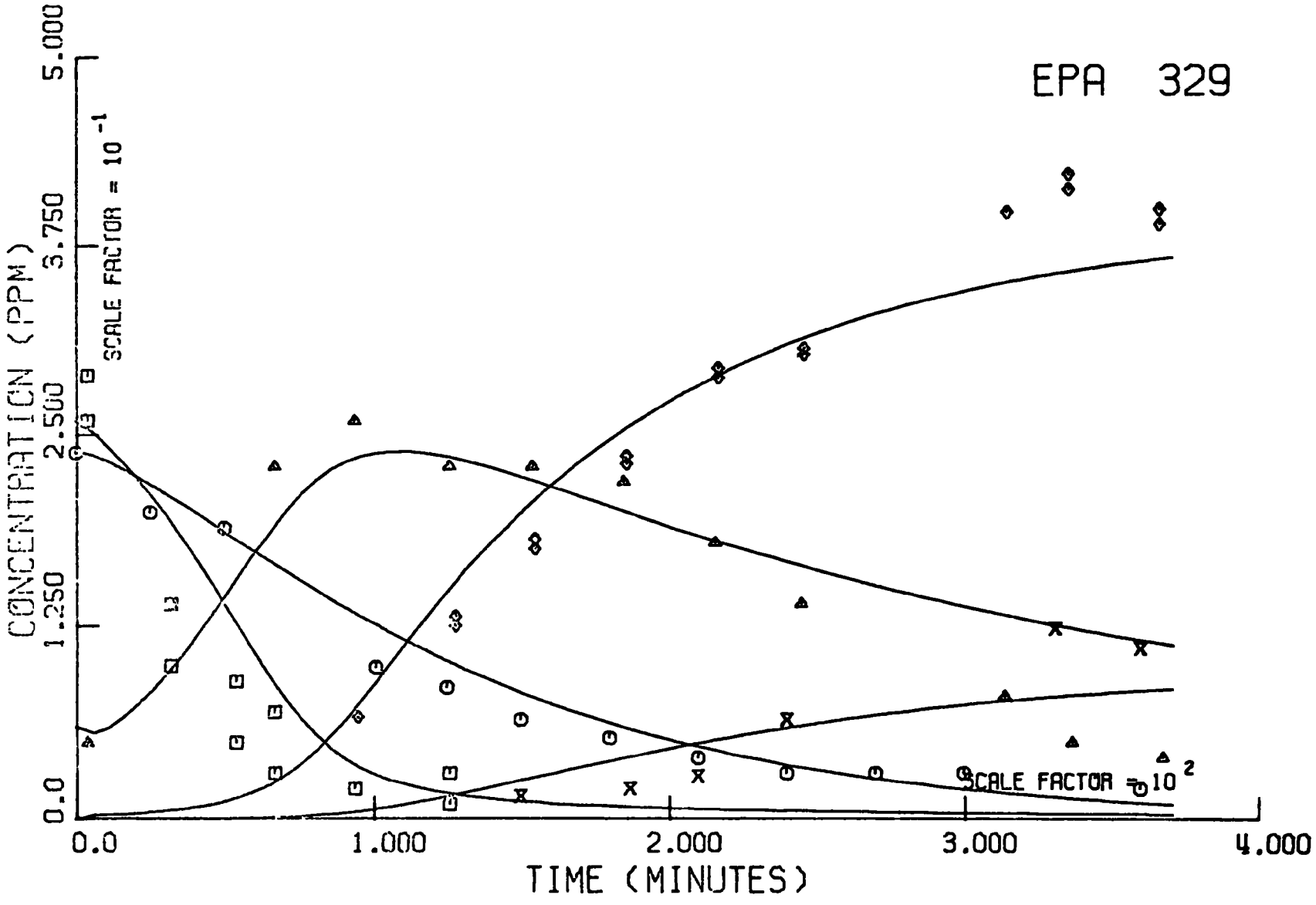

Figure 8a. EPA Run 329

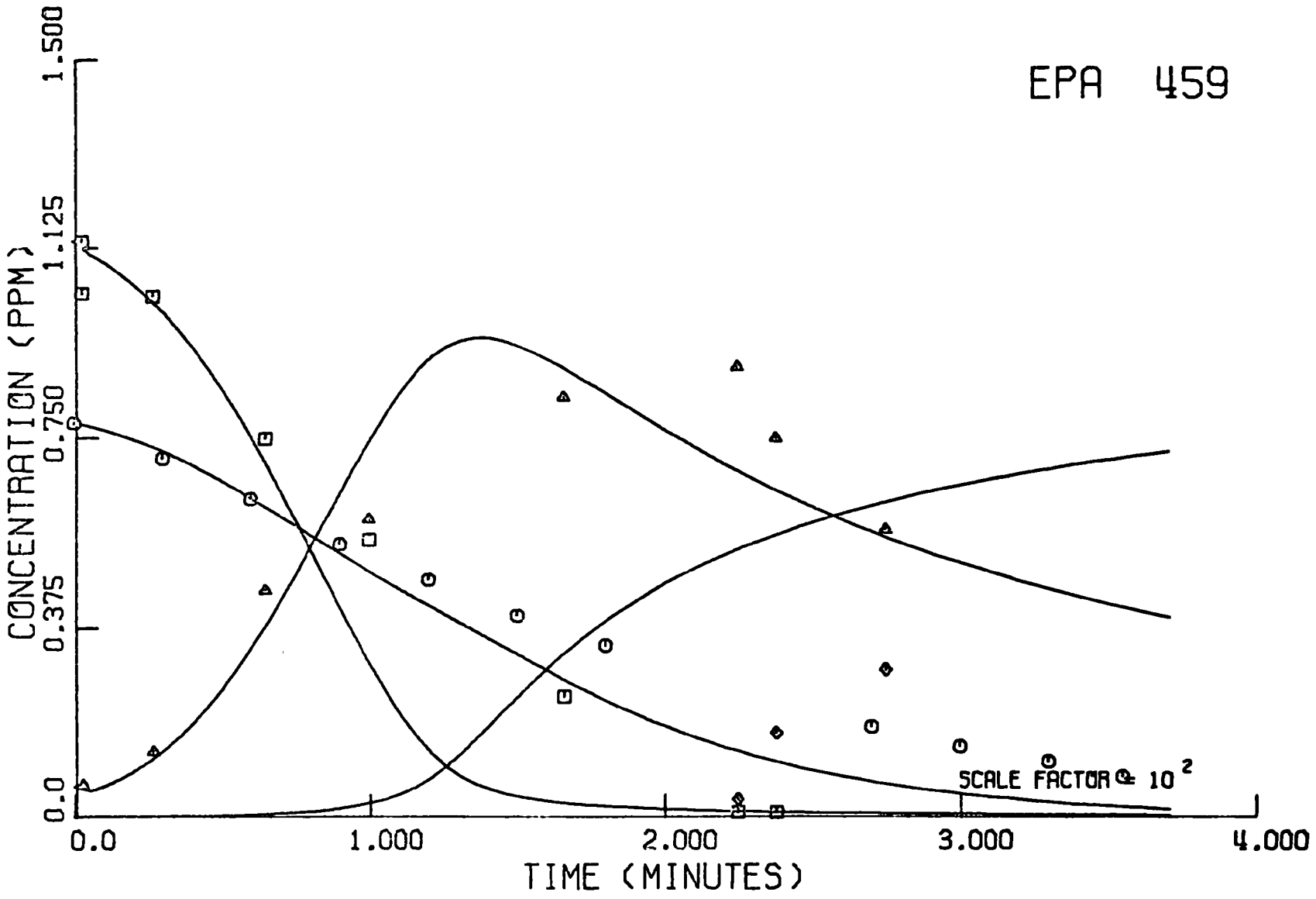

Figure 9a. EPA Run 459

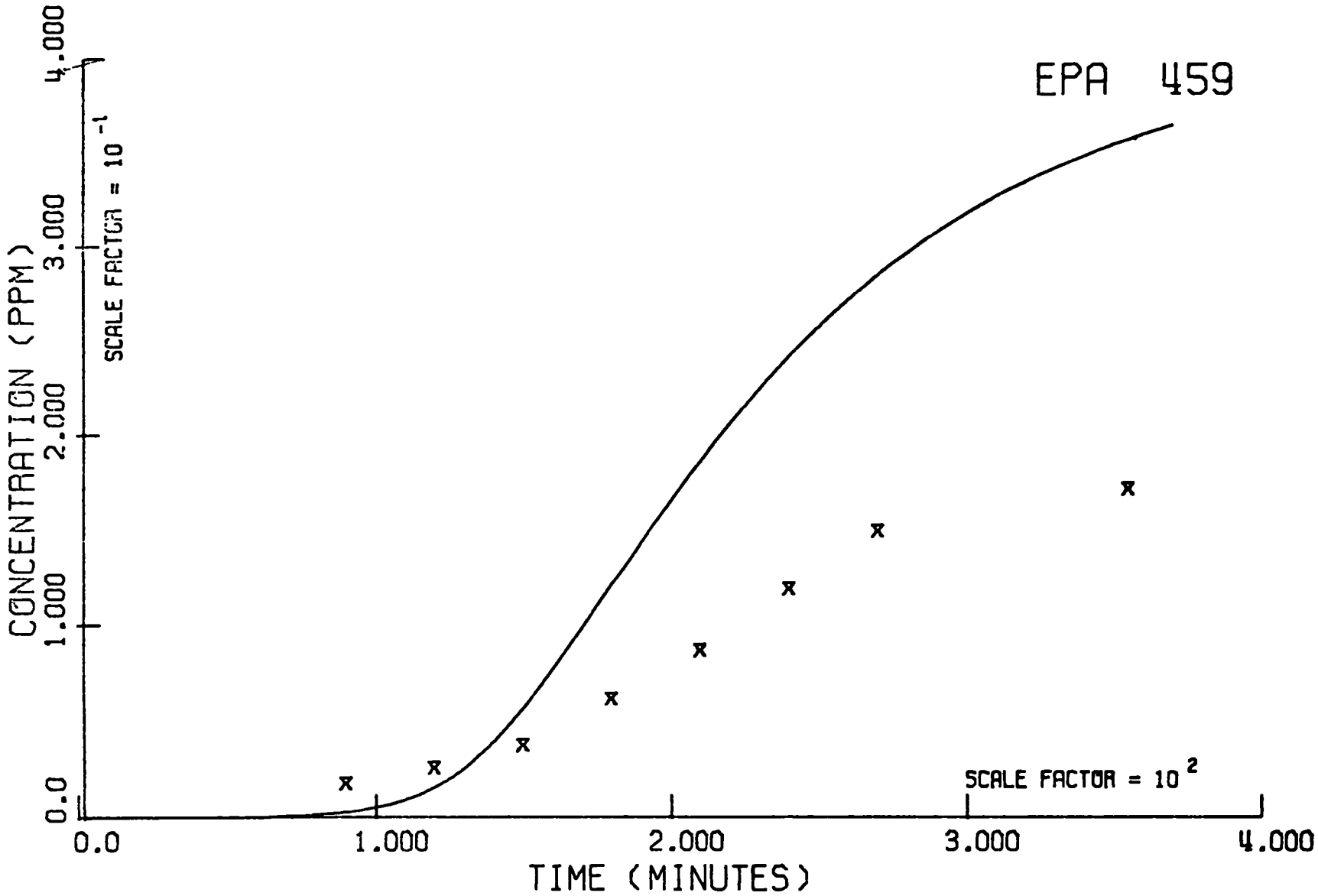

Figure 9b. EPA Run 459

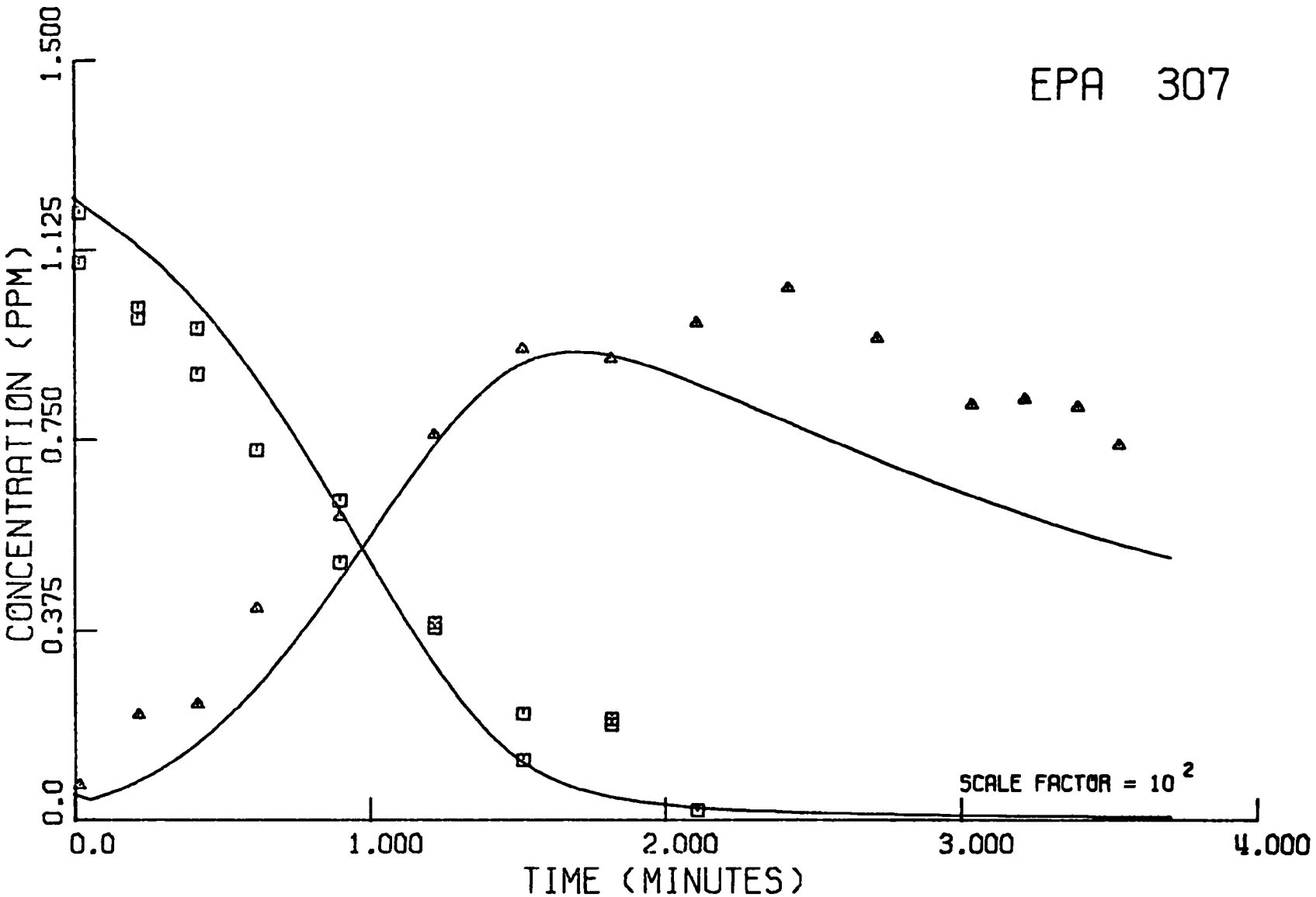

Figure 10a. EPA Run 307

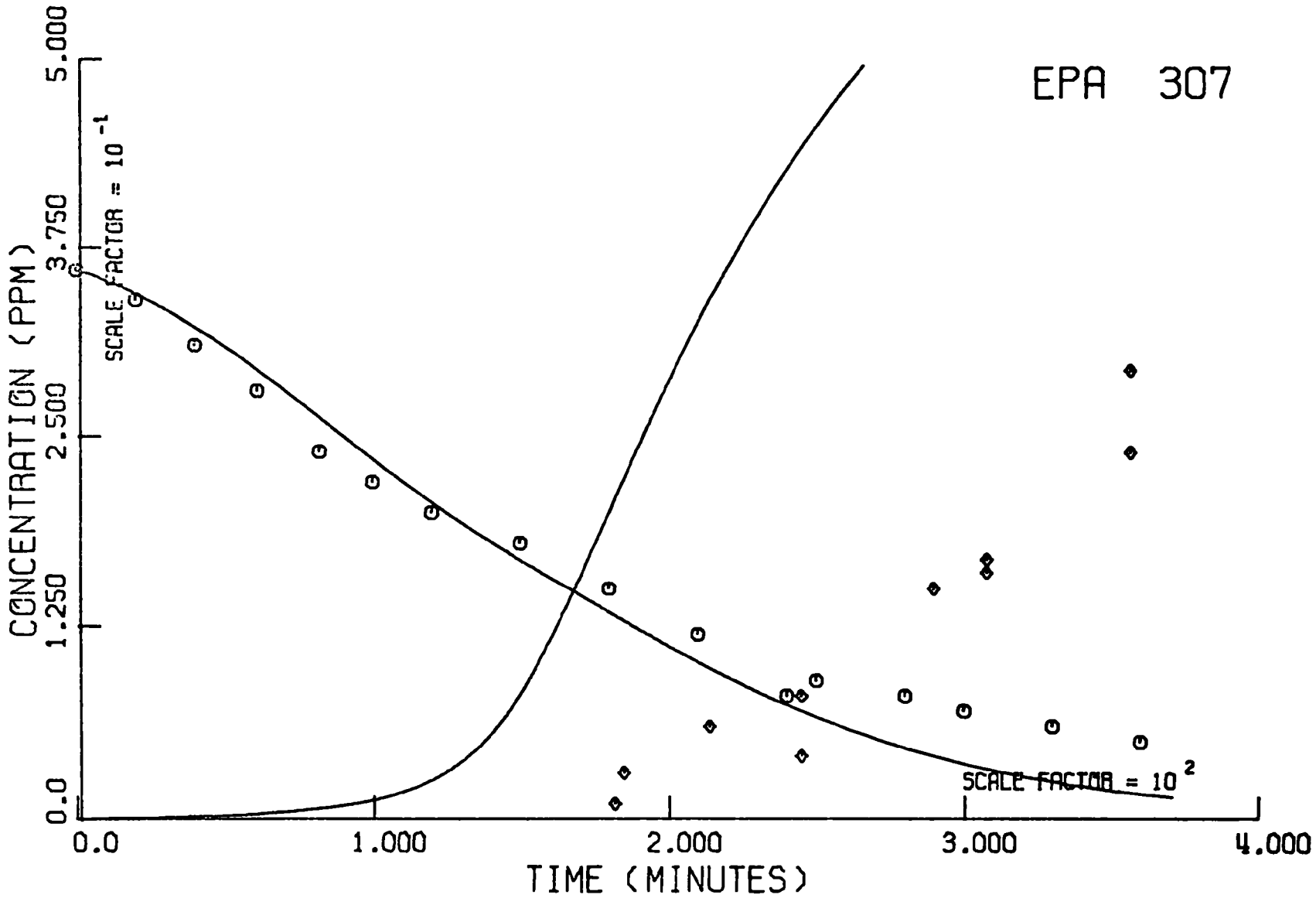

Figure 10b. EPA Run 307

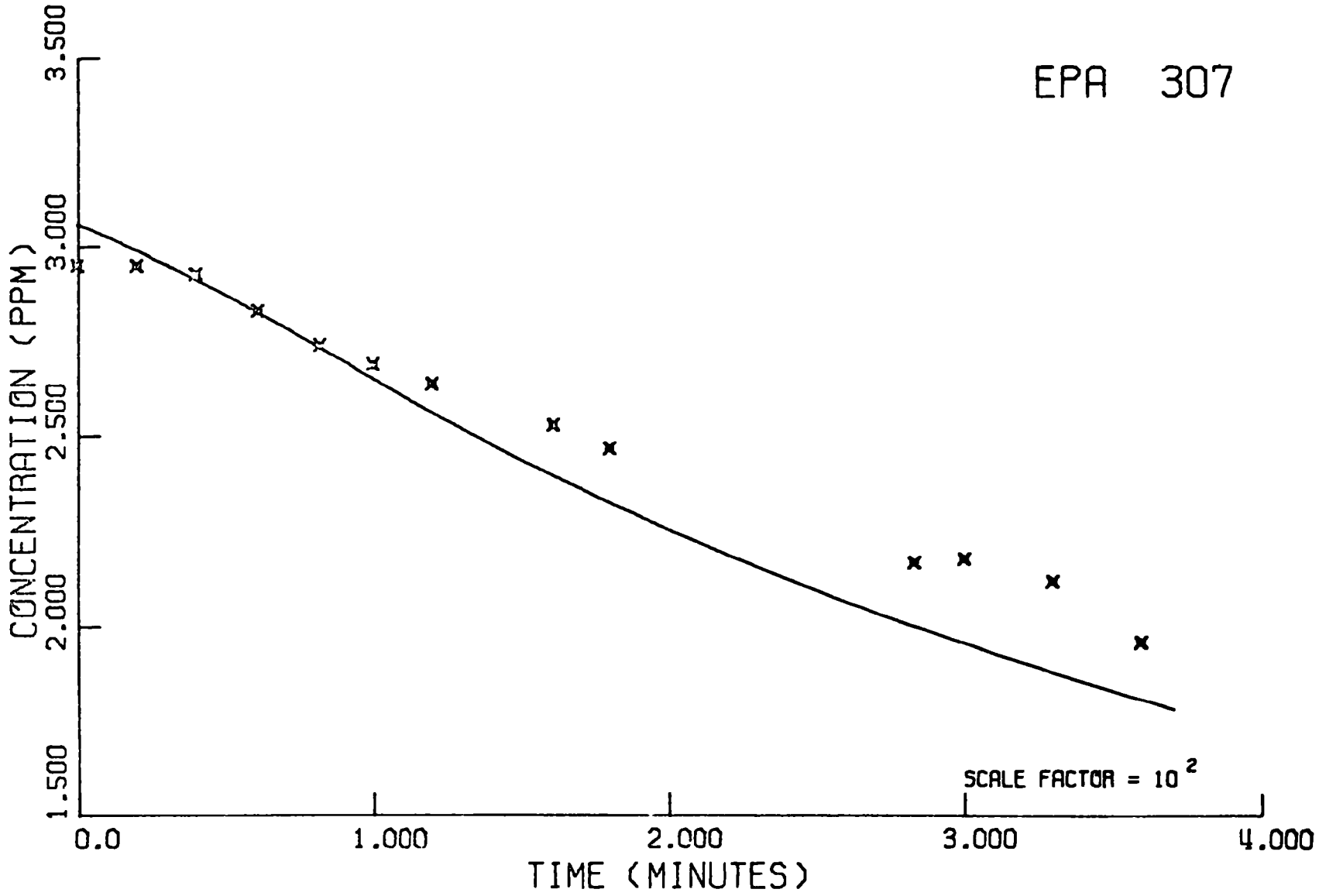

Figure 10c. EPA Run 307

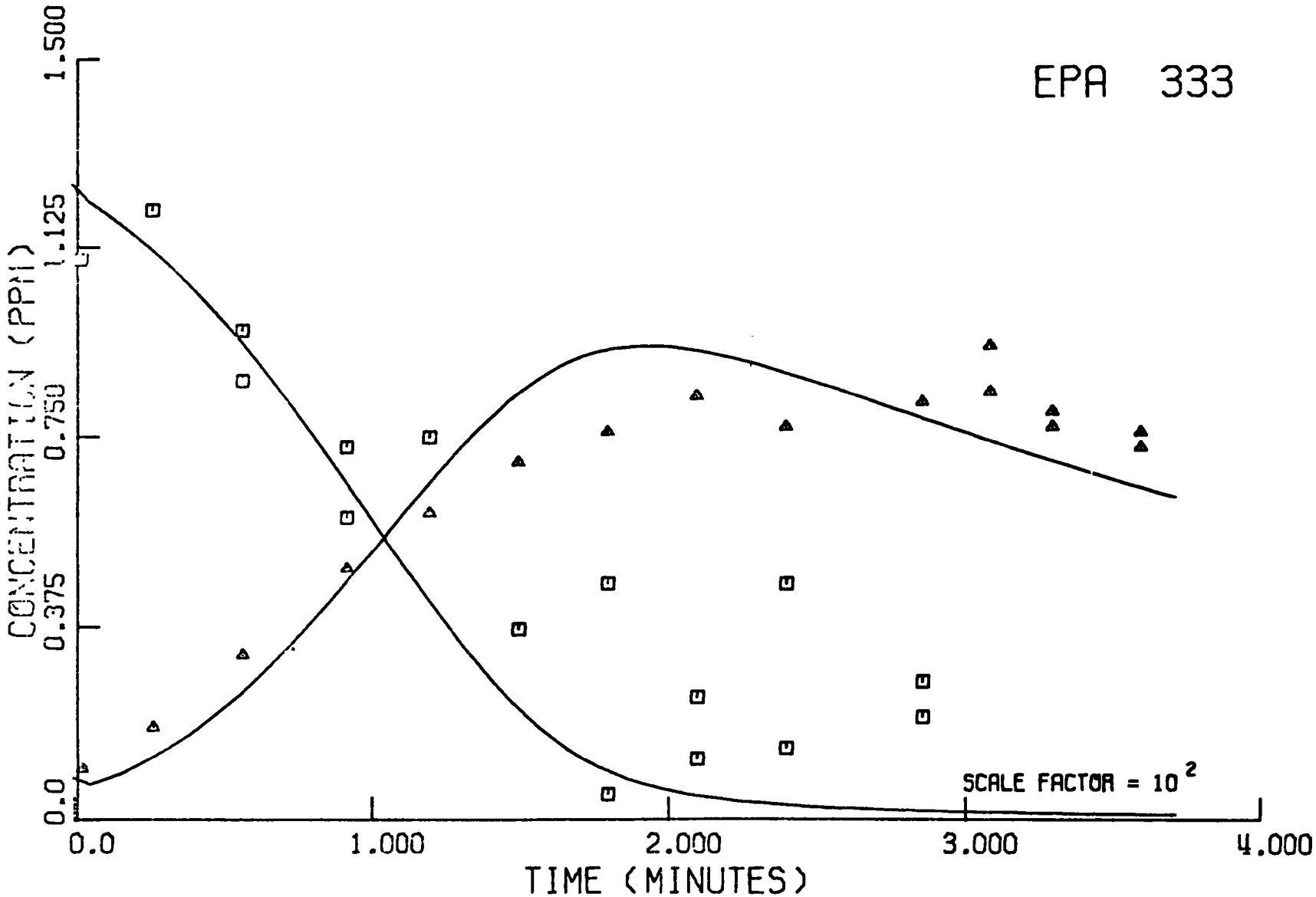

Figure 11a. EPA Run 333

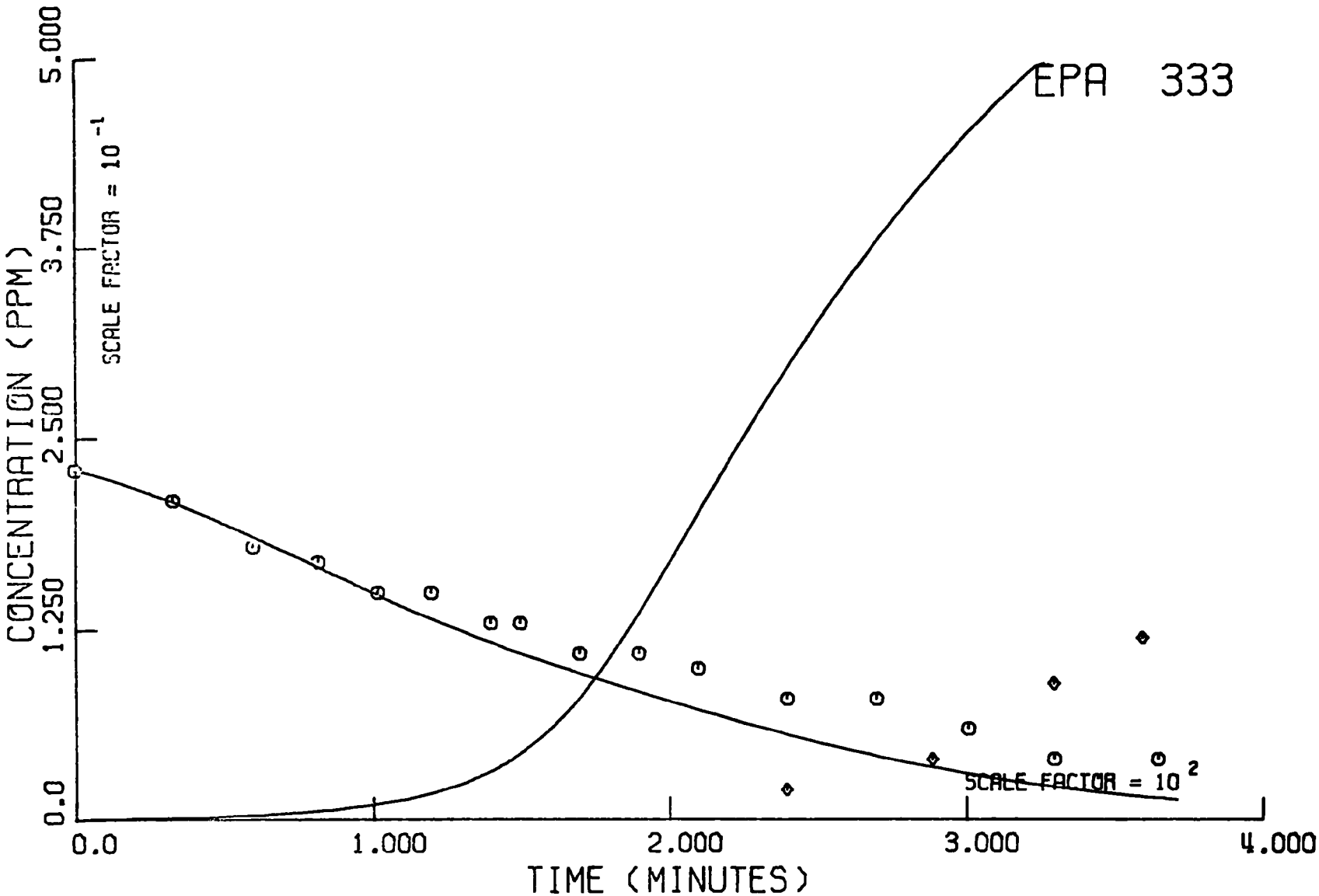

Figure 11b. EPA Run 333

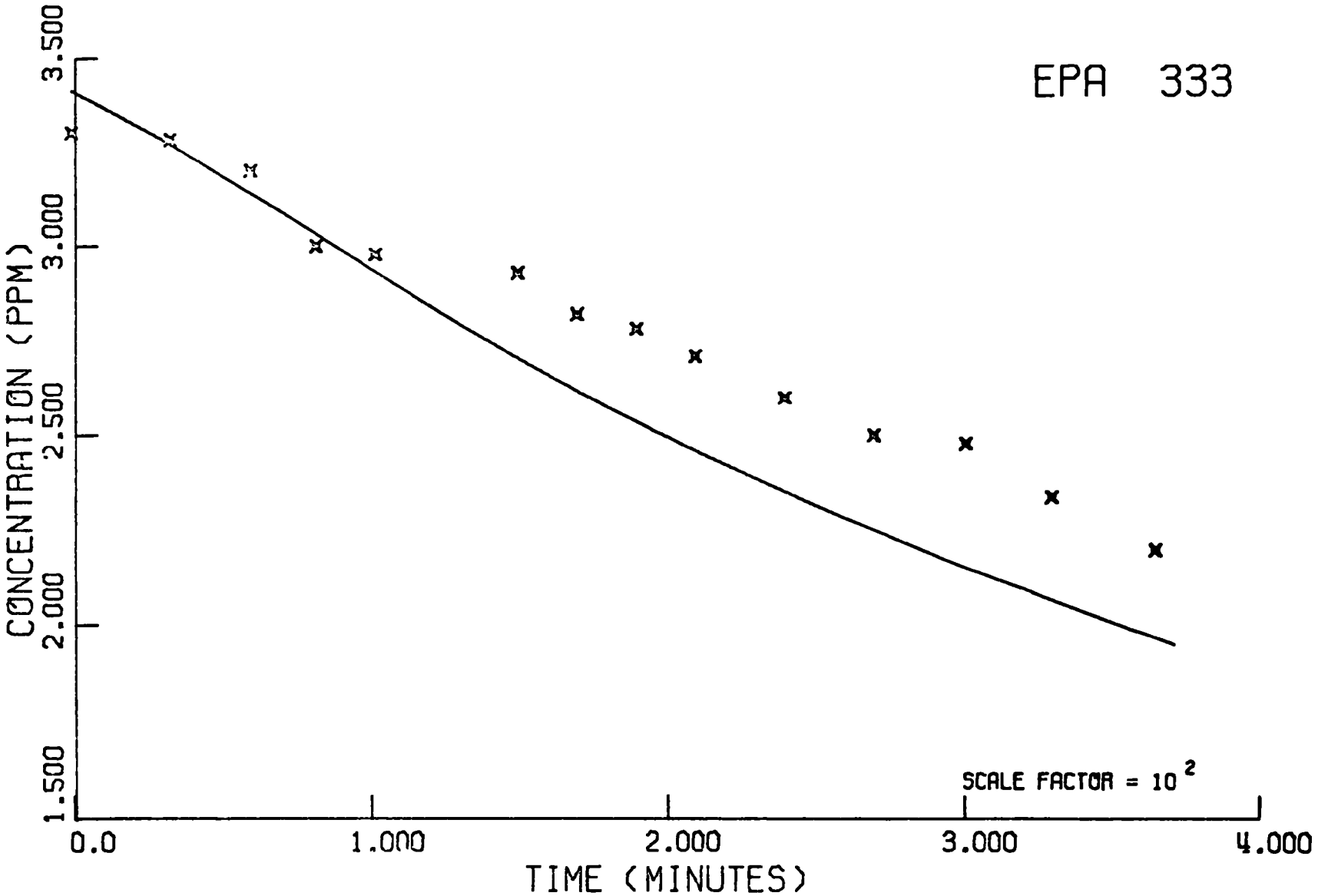

Figure 11c. EPA Run 333

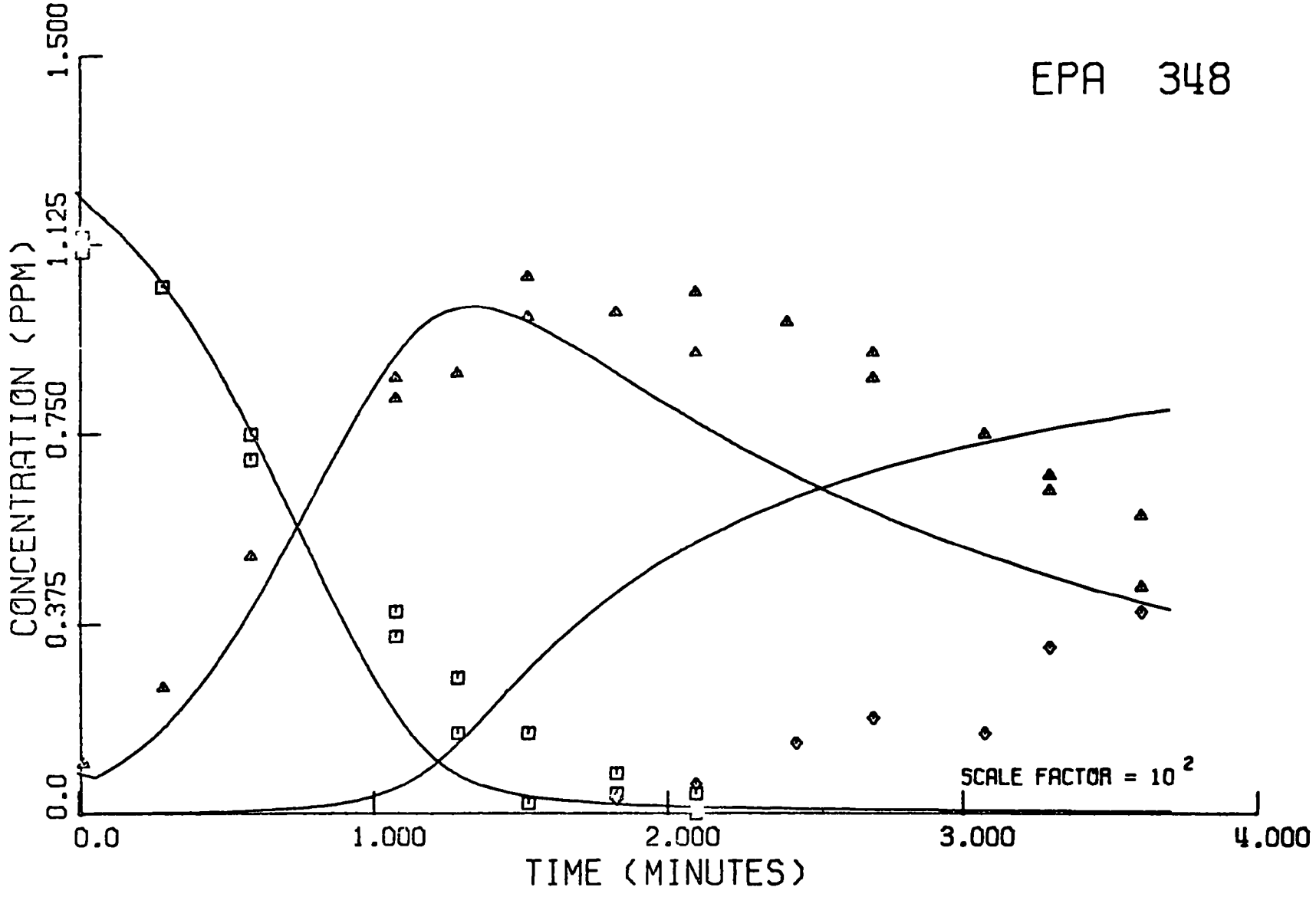

Figure 12a. EPA Run 348

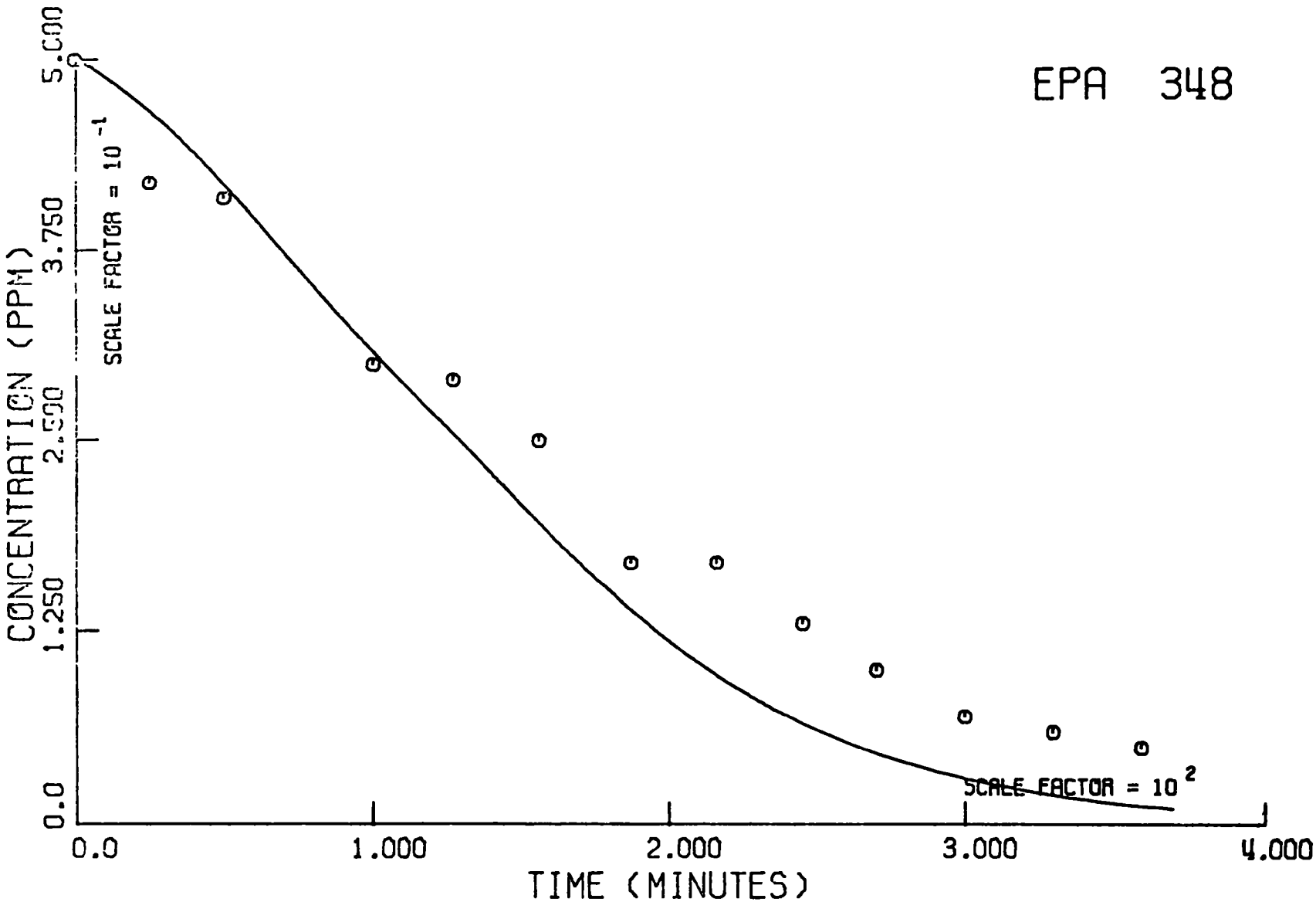

Figure 12b. EPA Run 348

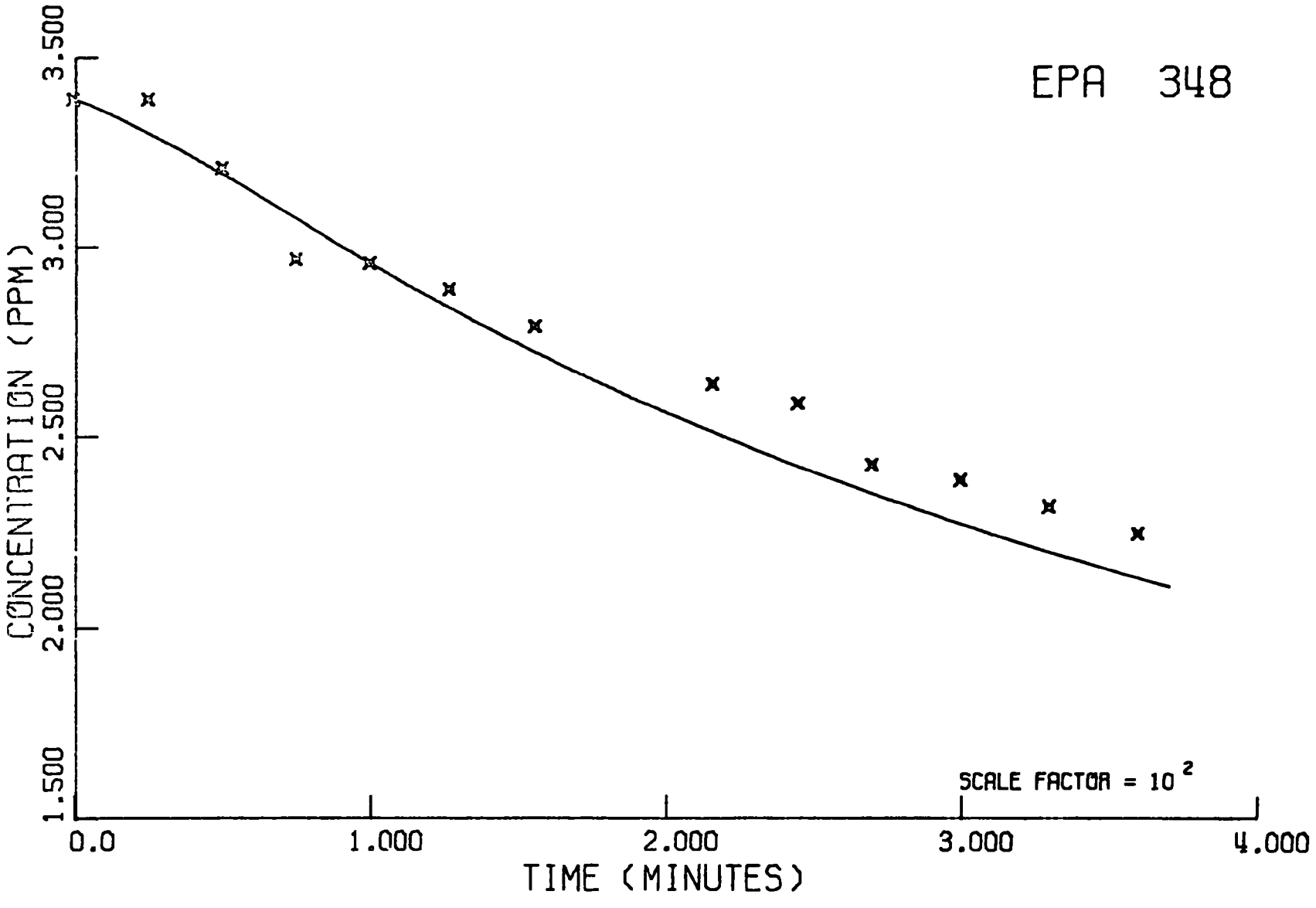

Figure 12c. EPA Run 348

FIGURE 13a.

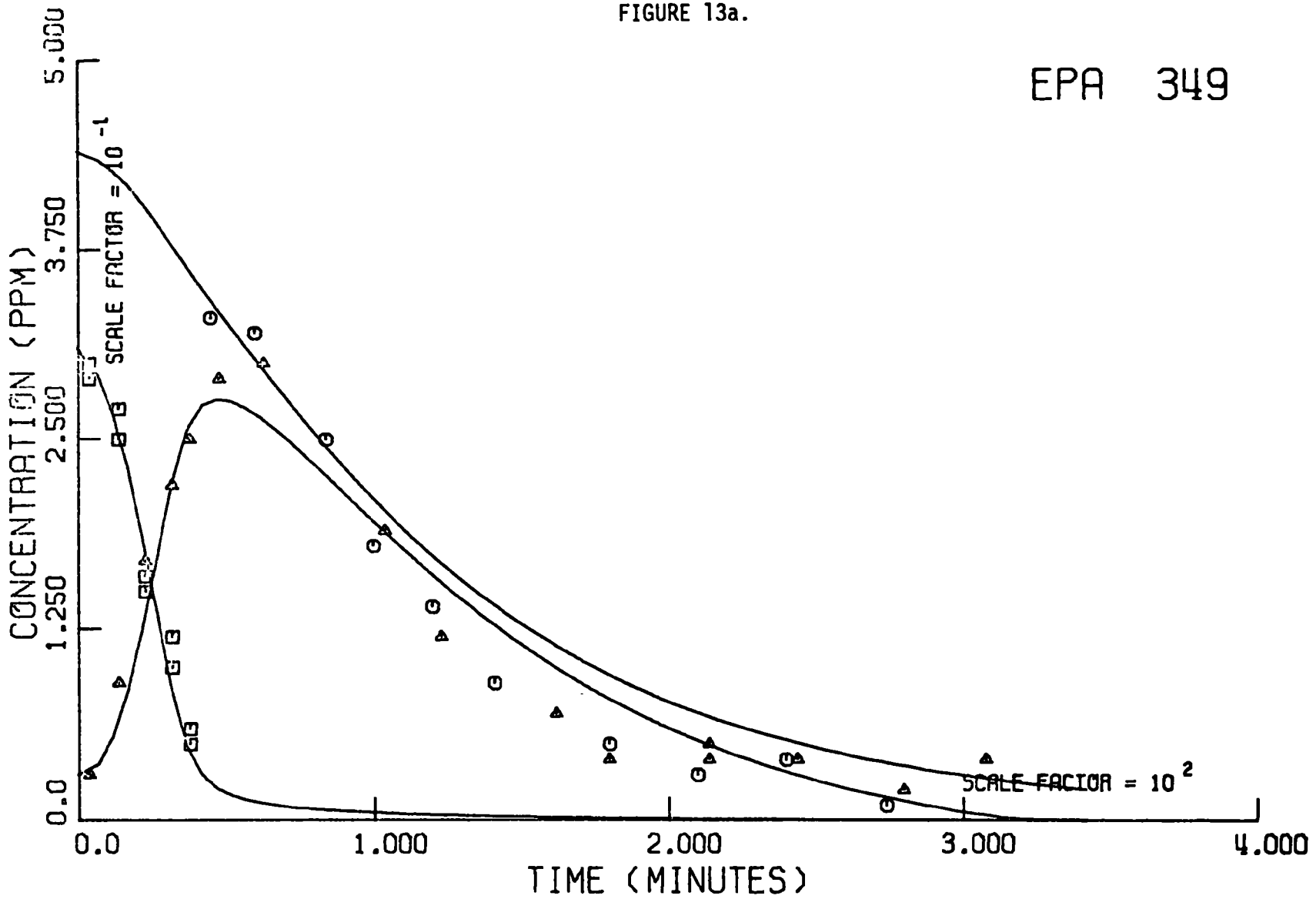

Figure 13a. EPA Run 349

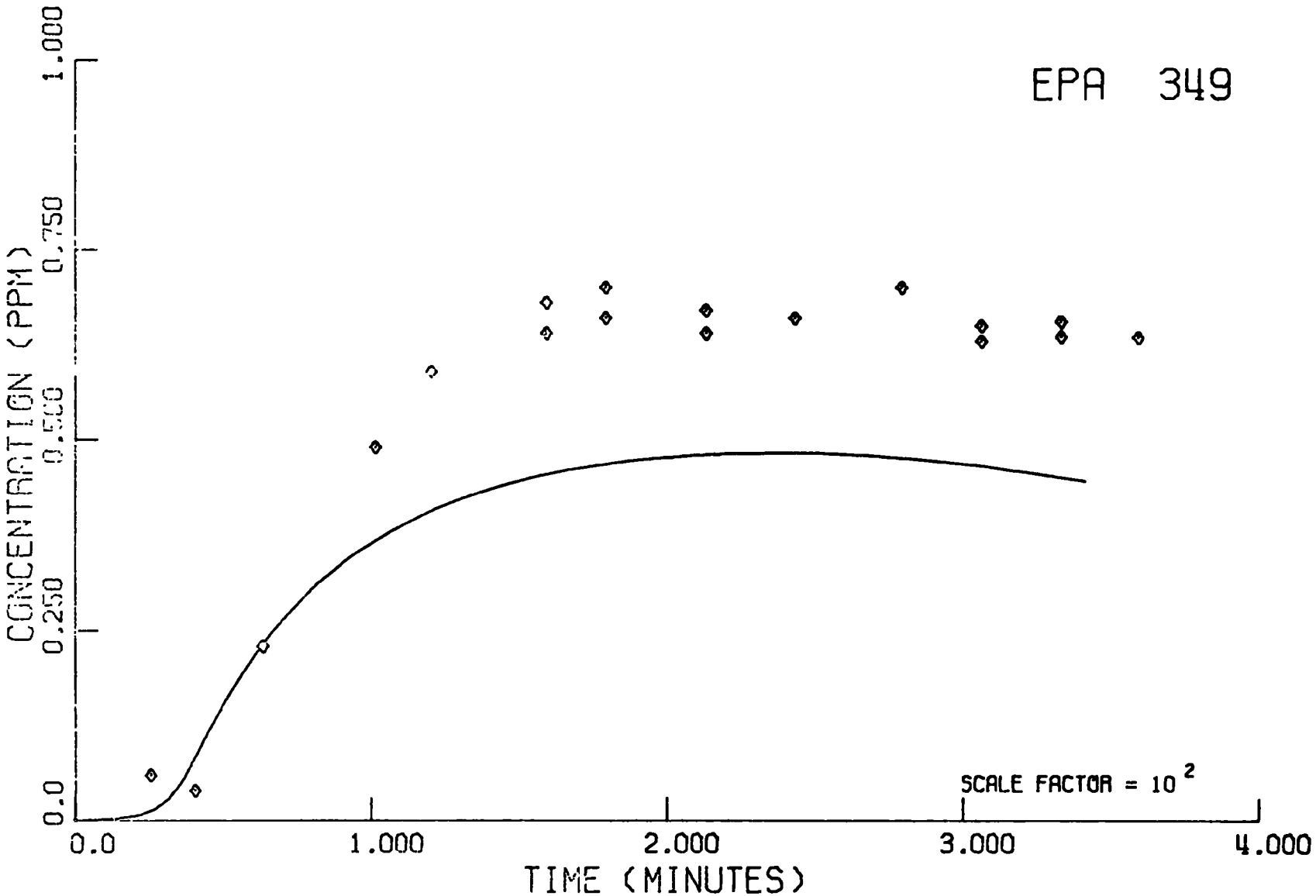

Figure 13b. EPA Run 349

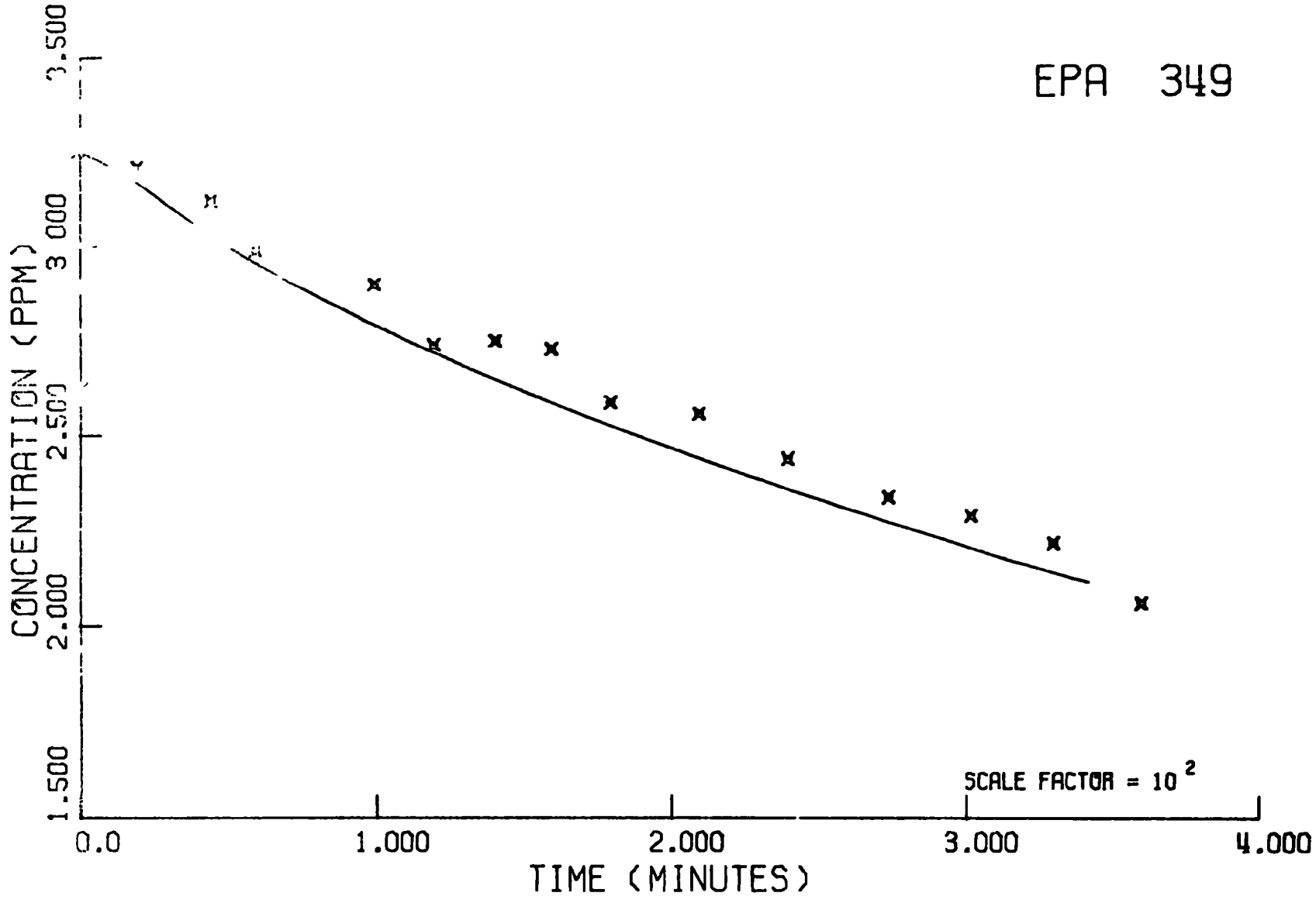

Figure 13c. EPA Run 349

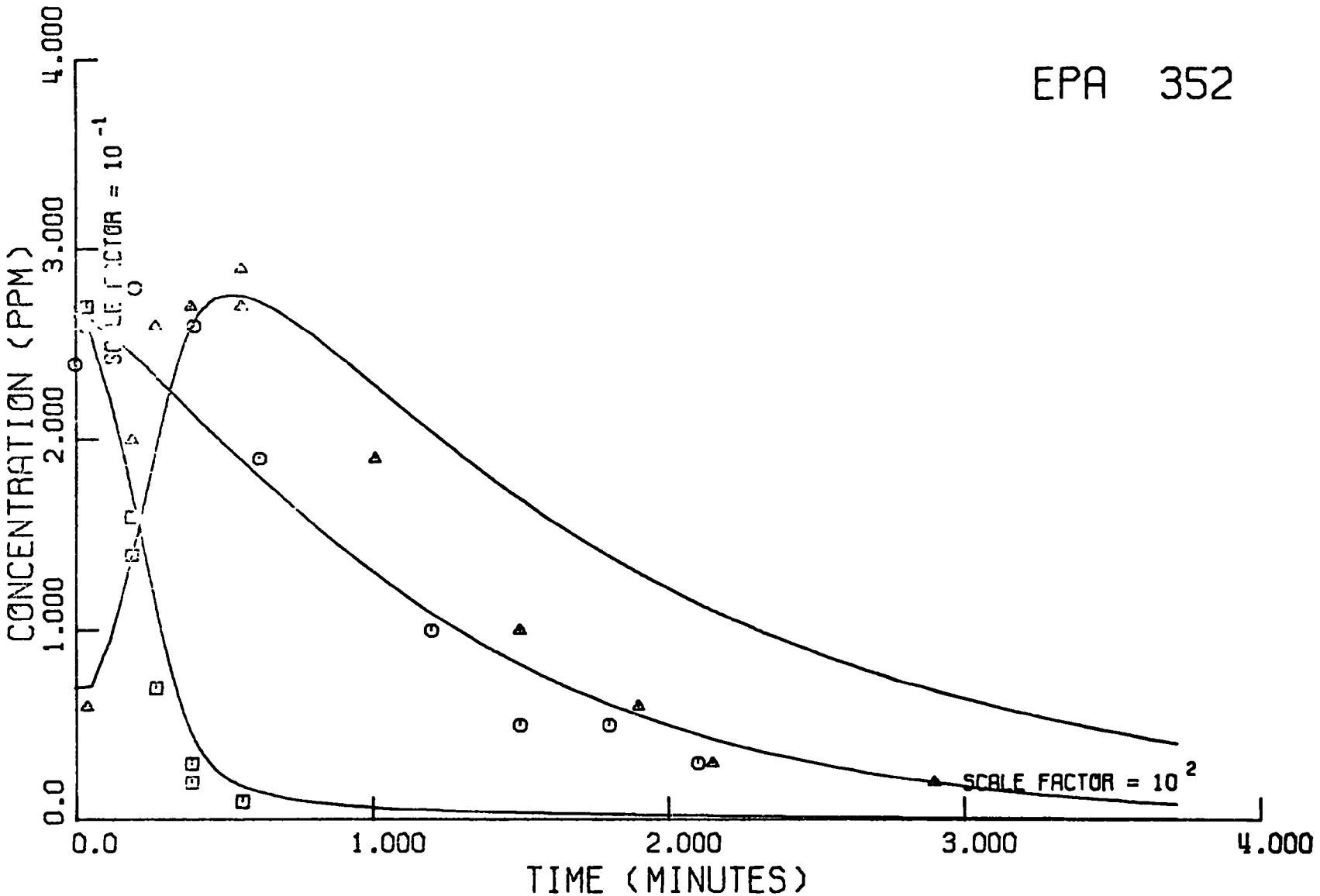

Figure 14a. EPA Run 352

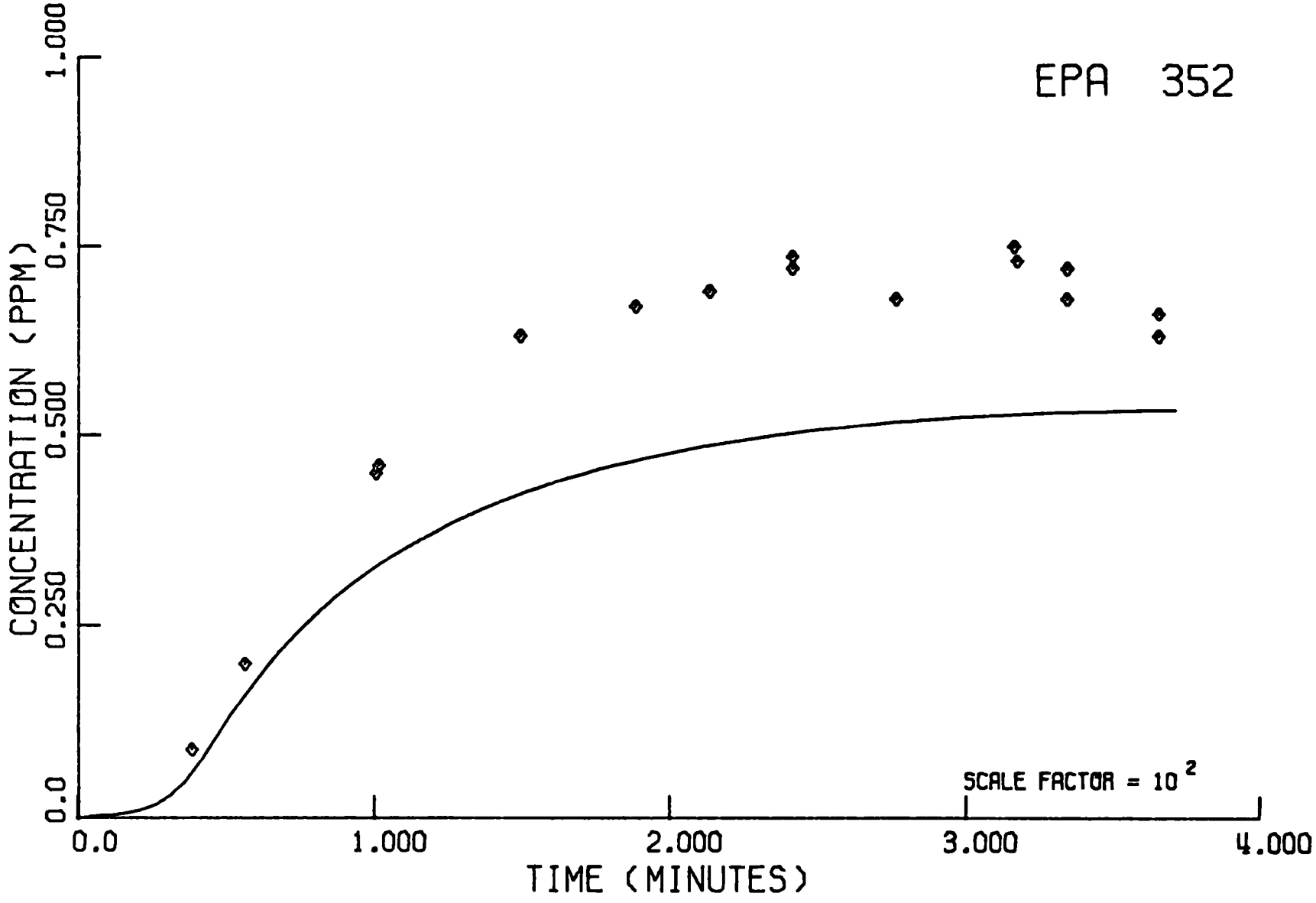

Figure 14b. EPA Run 352

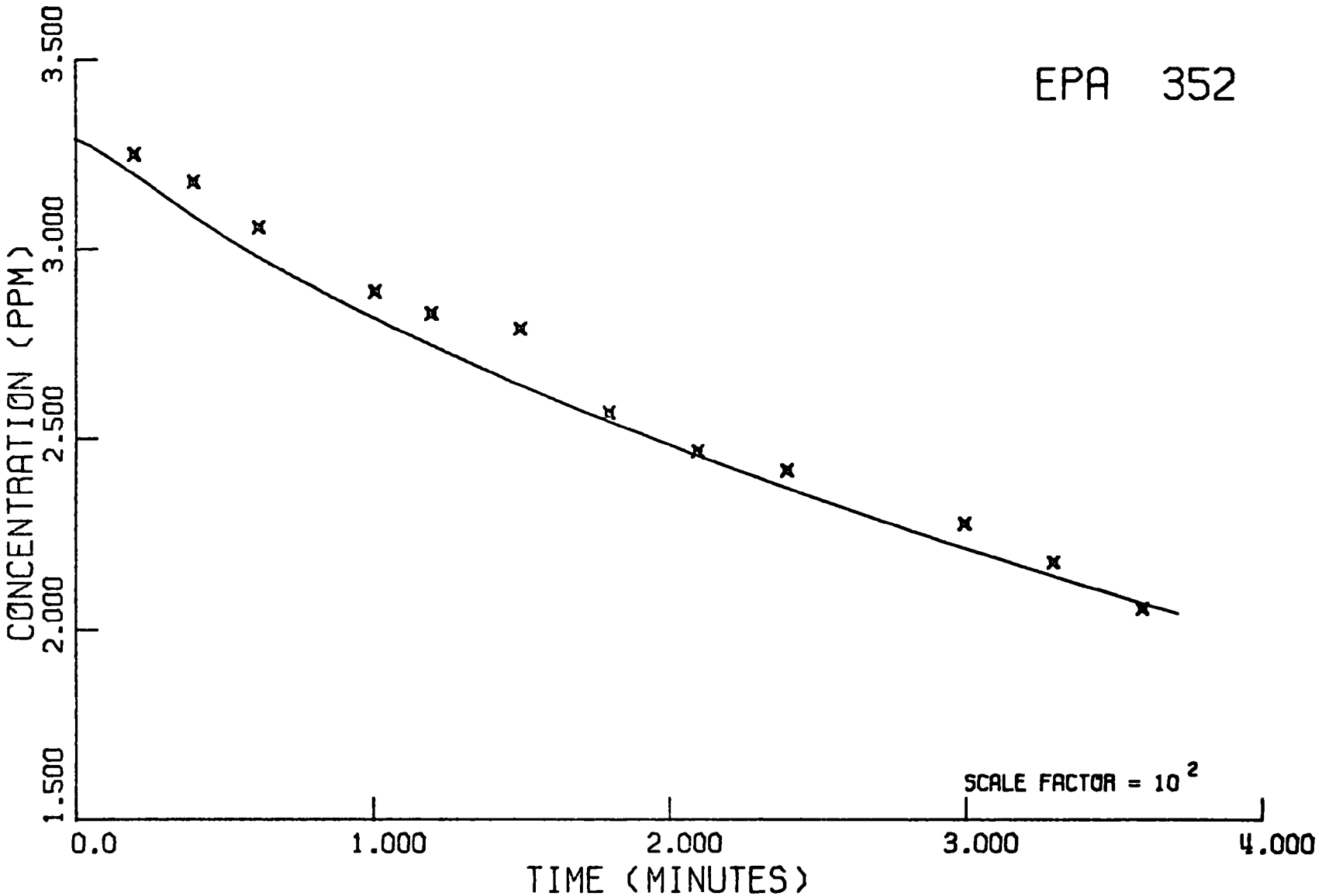

Figure 14c. EPA Run 352

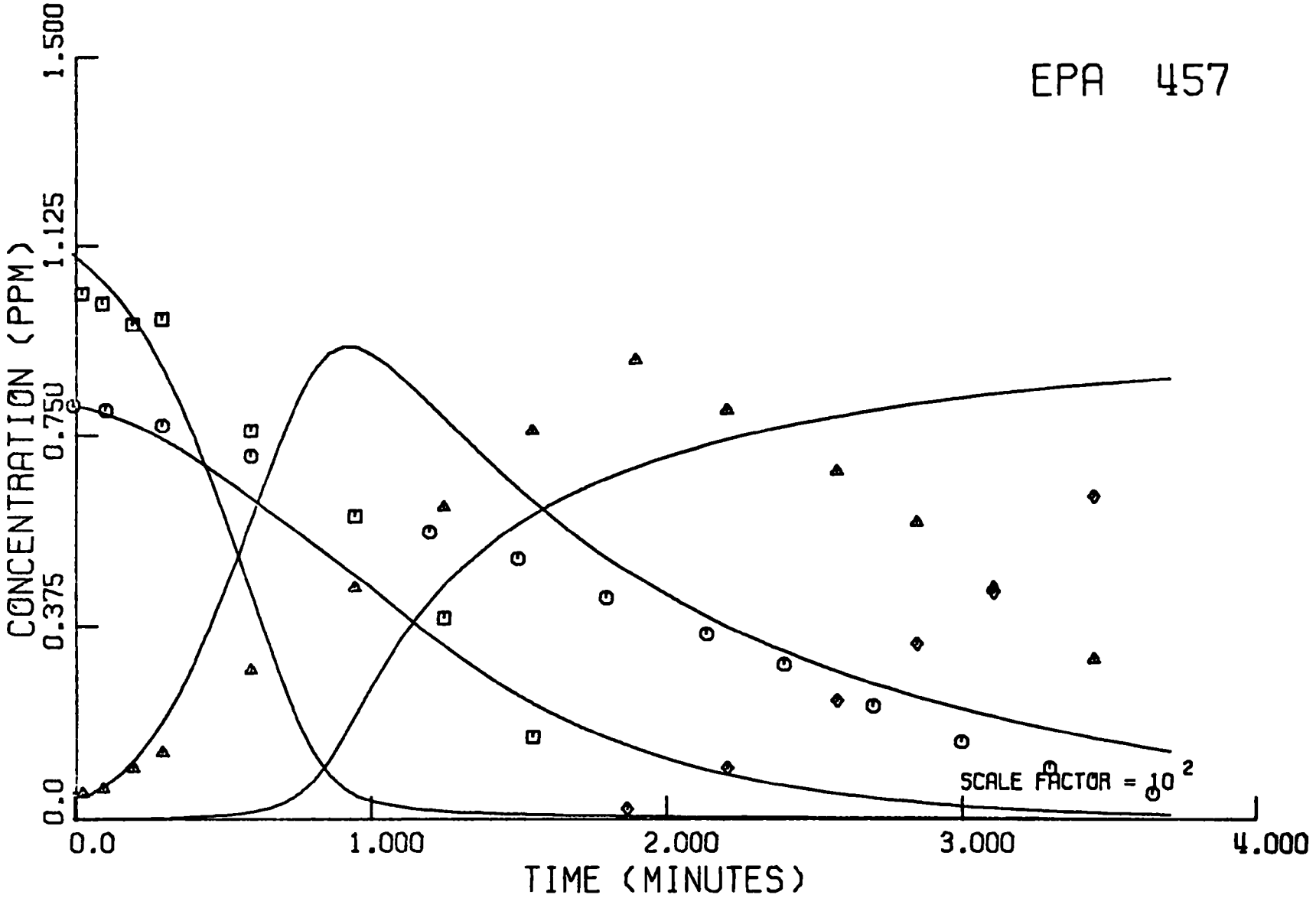

Figure 15a. EPA Run 457

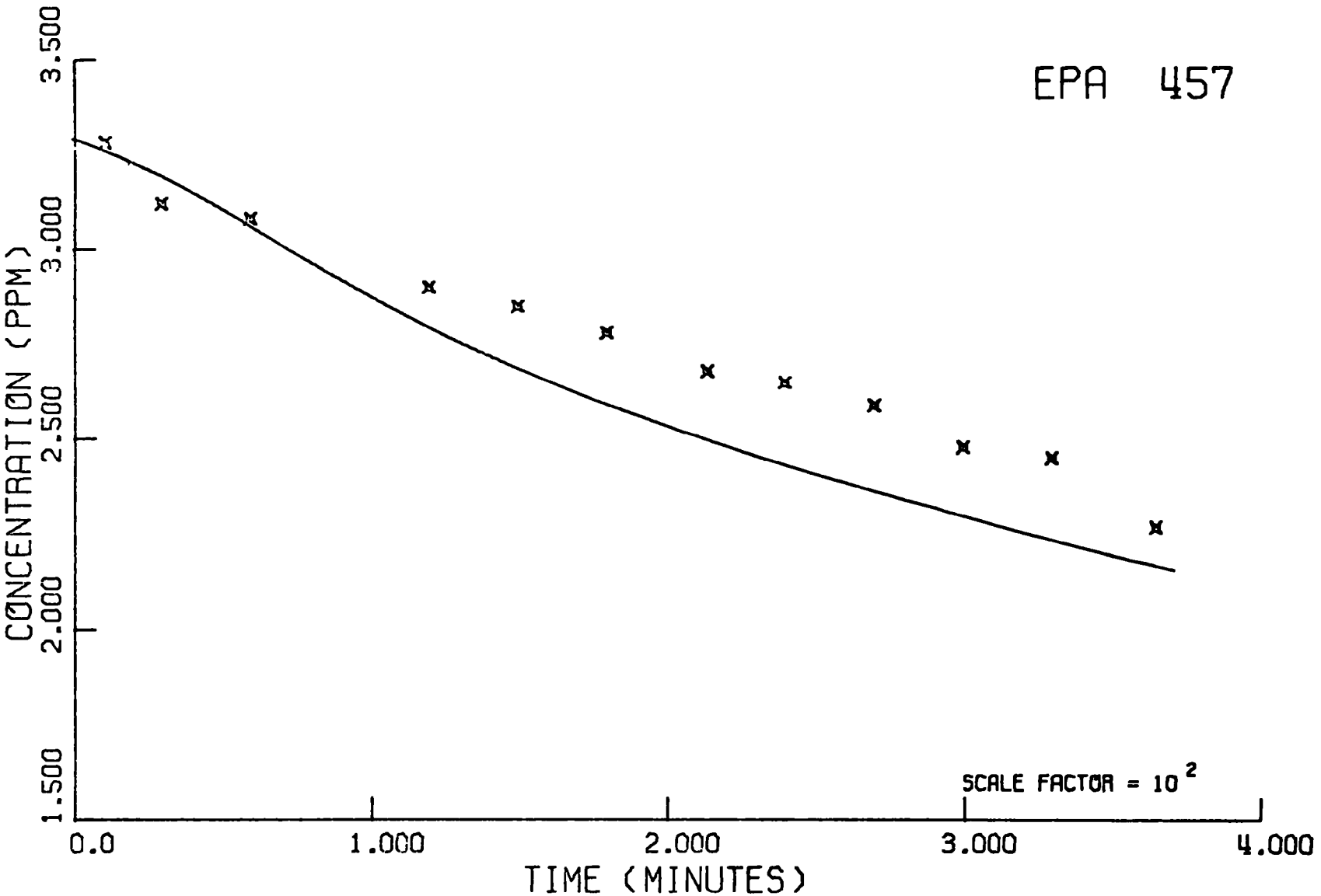

Figure 15b. EPA Run 457

$(\text{n-butane})_0/(NO_x)_0$ ratio ranges from 2.4 to 9.7 and the $(\text{propylene})_0/(NO_x)_0$ from 0.2 to 1.3.

C. Concluding Comments

The data base provided for the validation studies fulfills many of the important requirements that one would wish to place on it. The concentration levels of the hydrocarbons, nitrogen oxides, and oxidants are representative of those observed during smoggy days in Los Angeles. A variety of hydrocarbon systems have been studied; high and low reactivity hydrocarbons are represented in the data base, as are single reactants (n-butane and propylene) and a binary mixture. Initial conditions for the runs cover a broad range of hydrocarbon to nitrogen oxide ratios. This is a particularly important property of the data base if the validated mechanism is to be part of an airshed model which will be used to evaluate proposed alternative control strategies. On the whole, the accuracy and precision of the measurements is adequate, although there are a number of important expectations, which we will mention shortly.

While the data base possesses many desirable attributes, its shortcomings must be noted as well, for these determine the limits within which the model may be tested. Consider, for example, a data base for which concentrations have been determined with only passable accuracy. Wide ranging sets of parameters could easily produce predictions which fall within the broad limits of experimental uncertainty. Under such circumstances, it is not possible to satisfactorily

test the adequacy of the mechanism.

We have mentioned the most notable deficiences of the data base at one point or another in earlier sections. We summarize them here, with some comments.

(i) Inaccuracy in measurement and in analytical procedures. As noted earlier, Mast and KI readings were badly discrepant, initial NO_2 was imprecisely determined, and light intensity was not known with sufficient accuracy. Also, NO and NO_2 determinations were inaccurate at low concentrations.

(ii) Lack of measurement of certain species, both in the gas phase and on the wall. It would be of value to monitor nitric and nitrous acid concentrations in future studies. Determination of wall concentrations of these species is also desirable.

1. Discussion of the Chamber Validation Results

Turning now to the results of the validation efforts, we make a number of observations. First, we have been able to demonstrate that, in general, there is good agreement between predicted and measured concentrations. In making this statement, we must emphasize that substantial uncertainties exist in the magnitude of light intensity and initial NO_2 concentration, as well as in the values of measured concentrations of HC, NO, NO_2 and O_3, thus limiting the possibilities for critically testing the adequacy of the model. More specifically, the mechanism has shown good qualitative and quantititative agreement

with observed values of the time to the NO_2 peak and of final ozone levels reached for three different hydrocarbon-NO_x systems and for a wide range of hydrocarbon to NO_x ratios.

The predictions of the lumped mechanism agree most closely with the experimental data when the initial NO_x concentration is less than about 0.5 ppm--a condition typical of polluted atmospheres. At initial concentrations of NO_x greater than 1 ppm, the rates of oxidation of NO and accumulation of NO_2 predicted by the mechanism continue to agree well with the data; however, the rates of O_3 accumulation and NO_2 oxidation after the peak are more rapid than those observed experimentally. In many of the experiments the high initial concentrations of NO sufficiently delayed the attainment of the NO_2 peak that a maximum level of ozone was not achieved before the end of the irradiation (usually 375 minutes). As a result, while it is apparent that, under the conditions stated, the onset of O_3 accumulation predicted is somewhat premature, it is still not possible to fairly evaluate the accuracy of the simulated O_3 maximum. In those experiments during which ozone reached a maximum asymptotic level (e.g., runs 306, 325, and 349) the agreement between the data and the predicted ozone maxima are good. The rates of oxidation of propylene and n-butane predicted by the mechanism match the data uniformly well over the full range of initial concentrations and hydrocarbon/NO_x ratios studied. PAN validation data were available for only three sets of experiments, runs 325, 329, and 459. For the first two of these runs the predicted PAN concentrations are in good agreement with the data; for run 459, however, the predicted

onset of PAN formation occurs too early and the levels reached are unacceptably high, when compared with the data.

Earlier we noted that two of the experiments being used in our validation program were performed ten months after all the other data were obtained. In our attempts to validate the lumped mechanism against each of these experiments, runs 457 and 459, we have found that the predicted course of reaction, as displayed in the concentration-time traces, preceded that observed by about 80 minutes. Because, in at least one of these cases (run 459), the hydrocarbon/NO_x ratio is not appreciably different from that of another system successfully validated (run 329), it is possible that chamber conditions might have changed significantly during the 10 month interim period. In particular, the radiation intensity might have decreased substantially. While there is no way of checking, a posteriori, what changes, if any, occurred in the operating conditions of the smog chamber, this experience demonstrates the importance of continuously and accurately monitoring all the operating parameters of smog chambers.

As is apparent from the results, the data and predictions are not always in good agreement for all species over the full period of the irradiation. These discrepancies can be attributed to at least four possible sources of uncertainty:

(i) The mechanism may be incomplete. It has been our intent to include every reaction presently thought to be important to explaining smog formation in the lumped mechanism. In the future, new reactions may be discovered and/or

previously unsuspected products of elementary reactions may be found. Furthermore, reactions and products presently included in the mechanism may be shown to be unimportant (although this is unlikely).

(ii) The lumping process may introduce error. For example, we have assumed that the $CH_3\underset{OH}{C}HCH_2O_2\cdot$ radical (product of the OH-propylene reaction) to react in the same fashion as the $CH_3CH_2CH_2O_2\cdot$ radical. To the extent that their reactivities are different error will be introduced into the predictions.

(iii) There are uncertainties in the experimental data used for validation.

(iv) Chamber effects (such as surface effects) which are not accounted for in the model are potential sources of discrepancy.

(v) Not all of the rate constants are known with a high degree of certainty. Indeed, for a few of the reactions no experimental determination has yet been made of the rate constants. For the cases of those reactions for which several determinations of the rate constants have been carried out, there is often poor agreement between the various estimated values.

As a consequence of these uncertainties, we have not yet reached the point in model evaluation where we are in a position to quantitatively assess the "goodness" of the proposed mechanism or, for that matter, to draw unequivocal qualitative conclusions regarding its merits. Yet, the mechanism appears capable of predicting the concentration-time behavior of a variety of reactant systems over a wide range of initial

conditions. Clearly, however, a considerably more accurate and complete data base is required if the adequacy of the lumped mechanism is to be critically evaluated. We thus recommend that a carefully conceived experimental program be undertaken for the sole purpose of providing the data needed to carry out such an evaluation.

2. Effect of Initial Reactant Ratio on Ozone Formation

A well-documented characteristic of the photochemical smog system is that, for a series of experiments in which the ratio of initial hydrocarbon to NO_x ($NO + NO_2$) is continually decreased, either at fixed initial hydrocarbon or NO_x concentrations, the maximum concentration of ozone attained in each experiment increases, goes through a maximum, and then decreases (Hamming and Dickinson, 1966; Korth, 1966; Altshuller et al. 1967; Dimitriades, 1970; Glasson and Tuesday, 1970). While this phenomenon has been verified in many experimental smog chamber programs, no kinetic mechanism has to date been shown to be capable of predicting this behavior. Therefore, as a test of the mechanism, we undertook a study of the effect of variation in initial reactant mixtures on ozone formation.

Isopleths of maximum ozone concentration predicted by the mechanism given in Table 14 as a function of total initial hydrocarbon concentration and initial NO concentration are shown in Figure 16. The hydrocarbon mix consisted initially of 75% n-butane and 25% propylene. Further, 0.10 ppm of NO_2 was present initially in each case, so that the total initial NO_x is the sum of the indicated NO concentration

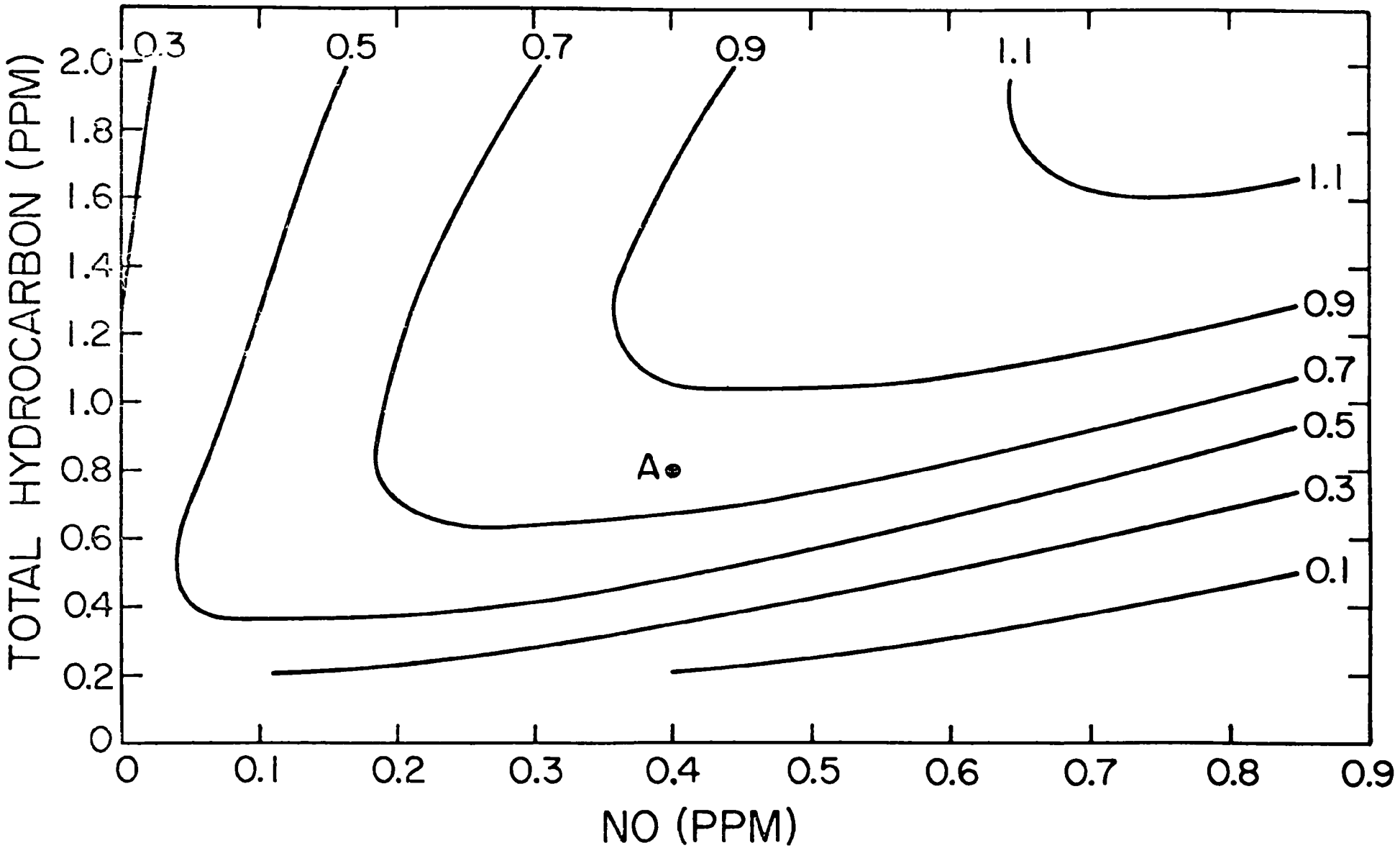

Figure 16. Isopleths of maximum ozone concentration achieved during an 8-hour irradiation of various mixtures of n-butane, propylene and NO. (NO_2 initially at 0.1 ppm.)

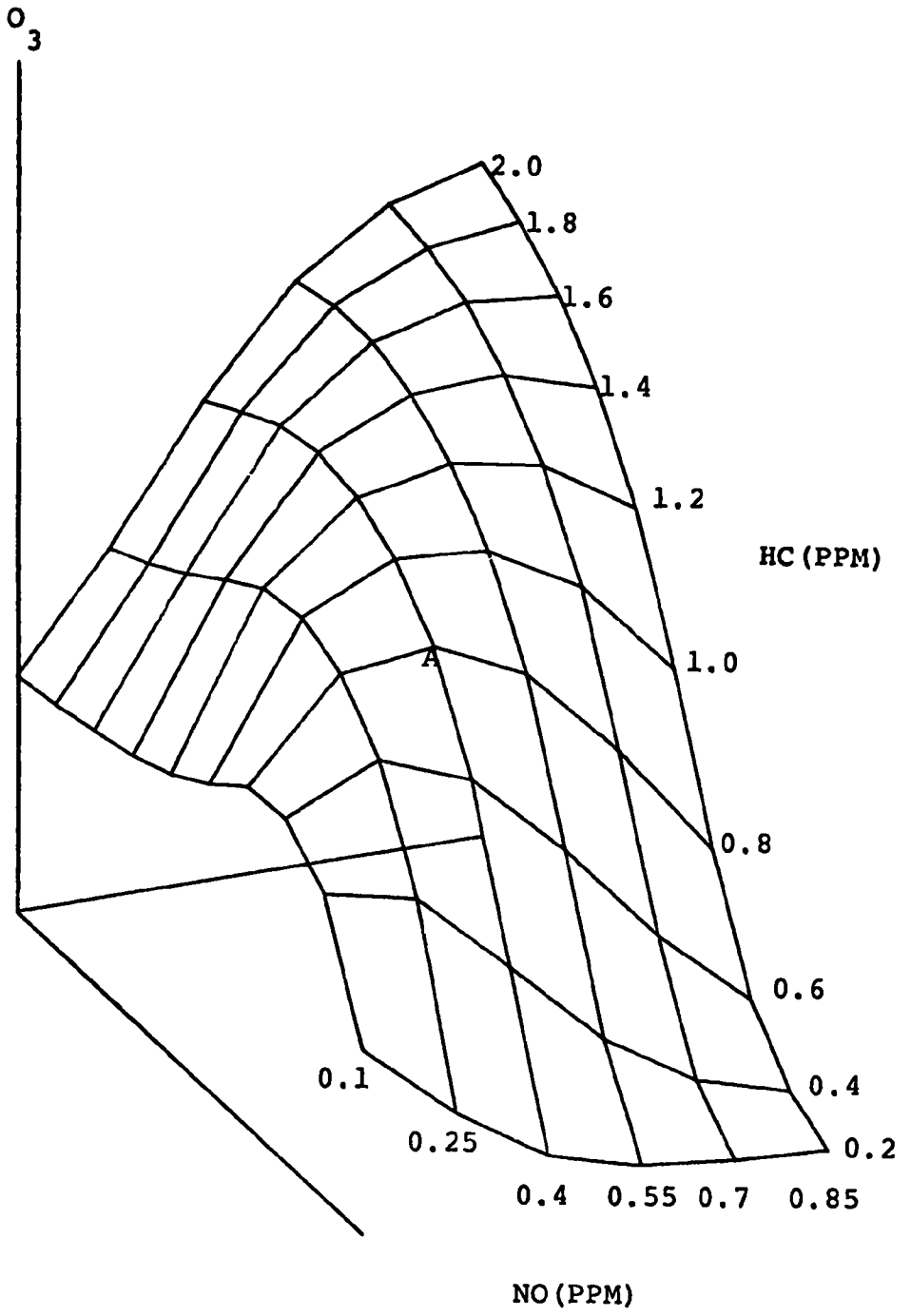

Figure 17a. Surface of maximum ozone concentrations achieved during an 8-hour irradiation of various mixtures of n-butane, propylene and NO. (NO_2 initially at 0.1 ppm). Note that the axes do not correspond to the origin of the NO-HC coordinate system. The smallest values of $[NO]_o$ and $[HC]_o$ are in the lower left hand corner of each figure.

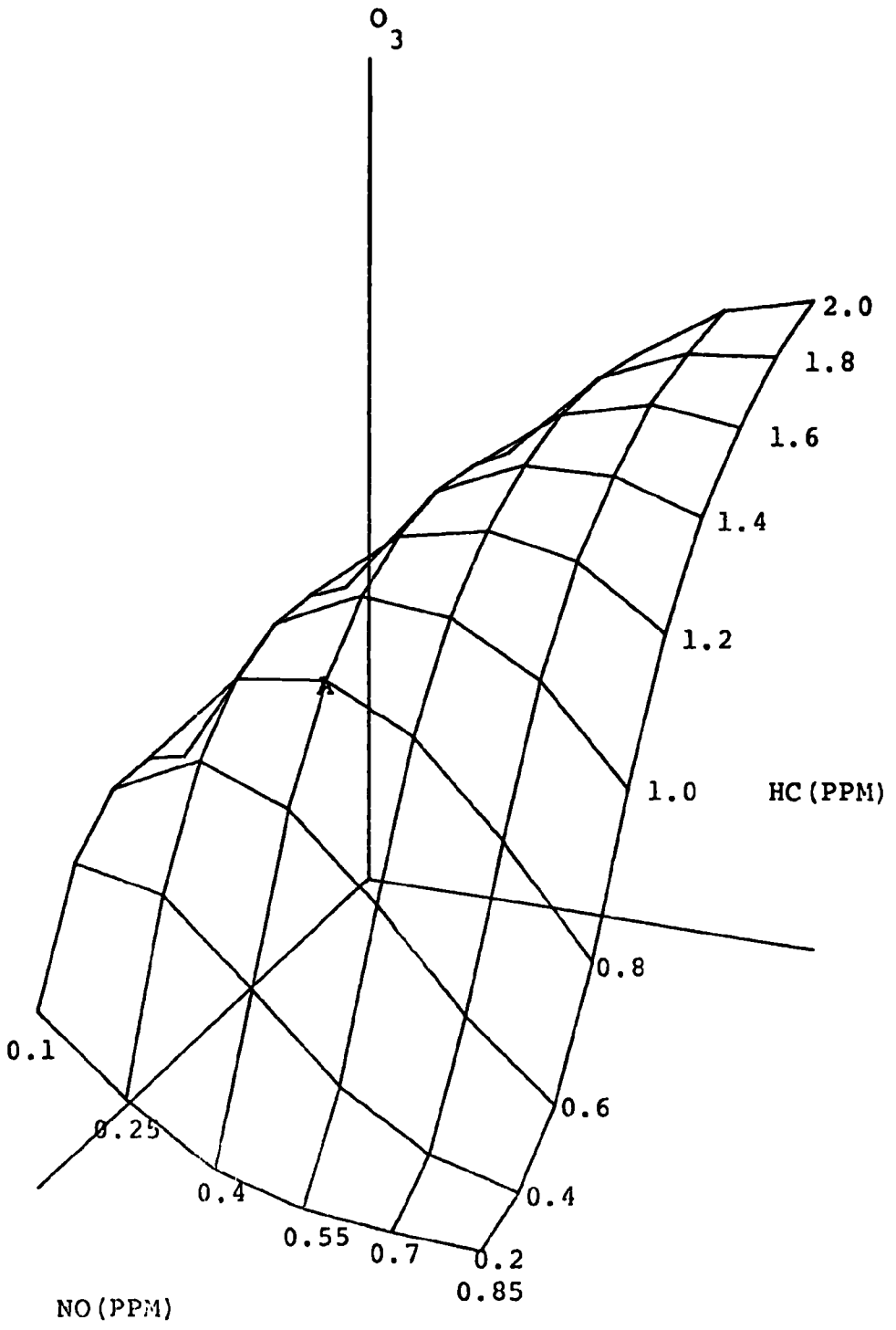

Figure 17b. Same as Figure 17a. except that axes have been rotated.

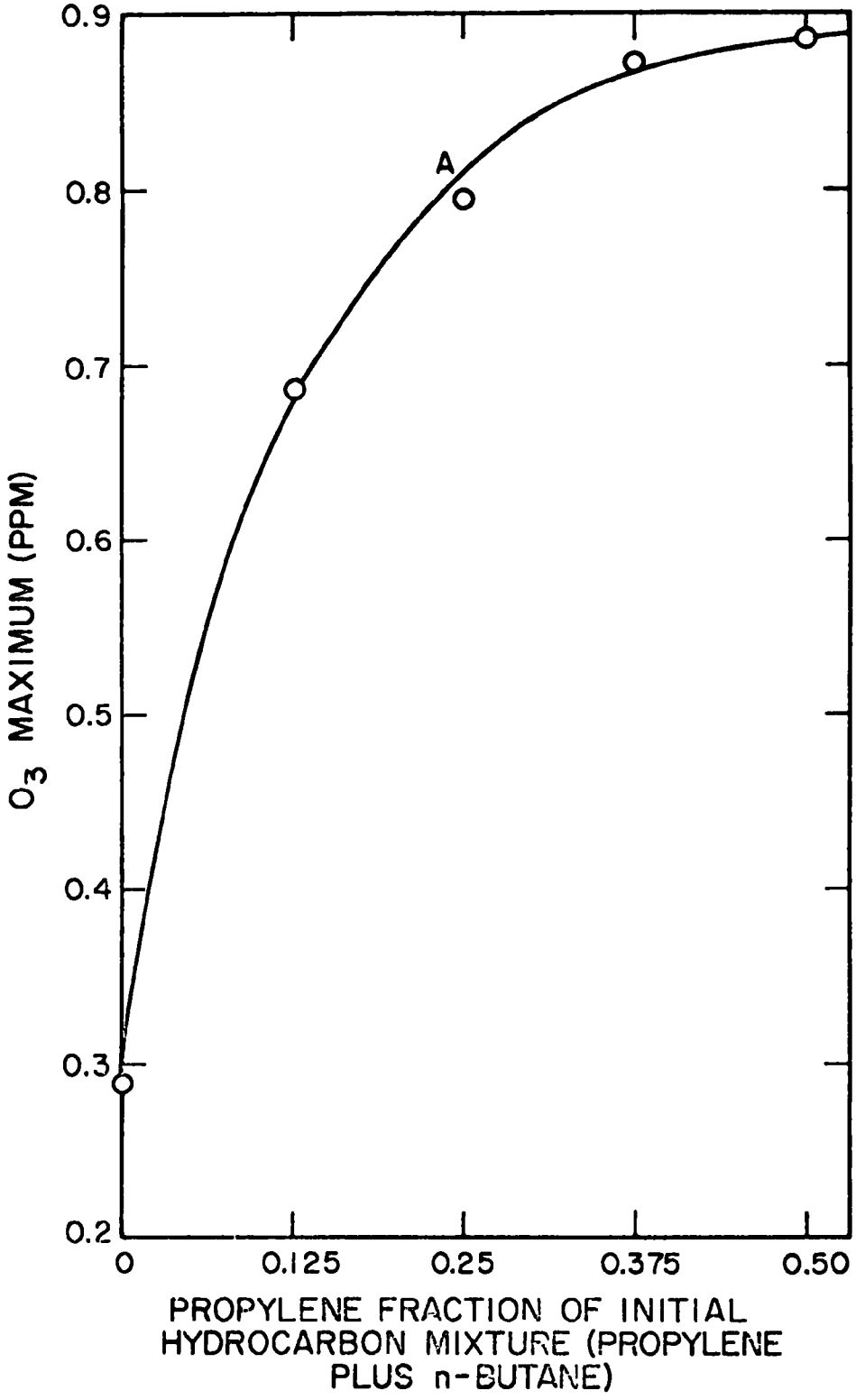

Figure 18. Maximum ozone concentration achieved during an 8-hour irradiation of an initial mixture of [HC] = 0.80 ppm, [NO] = 0.40 ppm, and [NO_2] = 0.10 ppm, for various initial mixtures of n-butane and propylene.

and 0.10 ppm. Viewed in three dimensions (Figures 17a and 17b), the predicted surface of peak ozone levels has a maximum both at fixed initial hydrocarbon and increasing initial NO and at fixed initial NO and increasing initial hydrocarbon, a result which is in qualitative agreement with the experimental results cited above. The maximum ozone ridge on the surface follows a line of constant $[HC]_o/[NO_x]_o = 2.5$ for the hydrocarbon mix and the range of concentrations studied.

The ozone values indicated in Figures 15 and 16 are the maximum values reached in eight simulated hours of irradiation. For all cases in which $[HC]_o/[NO_x]_o < 6$, the maximum ozone concentration occurred at the end of the eight hour irradiation. Thus, in these cases, the ozone levels reached after, say, ten hours of irradiation would be somewhat higher than those shown. The smallest ozone maxima are reached either under conditions of low initial hydrocarbon and high initial NO (not NO_2), or under conditions of high initial hydrocarbon and low inital NO. In the former case, high initial levels of NO inhibit the formation of ozone over the long incubation period during which NO is oxidized to NO_2; in the latter case, high levels of ozone cannot accumulate since the NO_2, which is necessary for ozone production, is rapidly consumed to form stable products. The general behavior depicted in Figures 16 and 17 matches closely that of eye irritation as a function of initial hydrocarbon and NO_x (Hamming and Dickinson, 1966; Los Angeles County Air Pollution Control District, 1971). In addition, Figures 16 and 17 exhibit the same behavior observed in a number of experimental programs (Altshuller et al., 1967; Dimitriades, 1970; Glasson and Tuesday, 1970), although precise quantitiative comparison is not possible because different systems were studied.

As noted, the results shown in Figures 16 and 17 are based on the study of an initial hydrocarbon mixture of fixed composition, 75% n-butane and 25% propylene. However, it is also important to determine the effect of altering the composition of the initial hydrocarbon mixture on the quantity of ozone formed. Figure 18 shows the maximum ozone concentration attained over an eight hour irradiation as a function of the composition of an initial hydrocarbon mixture of n-butane and propylene at $[NO]_0$ = 0.40 ppm and $[NO_2]_0$ = 0.10 ppm. We see that reduction in the olefin fraction of the mixture results in a substantial decrease in the amount of ozone formed. The reduction in ozone level is particularly effective between 0 and 10% olefin. Levy and Miller (1970) experimentally investigated this same issue through the study of organic solvent-NO_x mixtures and observed general behavior similar to that shown in Figure 18. In their study, n-octane and m-xylene were used as the low and high reactive species, respectively. They found that a reduction in the m-xylene to 3% of the solvent mixture resulted in a 32% reduction in the amount of ozone formed from that for a 50-50% mixture. Increasing the m-xylene fraction to 8% resulted in a sharp increase in the ozone level to 92% of that in the 50-50% mixture.

Point A on Figures 16 - 18 indicates the approximate composition of the Los Angeles atmosphere in 1969. At that time the ozone levels lay close to the "ridge" of observed maximum

values. While reductions in either or both of the hydrocarbon and NO emission levels can be expected to result in decreased ozone levels, it appears that hydrocarbon reductions will be more effective in reducing ozone formation since the surface of ozone levels declines more steeply in the direction of decreasing hydrocarbons at fixed NO than in the direction of decreasing NO at fixed hydrocarbon. Furthermore, a simultaneous reduction in both hydrocarbon and NO emissions will not be as effective as either of these other two routes. Finally, we see that reduction in the olefin (high reactivity) fraction in the atmosphere may also provide an attractive abatement strategy.

Based upon our results (Figures 3 - 16) and the principles of formulation, the kinetic mechanism developed here appears to hold substantial promise for incorporation in airshed models. The mechanism describes the important inorganic chemistry in detail, yet minimizes the overall number of reactions by taking advantage of the general behavior of specific groupings of similar hydrocarbons and free radicals. Further, the mechanism is free of arbitrarily assignable stoichiometric coefficients. Thus, the new lumped mechanism represents a reasonably rigorous, yet manageable, description of the photochemistry of air pollution.

VI. SUMMARY AND PROSPECTS

During the course of this project we have completed a multiplicity of tasks concerned with the mathematical modeling of photochemical smog. First, we have carried out an extensive sensitivity study for the simplified Hecht-Seinfeld mechanism. In this work we exposed the most notable shortcomings of simplified general mechanisms, the principal one being the strong dependence of predictions on the magnitudes of parameters which cannot be specified, with certainty, a priori. We then applied the simplified mechanism as an aid in planning a series of smog chamber experiments which are to be conducted this year in an outdoor chamber near Research Triangle Park, North Carolina. Specifically, we examined the effects that variations in the initial hydrocarbon to NO_x ratio, light intensity, and temperature have on such decision variables as the NO_2 and O_3 maxima and dosages. This work is noteworthy inasmuch as it marks the first time that a kinetic mechanism has been used to aid in planning an experimental program concerned with the study of air pollution. Third, we prepared an exhaustive recommendations document dealing with existing needs in the experimental and observational study of atmospheric chemical reactions. That document, which both appraises the current state of knowledge and identifies specific issues requiring further investigation, should be considered as a companion volume to this report. Finally, we have developed

and begun validation of a rigorous, yet general, lumped kinetic mechanism for photochemical smog. In the first phase of validation we have simulated the photo-oxidation of n-butane - NO_x propylene - NO_x and n-butane - propylene - NO_x mixtures when irradiated in an air-filled smog chamber. The results of this work are presented herein.

In reviewing the work carried out during the past year, we have concluded that the area of inquiry most likely to produce fruitful results is continued development of the 39-step lumped kinetic mechanism. We envision that the development program will be comprised of three groups of tasks:

(i) The validation of the mechanism using data for an aromatic-NO_x reactant system. To date we have evaluated the mechanism using an olefin, a paraffin and an olefin-paraffin mixture as reactants. However, aromatics constitute a significant percentage of the atmospheric hydrocarbon mix. It would, therefore, be extremely valuable to simulate aromatic, and aromatic-olefin-paraffin reactant systems, especially if the mechanism is ultimately to be applied in simulating atmospheric reactions.

(ii) The further validation of the mechanism using data presently being obtained at the new smog chamber research facility of the Statewide Air Pollution Research Center, University of California, Riverside. These data are being collected expressly for the purpose of

model validation and, as a consequence, should be subject to considerably less uncertainty, due to omissions and imprecisions in the data base, than have previous data.

(iii) The development of the mechanism for use as a planning tool. In Chapter II we demonstrated the utility of the simplified HS kinetic mechanism for this purpose. When satisfactorily validated, the new mechanism should prove even more useful in this regard. Before using the lumped mechanism as a planning aid, however, two tasks must be completed:

- A full sensitivity analysis of the mechanism must be made so that confidence bounds can be placed on the predictions.
- The mechanism must be extended so that variations in temperature, light intensity, and humidity can be accounted for.

It appears likely that, in the near future, the lumped kinetic mechanism will be incorporated into airshed models for use in predicting the concentrations of pollutants in urban areas. Before ambient smog can be accurately modeled, however, and, thus, before currently existing mechanisms are so used, the composition and reactivity

of the atmospheric organic mix must be carefully determined. The organic species in the atmosphere can then be rationally segmented into a number of mathematical "lumps". So that rational separation can be carried out, we recommend that

- the concentration distribution of organics in polluted air be determined from existing data
- alternative lumping techniques both for chamber and atmospheric applications be investigated
- the physical reasons for observed synergisms* be explicated.

To summarize, in this project we have demonstrated the shortcomings and limitations of simplified kinetic mechanisms and made progress in determining the level of complexity required in kinetic mechanisms in order to produce accurate predictions. A very promising kinetic representation has been developed, and with further work, this mechanism may well be of use both in planning experimental studies to be carried out in, and as part of, airshed simulation models which will ultimately find use in the evaluation of alternative emission control strategies.

---

* Synergism in this case refers to the change in the rate of oxidation of NO observed when mixtures of two or more hydrocarbons are irradiated in a system of NO_x and air relative to the rate which occurs when an NO_x-air system containing a single hydrocarbon is irradiated.

References

Altshuller, A. P., Kopczynski, S. L., Lonneman, W. A., Becker, T. L., Slater, R., *Environ. Sci. Technol.*, 1, 899 (1967)

Altshuller, A. P., Kopczynski, S. L., Lonneman, W. A., Sutterfield, F. D., Wilson, D. L., *Environ. Sci. Technol.*, 4, 44 (1970)

Altshuller, A. P., Kopczynski, S. L., Wilson, D., Lonneman, W., Sutterfield, F. D., *J. Air Pollut. Contr. Assn.*, 19, 791 (1969).

Bufalini, J. J., Gay, B. W., Jr., Kopczynski, S. L., *Environ. Sci. Technol.*, 5, 333 (1971).

Davis, D. D., Wong, W., Payne, W. A., Steif, L. F., "A Kinetics Study to Determine the Importance of HO_2 in Atmospheric Chemical Dynamics; Reactions with CO," presented at the Symposium on "Sources, Sinks, and Concentrations of CO and CH_4 in the Earth's Environment," St. Petersburg Beach, Fla., August 1972.

Demergian, K. L., Kerr, J. A., Calvert, J. G., The Mechanism of Photochemical Smog Formation, in press (1973).

Dimitriades, B., "On the Function of Hydrocarbon and Nitrogen Oxides in Photochemical Smog Formation," U.S. Department of the Interior, Bureau of Mines, Report 7433, 1970.

Dodge, M. C., private communication, Environmental Protection Agency, Research Triangle Park, N. C., 1973.

Eschenroeder, A. Q., Martinez, J. R., Advances in Chemistry, 113, Am. Chem. Soc., Washington, D.C., 1972

Gay, B. W., Jr., Bufalini, J. J., *Environ. Sci. Technol.*, 5, 422 (1971).

Gear, C. W., *Commun. of the Ass. for Computing Machinery*, 14, 176 (1971).

Glasson, W. A., Tuesday, C. S., *Environ. Sci. Technol.*, 4, 37 (1970).

Godt, H. C. Jr., Quinn, J. F., *J. Am. Chem. Soc.*, 78, 1461 (1956).

Hamming, W. J., Dickinson, J. E., *J. Air Pollut. Contr. Assn.*, 16, 317 (1966).

Hecht, T. A., "Further Validation of a Generalized Mechanism Suitable for Describing Atmospheric Photochemical Reactions," Report 72-SAI-26, Systems Applications, Inc., 9418 Wilshire Blvd., Beverly Hills, Calif., 1972.

Hecht, T. A., Seinfeld, J. H., *Environ. Sci. Technol.*, 6, 47 (1972).

Hill, A. C., *J. Air Pollut. Contr. Assn.*, 21, 341 (1971).

Johnston, H. S., Pitts, J. N., Jr., Lewis, J., Zafonte, L., Mottershead, T., "Atmospheric Chemistry and Physics," Project Clean Air, Task Force Assessments, Vol. 4, Univ. of California (1970).

Kopczynski, S. L. private communication, Environmental Protection Agency, Research Triangle Park, N. C., 1972.

Korth, M. S., "Effects of the Ratio of Hydrocarbon to Oxides of Nitrogen in Irradiated Auto Exhaust," U.S. Department of Health, Education and Welfare, Cincinnati, Ohio (1966).

Leighton, P. A., Photochemistry of Air Pollution, Academic Press, New York, N.Y., 1961

Levy, A., Miller, S. E., "Role of Solvents in Photochemical Smog Formation," Report 799, Battelle Memorial Institute, Columbus, Ohio, 1970.

Morris, E. D., Jr., Niki, H., *J. Phys. Chem.*, 75, 3640 (1971).

Niki, H., Daby, E., Weinstock, B., Advances in Chemistry, 113, Am. Chem. Soc., Washington, D.C., 1972.

"Profile of Air Pollution," Air Pollution Control Distric, County of Los Angeles, Los Angeles, Calif. (1971).

Schuck, E. A., Stephens, E. R., Schrock, P. R., *J. Air Pollut. Contr. Assn.*, 16, 695 (1966).

Wayne, L. G., Weisburd, M., Danchick, R., Kokin, A., "Final Report--Development of a Simulation Model for Estimating Ground Level Concentrations of Photochemical Pollutants," Technical Memorandum, System Development Corporation, Santa Monica, Calif., 1971.

APPENDIX A

Analog and Digital Sensitivity Analysis Techniques as Applied to the Hecht-Seinfeld Mechanism

R. Schainker
D. Stepner
C. Wells

Prepared by*

Systems Control, Inc.
260 Sheridan Avenue
Palo Alto, California 94306

for

Systems Applications, Inc.
950 Northgate Drive
San Rafael, California 94903

*Minor editing carried out at SAI

I. INTRODUCTION

This report summarizes the work accomplished under Phase I of Contract No. SAI-72-7, between Systems Applications, Inc., and Systems Control, Inc., dated July 15, 1972.

The two major objectives of Phase I were (1) to determine the feasibility of using an analog computer to assist in the estimation of photochemical reaction rate parameters, and (2) to evaluate the feasibility of, develop a methodology for, and perform sensitivity analyses for the H-S kinetic mechanism using the digital computer.

In the following sections of this appendix, the model used, the analog sensitivity experiments, the digital sensitivity methodology, and the digital sensitivity experiments are discussed and conclusions and recommendations are presented.

II. PHOTOCHEMICAL SMOG MODEL

The Hecht-Seinfeld (Seinfeld et al., 1971; Hecht and Seinfeld, 1972) kinetic mechanism for describing photochemical smog formation was used as the basis for the feasibility studies performed in Phase I. This mechanism was used because it appeared to be the best available at the time at which this work was undertaken. The complete mechanism is summarized in Table I of Chapter II. The kinetic and stoichiometric parameters for the toluene-NO_x and propylene-NO_x reactant systems, for which the studies reported here were carried out, can be found in Tables 2 and 6 of Chapter II.

The following assumptions were made in formulating the mass continuity

equations for the reaction mechanism:

1. Smog chamber is well mixed
2. Volumetric loss rate due to sample withdrawal is constant
3. Initial concentration of reactants are known with certainty

The resulting eleven unsteady-state mass balances that represent the kinetic model are given below:

Symbols used

$y_1 = NO_2$ $\quad$ $y_6 = OH\cdot$

$y_2 = NO$ $\quad$ $y_7 = HO_2\cdot$

$y_3 = O_3$ $\quad$ $y_8 = RO_2\cdot$

$y_4 = HC_1$ $\quad$ $y_9 = HNO_2$

$y_5 = HC_2$ $\quad$ $y_{10} = NO_3$

$y_{11} = O$

Unsteady-state mass balances

(1) NO_2

$$\dot{y}_1 = - R_1 + R_3 - R_4 + 2R_5 - R_6 - R_7 + R_8 + R_{11} - R_{12} - R_{17} + R_{16} - R_{21} - Qy_1$$

(2) NO

$$y_2 = R_1 - R_3 - R_5 - R_7 + R_8 + R_9 - R_{11} - R_{16} - Qy_2$$

(3) O_3

$$\dot{y}_3 = R_2 - R_3 - R_4 - R_{15} - R_{20} - Qy_3$$

(4) HC_1

$$\dot{y}_4 = - R_{13} - R_{14} - R_{15} - Qy_4$$

(5) HC_2

$$\dot{y}_5 = - R_{18} - R_{19} - R_{20} - Qy_5$$

(6) OH·

$$\dot{y}_6 = - R_{10} + R_9 + R_{11} - R_{14} - R_{19} + \varepsilon R_{16} - Qy_6$$

(7) HO_2·

$$\dot{y}_7 = R_{10} - R_{11} - R_{12} - Qy_7$$

(8) RO_2·

$$\dot{y}_8 = \alpha R_{13} + \beta R_{14} + \gamma R_{15} - R_{16} - R_{17} + \alpha_2 R_{18} + \beta_2 R_{19} + \gamma R_{20} - Qy_8$$

(9) HNO_2

$$\dot{y}_9 = 2R_7 - 2R_8 - R_9 + R_{12} - Qy'_9$$

(10) NO_3

$$\dot{y}_{10} = R_4 - R_5 - R_6 - Qy_{10}$$

(11) O

$$\dot{y}_{11} = R_1 - R_2 - R_{13} - R_{18} - Qy_{11}$$

Rate functions

$R_1 = RK_1 \cdot y_1$

$R_2 = RK_2 \cdot y_{11}$

$R_3 = RK_3 \cdot y_2 \cdot y_3$

$R_4 = RK_4 \cdot y_1 \cdot y_3$

$R_5 = RK_5 \cdot y_2 \cdot y_{10}$

$R_6 = RK_6 \cdot y_1 \cdot y_{10}$

$R_7 = RK_7 \cdot y_2 \cdot y_1$

$R_8 = RK_8 \cdot y_9^2$

$R_9 = RK_9 \cdot y_9$

$R_{10} = RK_{10} \cdot y_6$

$R_{11} = RK_{11} \cdot y_2 \cdot y_7$

$R_{12} = RK_{12} \cdot y_7 \cdot y_1$

$R_{13} = RK_{13} \cdot y_4 \cdot y_{11}$

$R_{14} = RK_{14} \cdot y_4 \cdot y_6$

$R_{15} = RK_{15} \cdot y_4 \cdot y_3$

$R_{16} = RK_{16} \cdot y_2 \cdot y_8$

$R_{17} = RK_{17} \cdot y_1 \cdot y_8$

$R_{18} = RK_{18} \cdot y_5 \cdot y_{11}$

$R_{19} = RK_{19} \cdot y_5 \cdot y_6$

$R_{20} = RK_{20} \cdot y_3 \cdot y_5$

$R_{21} = RK_{21} \cdot y_1$

Two methods of solution of these reaction equations were investigated in Phase I, one involving use of the analog computer, the second involving use of the digital computer. In both cases the purpose was to determine the feasibility of performing sensitivity calculations using the device in question.

In past work it has been standard practice to assume that the free radical reactions (reactions 6-11) are always in an equilibrium state (Seinfeld, et al, 1971; Hecht and Seinfeld, 1972). If this assumption is made, the set of eleven differential equations reduces to a set of four differential equations (for a single hydrocarbon system) and six non-linear algebraic equations. However, analog computers are not well suited to solving non-linear algebraic equations. It was thus decided to solve equations (1-11) as a set of eleven simultaneous differential equations. In the course of this work it was shown that there is no appreciable difference between the simulated time histories of the measurable chemical species using the free radical equilibrium assumption and the time histories generated from the solution of the full set of unsteady-state material balances.

In the following sections the analog and digital sensitivity results are outlined. Working wiring diagrams and pot setting sheets for the analog computer runs have been furnished directly to EPA.

III. ANALOG SENSITIVITY RUNS

The NASA Ames EAI 8800 Hybrid computer was used on a no-cost contract basis to solve the eleven differential equations describing photochemical

reaction kinetics.

Analog Computer System Description

The EAI 8800 computer is one of the largest and most accurate analog computers built. It is in nearly constant use at NASA Ames and undergoes daily preventive maintenance and calibration. The analog portion of the machine consists of the following analog computer hardware: 240 precision potentiometers, 60 high gain amplifiers, 60 integrating amplifiers, 60 summing amplifiers, 48 multipliers, and numerous additional analog computer components, e.g., resolvers, clocks, logic circuits, etc. The computer has an accuracy of 1 part in 10,000, which is essential in developing a valid solution to the H-S Photochemical Smog Model. Time scaling capacitor logic of 0.01, 0.1, 1.0, 10, 100, 1000 is also available.

The computer system has several integral output devices including: X-Y plotter, 4 variable CRT display, and multiple strip chart recorders. In addition, potentiometer settings can be made through the digital computer portion of the hybrid system.

Programming the H-S Photochemical Smog Model

Time and amplitude scaling are basic difficulties inherent in programming analog computers. Time scaling is relatively straightforward and is attained simply by multiplying the right hand side of the differential equations by the appropriate scaling factor. Amplitude scaling, however, must be performed on the output of each amplifier. Amplitude scaling can be accomplished by normalizing the differential equations by the maximum

voltage level of the particular machine. In the H-S Photochemical Smog Model normalization factors were obtained directly from the digital computer solutions. Without this information, a successful simulation of the mechanism would have been much more difficult to obtain.

Criteria Used in Sensitivity Runs

The analog computer was time scaled to produce a solution to the H-S mechanism in from 0.4 to 40 seconds, depending on the integration speed settings on the operator's panel. The 40 second runs were used for producing a solution on the X-Y plotter. The 0.4 second runs were used to display the solution on the CRT in high speed repetitive operation.

The objective of the analog computer experiments was to display a solution to the photochemist so that, based on his judgment, parameters could be adjusted to obtain the best possible fit to experimental data. After several iterations in this mode of operation, it was apparent that some form of goodness-of-fit criterion should be selected to compare different solutions.

The major element of the criteria finally selected was the time to the NO_2 peak, T. Other elements in the criteria included maximum O_3 values, and the time at which the NO and NO_2 concentrations were equal (toluene system only).

The utility of using phase plane plots to display characteristics of the solution was examined. A phase plane plot is a cross plot of one dependent variable versus another, for example NO versus NO_2. The time axis is represented parameterically along the trajectory which begins at

the initial condition (I.C.) and ends at the equilibrium condition (E.C.). The location of the maximum NO_2 is readily apparent in this type of display and, in cases where flat peaks occur in the time domain plots, the phase plane plot often greatly sharpens the peak. An example of a phase plane plot for (NO_2, NO) is shown below:

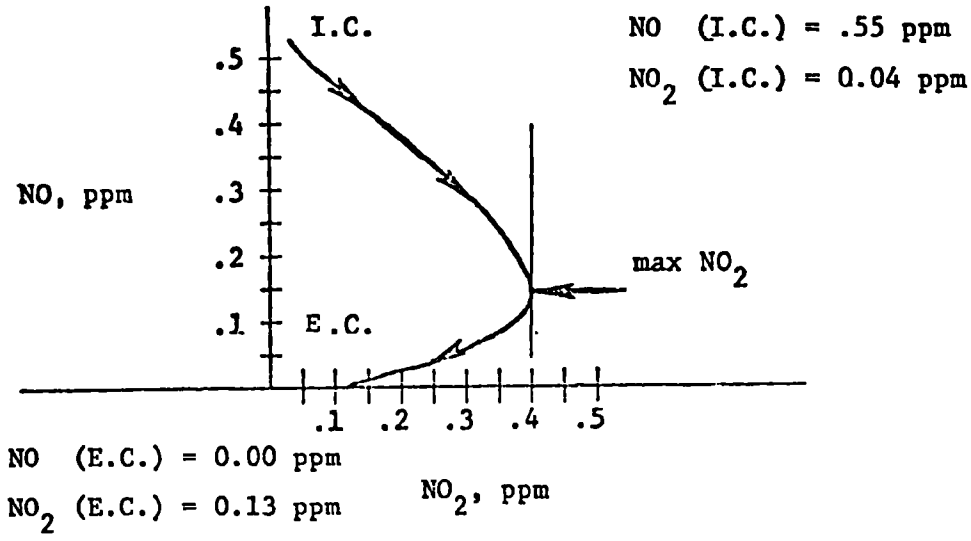

Figure 1. Phase Plane Plot of NO/NO_2 (Toluene System)

In this figure the trajectory begins at the initial condition I.C. point (0.04, 0.55) and terminates at the equilibrium condition E.C. (0.13, 0.00). The location of maximum predicted NO_2 could be used as a sensitive indicator when compared with experimentally measured values of (NO_2, NO).

This type of plot is frequently used in the study of non-linear systems and, in particular, is used extensively in the development of control systems for non-linear systems. Phase plane trajectory analysis could prove useful in the preliminary validation of smog chamber experiments. The phase plane diagram based on the measured data from a smog chamber run could be plotted and the model outputs compared in the phase

plane instead of the state-time plane.

In this task of Phase I it was shown that the H-S photochemical smog model could be solved on the analog computer for two HC species, namely toluene and propylene. For both systems analog sensitivity studies were performed. Time history plots of the four measured variables, NO_2, NO, O_3, and HC, were obtained for perturbations about nominal rate constant values and for different initial conditions. The resulting plots were forwarded to Systems Applications, Incorporated for further analysis.

IV. DIGITAL SENSITIVITY RUNS

Task II of Phase I of the contract included the development of the digital sensitivity functions for subsequent use in the SCI maximum likelihood identification program. The toluene system was used as the test case.

As indicated earlier, a solution to the set of 11 differential equations was required in order to scale the analog computer program. For this reason, all 11 differential equations were solved simultaneously on the digital computer. Several integration programs were examined for possible use in obtaining solutions to the system of equations. The Fourth Order Runge Kutta method and the Adams Moulton predictor-corrector methods proved to be unsuitable for this model because of numerical instabilities. The original GEAR and the modified GEAR (provided by Systems Applications, Inc.) were used to obtain an accurate solution of the equations. It was found that an initial transient occurred in the solution for the free radical species because of the mismatch between equilibrium concentrations and the assumed zero concentrations of these chemical species. Computation times

were thus slightly lengthened due to the small time step required during the first several milliseconds of the simulation.

Basis for Sensitivity Calculations

The sensitivity equations, as defined herein, are the partial derivatives of the dependent variables with respect to the unknown parameters. Parameters include rate constants, stoichiometric coefficients, and initial conditions. There are 11 dependent variables and up to 25 parameters requiring up to 275 sensitivity equations.

Symbolically, the reaction and sensitivity equations may be written as a set of coupled nonlinear first order differential equaitons. In the vector-matrix notation these can be summaried as

$$\dot{\underline{y}} = \underline{f}\,(\underline{y},\underline{p}) \qquad (1)$$

$$\frac{d}{dt}\left(\frac{\partial \underline{y}}{\partial \underline{p}}\right) = \frac{\partial \underline{f}}{\partial \underline{p}} + \frac{\partial \underline{f}}{\partial \underline{y}} \cdot \frac{\partial \underline{y}}{\partial \underline{p}} \qquad (2)$$

where $\underline{y}$ = (11 x 1) vector, $\underline{p}$ = (25 x 1) vector, $\underline{f}$ = (11 x 1) vector function, $(\partial \underline{y} / \partial \underline{p})$ = (11 x 25) matrix of sensitivities, and $\partial \underline{f} / \partial \underline{p}$ = (11 x 25) matrix of first order partial derivatives (Jacobian). The Jacobian is an integral part of the SCI Maximum Likelihood Identification program. The simultaneous integration of Eq. (1) and Eq. (2) generates the time histories of the sensitivities.

The sensitivity at any time means little when compared to the overall "shape" of the solution for any specified set of parameters. A useful measure of the overall sensitivity, as derived in the following section, is based on the "Information" contained in the output data with respect to the unknown parameters. The "Information" is defined as,

$$I = \int_0^t \left(\frac{\partial \underline{\underline{y}}}{\partial \underline{\underline{p}}}\right) \left(\frac{\partial \underline{\underline{y}}}{\partial \underline{\underline{p}}}\right) dt \qquad (3)$$

where T denotes transpose. The "Information" is a quantitative measure of degree of certainty with which we can estimate the individual parameters contained in a set of equations.

In order to illustrate the method of sensitivity analysis outlined below, five parameters were selected. These were: RK_1, RK_{11}, RK_{16}, RK_3, RK_4. For this set of parameters sixty-six equations were needed to calculate sensitivities, the original 11 differential equations plus 55 sensitivity equations. Twenty-five additional equations were integrated to generate the Information Matrix. A summary of the sensitivity analysis that was carried out is outlined below.

Digital Sensitivity Analysis

Although analog computer simulation of the smog mechanism is a flexible tool for allowing visual, qualitative sensitivity studies, the precise ordering of the reaction coefficients must be done on a digital computer, and with specialized alogrithms. The relative importance of the reaction coefficients is found by computing the sensitivity of the time histories, over a specified length of time and for all eleven reaction constituents, to a fixed percentage change in each of the reaction coefficients, in turn. At the heart of this analysis is the computation of the information matrix, from which the reaction coefficient sensitivities are easily determined.

For small changes in a given rate constant, RK_j, with all the other rate constants fixed, the variation in the concentration of species y_i at a given moment in time from that observed at the same time in the integration with all input parameters at their base values, δy_i, is given by

$$\delta y_i = \frac{\partial y_i}{\partial RK_j} \cdot \delta RK_j$$

and the total squared variation for all 11 constituents, integrated over the total reaction time, is

$$\sum_{i=1}^{11} \int_0^t (\delta y_i)^2 dt = \sum_{i=1}^{11} \int_0^t \left(\frac{\partial y_i}{\partial RK_j}\right)^2 (\delta RK_j)^2 dt = \int_0^t \sum_{i=1}^{11} \left(\frac{\partial y_i(t)}{\partial RK_j}\right)^2 (\delta RK_j)^2 dt$$

A convenient measure of the sensitivity of the constituent level to RK_j is the root sum square variation given by

$$\left[\sum_{i=1}^{11} \int_0^t (\delta y_i)^2 dt\right]^{1/2} = \left[\int_0^t \sum_{i=1}^{11} \left(\frac{\delta y_i(t)}{\delta RK_j}\right) dt\right] \cdot \delta RK_j = M_j \cdot \delta RK_j \quad (4)$$

the appearance of the value of the change in the j^{th} rate constant, δRK_j, in this equation is extremely important since this acts to normalize the sensitivity of the constituent's level with respect to the magnitude of the rate constants. Clearly, a change of 1 (unit) for each RK_j would indicate that the smaller rate constants have a larger sensitivity than the larger rate constants. This is reflected in the values for the first

order partial derivatives, $\frac{\partial y_i(t)}{\partial RK_j}$. Multiplying these first order partials by a fixed percentage of the values of the rate constants (e.g., δRK_j = 1% of RK_j) provides a normalized measure.

The quantities, $M_1, \ldots, M_{21}$, can all be computed simultaneously through the use of the information matrix. This matrix, presented as a function of time, is given by

$$I = \int_0^t \left(\frac{\partial \underline{y}}{\partial \underline{RK}}\right)^T \left(\frac{\partial \underline{y}}{\partial \underline{RK}}\right) dt \qquad (5)$$

where $\underline{y}$ is a vector of the 11 reaction constants and $\underline{RK}$ is a vector of the 21 rate constants. The first order partial $\frac{\partial \underline{y}}{\partial \underline{RK}}$ is an (11 x 21) matrix. Each concentration-time history is given by a differential equation

$$\frac{d}{dt}(y_i) = f_i(\underline{y}, \underline{RK}) \quad , \quad i = 1, 11$$

For example, for y_{10} (NO_3)

$$\frac{d}{dt}(y_{10}) = RK_4\, y_1 y_3 - RK_5 y_2 y_{10} - RK_6 y_1 y_{10}$$

Differentiating with respect to RK_4 yields

$$\frac{d}{dt}\left(\frac{\partial y_{10}}{\partial RK_4}\right) = y_1 y_3 + RK_4 \frac{\partial y_1}{\partial RK_4} y_3 + RK_4 y_1 \frac{\partial y_3}{\partial RK_4} - RK_5 \left(y \frac{\partial y_{10}}{2\partial RK_4} + \frac{\partial y_2}{\partial RK_{10}}\right) \cdot y_{10}$$

$$-RK_6 \left(y_1 \frac{\partial y_{10}}{\partial RK_4} + \frac{\partial y_1}{\partial RK_4} \cdot y_{10}\right)$$

Inspection of equation (5) shows that a diagonal element of the information matrix, I, is identically the square of one of the M_j's of Eq. (4). Therefore, to determine the sensitivities of the reaction constituents to any set of rate constants, the information matrix for the first order partials is computed. After a fixed length of integration time, the square roots of the diagonal elements are calculated and the sensitivities are found via Eq. (4).

As an illustrative example, the sensitivities of the constituents with respect ot the five rate constants RK_1, RK_{11}, RK_{16}, RK_3, and RK_4 were computed. These five rate constants were selected because of their broad range in magnitude and, thus, the potential for numerical instability problems. In this example, all other rate constants remained constant, and thus their sensitivities were not evaluated. As we have noted, even this simple example involves the solution of 66 simultaneous differential equations (11 for y_i, . . . , y_{11}, and 55 first order partials for $\frac{\partial y_i}{\partial RK_j}$, $j = k,3,4,11,16$ and $i = 1....11$). The nominal values for the rate constants were those used for the toluene base case. The square roots of the diagonal elements of the information matrix were computed to be:

$RK_1(5.64)$, $RK_{11}(1.37\times10^{-18})$, $RK_{16}(1.50\times10^{-4})$, $RK_3(1.17\times10^{-2})$, $RK_4(24.05)$

The sensitivities for these constants are:

$$RK_1: \quad (5.64)(2.66 \times 10^{-3}) = 1.46 \times 10^{-2}$$
$$RK_{11}: \quad (1.37 \times 10^{-18})(18) = 0.0$$

$$RK_{16}: \quad (1.56 \times 10^{-4})(18) = 2.71 \times 10^{-3}$$
$$RK_{3}: \quad (1.17 \times 10^{-2})(.218) = 2.56 \times 10^{-3}$$
$$RK_{4}: \quad (24.05)(6 \times 10^{-5}) = 1.44 \times 10^{-3}$$

The importance of these five rate constants can be ordered as (from most to least important)

$$RK_1, RK_{16}, RK_3, RK_4, RK_{11}.$$

The results of this experiment indicate that digital sensitivities can be generated using the H-S model and the modified GEAR program. It is estimated that up to 15 simultaneous sensitivity analyses may be performed without excessive accumulation of computer time. Because this method of sensitivity analysis is an integral part of the maximum likelihood estimation procedure, it can be used to order the parameters to be identified in terms of thier relative sensitivity.

V. DISCUSSION AND CONCLUSIONS

Discussion

In phase I of this study, two different approaches to the problem of determining the sensitivity of photochemical smog reaction parameters were evaluated. The analog computer was used to study the effect of large parameter changes that often result when a new set of experimental smog chamber data is being validated. The analog computer produces accurate

results for any desired parameter values as long as the amplitude scaling for the parameter has been properly carried out in programming the solution. In our first attempt at solving the reaction model on the analog computer, the ranges allowed for the parameter changes were far too limited, and, consequently, solutions for small changes in parameter values often required several hours of program modification. This problem can be avoided by allowing for larger ranges of parameter variations in the inital amplitude scaling.

Peripheral devices, used as aids in plotting, display, and other functions, have proven to be valuable tools in the photochemical smog model validation studies. The CRT and the use of cross (phase plane) plots were also helpful in guiding the sensitivity studies.

One major advantage of the anlog computer over the digital computer is that of stability of the solution procedure. If amplitude scaling is correctly carried out, the analog computer will always produce valid integration of the equations, whereas roundoff error and numerical stability problems can result in inaccurate solutions on a digital computer.

The digital computer provides a means for quantitatively determining a measure of the sensitivity of parameter values. A method of simultaneously solving the sensitivity equations was developed, and an example of a means for rank ordering the parameters was given for the toluene system. The sensitivity calculations are required in the maximum likelihood identification program, and consequently the sensitivities are determined automatically when parameter estimation is carried out.

The major problem in using a digital computer for sensitivity studies is that of achieving valid integrations. The modified GEAR program does not always yield an accurate solution, even when the error function test is successful. Each solution should be tested for convergence using certain options available in the program. In the results contained herein, only those solutions that result in FLAG = 1 were considered successful.

A major advantage of the digital computer is that its use, on the average, minimizes the time required to obtain new results. However, as indicated above, caution should be exercised in drawing conclusions from the digital solution unless convergence is assured.

Recommendations

We recommend that, in future sensitivity studies, the digital computer be used as the basic tool for the experimental planning activities because of the lower manpower requirements. We further recommend that the analog and digital computers continue to be used in a complementary manner to insure that accurate integrations are obtained.

REFERENCES

1. Hecht, Thomas A. and John H. Seinfeld, "Development and Validation of a Generalized Mechanism for Photochemical Smog," *Environmental Science and Technology*, *6*, 47. (1972).

2. Seinfeld, John H., Thomas A. Hecht, and Philip M. Roth, "A Kinetic Mechanism for Atmospheric Photochemical Reactions," Appendix B of Report 71-SAI-9 , Systems Applications, Inc., Beverly Hills, California, under Contract CPA 70-148, May (1971).

TECHNICAL REPORT DATA
(Please read Instructions on the reverse before completing)

1 REPORT NO	2	3 RECIPIENT'S ACCESSION NO.
EPA-650/4-74-011		

4. TITLE AND SUBTITLE	5 REPORT DATE
Mathematical Simulation of Atmospheric Photochemical Reactions: Model Development, Validation and Application	July 1973
	6. PERFORMING ORGANIZATION CODE

7 AUTHOR(S)	8 PERFORMING ORGANIZATION REPORT NO
Thomas A. Hecht, Philip M. Roth, John H. Seinfeld	R73-28

9 PERFORMING ORGANIZATION NAME AND ADDRESS	10. PROGRAM ELEMENT NO
Systems Applications, Inc. 950 Northgate Drive San Rafael, California 94903	26AAD, Task 10
	11 CONTRACT/GRANT NO.
	68-02-0580

12 SPONSORING AGENCY NAME AND ADDRESS	13. TYPE OF REPORT AND PERIOD COVERED
Environmental Protection Agency Office of Research & Monitoring National Environmental Research Center Research Triangle Park, NC 27711	Final
	14. SPONSORING AGENCY CODE

15. SUPPLEMENTARY NOTES

16 ABSTRACT

The development and evaluation of a kinetic mechanism, for use in air quality simulation models to describe photochemical smog formation, is described. The mechanism, which treats inorganic reactions in detail and organic reactions in general terms, was formulated to achieve a balance between accuracy of prediction and compactness of representation. The results of the evaluation of this mechanism using n-butane/NO_x, propylene/NO_x, and n-butane/propylene/NO_x smog chamber data are included.

17. KEY WORDS AND DOCUMENT ANALYSIS

a DESCRIPTORS	b IDENTIFIERS/OPEN ENDED TERMS	c. COSATI Field/Group
Computer Modeling Chemical Kinetics Photochemistry Atmospheric Chemistry		

18 DISTRIBUTION STATEMENT	19. SECURITY CLASS *(This Report)*	21. NO. OF PAGES
Unlimited	Unclassified	156
	20 SECURITY CLASS *(This page)*	22. PRICE
	Unclassified	

EPA Form 2220-1 (9-73)